

2007

C2- and C3-Symmetric Meta-substituted Thienyl Benzenes: A Comparative Synthetic and Structural Study

Angelica Lee Petrina Cornacchio
Western University

Follow this and additional works at: <https://ir.lib.uwo.ca/digitizedtheses>

Recommended Citation

Cornacchio, Angelica Lee Petrina, "C2- and C3-Symmetric Meta-substituted Thienyl Benzenes: A Comparative Synthetic and Structural Study" (2007). *Digitized Theses*. 4670.
<https://ir.lib.uwo.ca/digitizedtheses/4670>

This Thesis is brought to you for free and open access by the Digitized Special Collections at Scholarship@Western. It has been accepted for inclusion in Digitized Theses by an authorized administrator of Scholarship@Western. For more information, please contact wlsadmin@uwo.ca.

C_2 - and C_3 -Symmetric Meta-substituted Thienyl Benzenes:
A Comparative Synthetic and Structural Study

(Spine Title: C_2 - and C_3 -Symmetric Meta-substituted Thienyl Benzenes)
(Integrated-Article Format)

by
Angelica Lee Petrina Cornacchio

Graduate Program in Chemistry

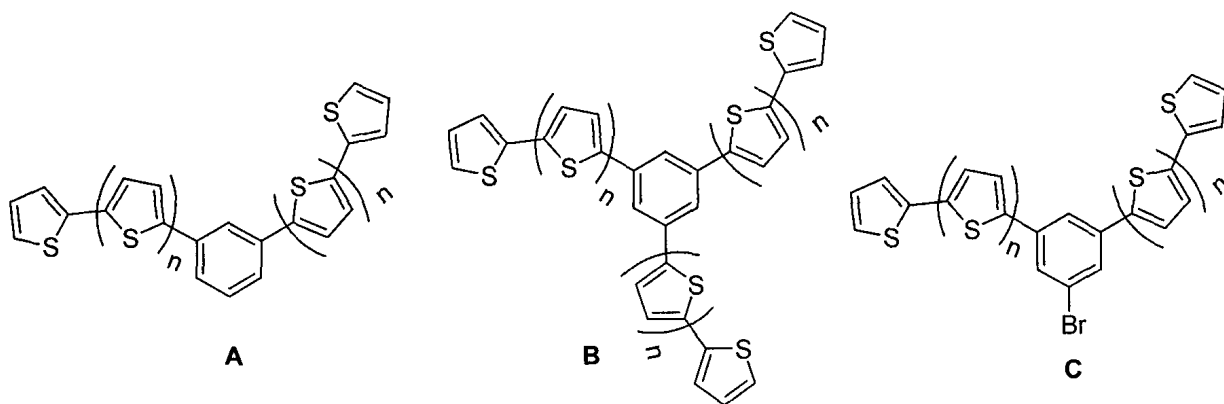
A thesis submitted in partial fulfillment
of the requirements for the degree of
Master of Science

Faculty of Graduate Studies
The University of Western Ontario
London, Ontario
May, 2007

ABSTRACT

Suzuki, Stille and Kumada coupling approaches to the syntheses of various C_2 - and C_3 -symmetric thienylbenzene compounds (**A** and **B**, respectively) are systematically compared. Novel routes are reported for the syntheses of C_3 -symmetric compounds using Kumada ($n = 0$) and Stille ($n = 1$) coupling reactions. Potentiodynamic treatment of these compounds produces polymers whose properties as a function of the length of the thienyl substituent ($n = 1$ vs. $n = 2$), and of cross-linking (C_2 vs. C_3), are compared. The solid-state structures of C_2 - and C_3 -symmetric ($n = 1$) compounds are also discussed.

Furthermore, the syntheses of novel meta-substituted benzenes that bear both thiophene and halogen groups are reported (**C**, $n = 0$ or 1). Further elaboration of the third meta position using Kumada, Stille and Sonogashira coupling methods gives a family of C_2 -symmetric compounds of the general structure 1,3-bis(thienyl)-5-R-benzene, where R is either an electron-donating or -withdrawing group. The physical and optical properties of these compounds are compared using spectroscopic (UV-visible absorption and fluorescence) and electrochemical measurements. The anodic peak potentials (E_{pa}) obtained for these compounds do not correlate with their σ_m Hammett parameters.



ACKNOWLEDGEMENTS

First and foremost, I would like to thank my supervisor, Dr. Nathan Jones, for the opportunity to work in his lab and especially for his guidance, support and encouragement during this project. Thanks for making the lab a positive and friendly place to work and for the countless hours you spent editing this thesis.

I also wish to thank Dr. Oleg Semenikhin and Dr. Ding for use of their electrochemistry instruments, and Trissa Kantzas for her patience and assistance while conducting experiments.

Financial assistance from UWO Faculty of Graduate Studies, UWO Chemistry Department, the Government of Ontario and the Natural Sciences and Engineering Research Council of Canada (NSERC) are gratefully acknowledged.

I would like to extend my gratitude to the members of the Jones group, especially Jackie and Christine, and past members: Florentino Carneiro, David Dodd, Heather Toews, Brendan Flowers and Mike Trevail. It has been an unforgettable experience to work with all of you – thank you for your friendship and support.

A very special thanks to my parents, Tracy and Peter, for always believing in me and giving me the love and support I needed to accomplish my dreams.

Thank you to Luke MacLennan for keeping me grounded and always being there when I needed a break from chemistry and finally, to my extended family, the MacLennans, for making me a part of their family and giving me a place to call home.

TABLE OF CONTENTS

Certificate of Examination.....	ii
Abstract.....	iii
Acknowledgements.....	iv
Table of Contents.....	v
List of Tables.....	x
List of Figures.....	xi
List of Schemes.....	xiii
List of Appendices.....	xv
Abbreviations.....	xvi
1 General Introduction	1
1.1 Conjugated Polymers	1
1.1.1 Syntheses of Poly(thiophenes) (PT)s	2
1.1.1.1 Mechanism of Anodic Electropolymerization of Heterocycles	4
1.2 Dendrimers.....	5
1.2.1 Previous Work with Star-Shaped Oligothiophenes Dendrimers	7
1.3 Cross-Coupling Reactions	11
1.4 Goals and Scope of this Thesis	13
1.5 References.....	16
2 Experimental Details.....	18
2.1 General Considerations	18

2.2	Electrochemical Experiments	19
2.3	Syntheses of Coordination Complexes	20
2.3.1	<i>trans</i> -PdCl ₂ (PhCN) ₂	20
2.3.2	PdCl ₂ (dppf)	21
2.4	Syntheses of Precursors to Coupling Reactions.....	21
2.4.1	3-hexylthiophene.....	21
2.4.2	2,5-dibromothiophene	22
2.4.3	2-thienylmagnesium bromide	23
2.4.4	2,2'-bithiophene	24
2.4.5	2,2':5',2''-terthiophene.....	25
2.4.6	5,5'-dibromo-2,2'-bithiophene	26
2.4.7	5'-bromo-2,2'-bithiophene.....	27
2.4.8	Syntheses of 5'-substituted bithiophenes and 2''-substituted terthiophene.....	28
2.4.8.1	2,2'-bithienyl-5'-boronic acid.....	28
2.4.8.2	2,2':5',2''-terthienylboronic acid	29
2.4.8.3	5'-acetyl-2,2'-bithiophene.....	29
2.4.8.4	5'-tributylstannyl-2,2'-bithiophene.....	30
2.4.9	Tri(ⁿ butyl)stannylferrocene.....	31
2.4.10	1,3,5-triiodobenzene	32
2.5	Cross-Coupling Reactions to Yield Thienylbenzene “Monomers”	33
2.5.1	Kumada Couplings.....	34
2.5.1.1	1,3-bis(2'-thienyl)benzene (1)	34
2.5.1.2	1-bromo-3,5-bis(2'-thienyl)benzene (7^{Br})	35

2.5.1.3	1,3-dibromo-5-(2'-thienyl)benzene (5^{Br}).....	35
2.5.1.4	1,3,5-tris(2'-thienyl)benzene (3).....	36
2.5.1.5	1,3,5-tris(2'-bromo-5'-thienyl)benzene	37
2.5.2	Stille Couplings.....	38
2.5.2.1	1,3-bis{5'-(2',2''-bithienyl)}benzene (2)	38
2.5.2.2	1-bromo-3,5-bis{5'-(2',2''-bithienyl)}benzene (8^{Br}).....	39
2.5.2.3	1,3-dibromo-5-{5'-(2',2''-bithienyl)}benzene (6^{Br}).....	40
2.5.2.4	1,3,5-tris{5'-(2',2''-bithienyl)}benzene (4).....	41
2.5.3	Suzuki Coupling.....	42
2.5.3.1	1,3,5-tris{5'-(2',2''-bithienyl)}benzene (4).....	42
2.6	Onward Reaction of Bromothienylbenzene Monomers.....	43
2.6.1	Kumada Coupling	43
2.6.1.1	1-methyl-3,5-bis(2'-thienyl)benzene (9).....	43
2.6.1.2	1-phenyl-3,5-bis(2'-thienyl)benzene (10).....	44
2.6.1.3	1,1'-(4'-fluorophenyl)-3,5-bis(2''-thienyl)benzene (12)	45
2.6.1.4	1,1'-(4'-methoxyphenyl)-3,5-bis(2''-thienyl)benzene (11).....	46
2.6.1.5	1,1',5,5'-tetra(2''-thienyl)-3,3'-biphenyl (18)	47
2.6.1.6	1-phenyl-3,5-bis{5'-(2',2''-bithienyl)}benzene (15).....	48
2.6.1.7	1,1'-(4'-fluorophenyl)-3,5-bis{5''-(2'',2'''-bithienyl)}benzene (17) ..	49
2.6.1.8	1,1'-(4'-methoxyphenyl)-3,5-bis{5''-(2'',2'''-bithienyl)}benzene (16)	50
2.6.2	Stille Coupling	51
2.6.2.1	1-ferrocenyl-3,5-bis(2'-thienyl)benzene (14)	51
2.6.3	Sonogashira Coupling.....	52

2.6.3.1	1,1'-(2'-phenylacetylene)-3,5-bis(2''-thienyl)benzene (13).....	52
2.7	References	54
3	C_3 – Symmetric Thienyl Benzenes and Related Compounds	56
3.1	General Introduction	56
3.2	Syntheses of Compounds 1 , 2 , 3 and 4	58
3.3	Results and Discussion	58
3.3.1	Syntheses of 1,3-bis- and 1,3,5-tris(2'-thienyl)benzene	58
3.3.2	Syntheses of 1,3-bis- and 1,3,5-tris{5'-(2',2''-bithienyl)benzene.....	64
3.3.3	Crystal Structures	68
3.3.3.1	1,3-bis{5'-(2',2''-bithienyl)}benzene (2).....	68
3.3.3.2	1,3,5-tris{5'-(2',2''-bithienyl)}benzene (4).....	70
3.3.4	Electronic Spectroscopy.....	72
3.3.5	Electrochemical Experiments	76
3.3.5.1	Electrochemical Polymerization	76
3.3.5.2	Cyclic Voltammetry (CV) of Polymers	80
3.3.5.3	Spectroelectrochemical Studies	84
3.4	References	88
4	C_2 -Symmetric Thienyl Benzene Compounds	90
4.1	General Introduction	90
4.2	Synthesis of 1,3-bis(thienyl)-5-R-phenyl compounds	92
4.3	Results and Discussion	92
4.3.1	Synthesis of 1,3-bis(thienyl)-5-R-phenyl compounds	92
4.3.2	Electronic Spectroscopic and Electrochemical Measurements.....	96

4.4	References	102
5	Conclusions and Plans for Future Work	103
	Appendices.....	106
	Curriculum Vitae.....	110

LIST OF TABLES

<u>Table 1.1:</u> Reactants and catalysts for various cross-coupling reactions.....	12
<u>Table 3.1:</u> Syntheses of 1,3-bis- (1) and 1,3,5-tris(2'-thienyl)benzene (3) <i>via</i> Ni- or Pd-catalyzed cross-coupling reactions.....	60
<u>Table 3.2:</u> Syntheses of 1,3,5-tris(2'-thienyl)benzene (3) <i>via</i> cyclotrimerization reactions... ..	62
<u>Table 3.3:</u> Syntheses of 1,3-bis- (2) and 1,3,5-tris{5'-(2',2''-bithienyl)}benzene (4) <i>via</i> Ni- and Pd-catalyzed cross coupling reactions.	66
<u>Table 3.4:</u> Selected bond distances (Å) and torsion angles (°) for 2 with estimated standard deviations in parentheses.....	69
<u>Table 3.5:</u> Selected bond distances (Å) and torsion angles (°) for 4 with estimated standard deviations in parentheses.....	71
<u>Table 3.6:</u> Absorption and fluorescence data for compounds 3 – 8	73
<u>Table 3.7:</u> Absorption and fluorescence maxima for selected oligothiophenes.	74
<u>Table 3.8:</u> Electropolymerization potentials of monomers 1 - 4	79
<u>Table 3.9:</u> p-Doping and n-doping potentials and voltammetry scan limits for P1 – P4 . ..	81
<u>Table 4.1:</u> Reaction type and yields for the synthesis of compounds 9 – 17	93
<u>Table 4.2:</u> Absorption, fluorescence and anodic peak potential (E_{pa}) data for compounds 1, 7^{Br} and 9 – 14	97
<u>Table 4.3:</u> Absorption, fluorescence and anodic peak potential (E_{pa}) data for compounds 2, 8^{Br} and 15 – 17	98
<u>Table A1:</u> Crystallographic Experimental Details for 2	106
<u>Table A2:</u> Crystallographic Experimental Details for 4	108

LIST OF FIGURES

<u>Figure 1.1:</u> Schematic diagram of a G2 dendrimer, where R = peripheral functional group.	6
<u>Figure 1.2:</u> Reported star-shaped benzene-cored thienyl dendrimers (\leq G2).	9
<u>Figure 1.3:</u> Catalytic cycle for a Pd-catalyzed cross-coupling reaction.	12
<u>Figure 1.4:</u> Target Compounds.	14
<u>Figure 1.5:</u> C ₂ -Symmetric Target Compounds	15
<u>Figure 3.1:</u> ORTEP representation of 2 (20 % ellipsoids). Hydrogen atoms have been omitted for clarity.	69
<u>Figure 3.2:</u> Alternative view of 2	69
<u>Figure 3.3:</u> ORTEP representations of the two crystallographically independent molecules of 4 (20% ellipsoids). Hydrogen atoms have been omitted for clarity.	70
<u>Figure 3.4:</u> Alternative views of molecules A and B.	71
<u>Figure 3.5:</u> Absorption (blue) and fluorescence (red) spectra for 3 and 4	72
<u>Figure 3.6:</u> Potentiodynamic syntheses of polymers from monomers 1 and 3 (in CH ₃ CN solution over the potential range of 0 – 1.6 V and 0.1 – 1.6 V, respectively), and 2 and 4 (in CH ₂ Cl ₂ solution over the potential range of 0 – 1.4 V).	78
<u>Figure 3.7:</u> Cyclic voltammograms (3 cycles) of P1 and P3 . Polymers were deposited on a Pt electrode by potentiodynamic synthesis over 10 cycles (0 to 1.7 V).	80
<u>Figure 3.8:</u> Cyclic voltammograms of P1 and P3 . Polymers were deposited on a Pt electrode by galvanostatic synthesis (3×10^{-5} A/cm ² for 50 s, discharged at 0 V for 100 s to convert to the undoped state.)	82

<u>Figure 3.9:</u> Cyclic voltammograms (5 cycles) of P2 and P4 . Polymers were deposited on a Pt electrode by galvanostatic synthesis (3×10^{-5} A/cm ² for 50 s, discharged at 0 V for 100 s to convert it to the undoped state).....	83
<u>Figure 3.10:</u> Electronic absorption spectra of P2 as a function of oxidation potential from 0 to 1.2 V (A) and reduction potential from -1.0 to -2.0 V (B) vs. Ag/Ag ⁺	85
<u>Figure 3.11:</u> Electronic band diagram for nondegenerate ground-state conjugated polymers showing (A) neutral state, (B) polaron states, (C) bipolaron states, (D) bipolaron bands, and (E) metallic-like bands.	86
<u>Figure 3.12:</u> Electronic absorption spectra of P4 as a function of oxidation potential from 0 to 1.2 V (A) and reduction potential from -1.0 to -2.0 V (B) vs. Ag/Ag ⁺	87
<u>Figure 4.1:</u> Plot of the oxidation potentials of 3-(<i>p</i> -R-phenyl)thiophene monomers against σ_p values of the R group.	91
<u>Figure 4.2:</u> Plot of oxidation potentials for the polymers of 3-(<i>p</i> -R-phenyl)thiophene against σ_p values for the R group.....	91
<u>Figure 4.3:</u> Structures of compounds 1 , 2 and 9 – 17	96
<u>Figure 4.4:</u> Absorption (blue) and fluorescence (red) spectra of 12	99
<u>Figure 4.5:</u> Plot of oxidation potentials of 1 , 7^{Br} and 9 – 14 against σ_m values of the R group.	100
<u>Figure 4.6:</u> Plot of oxidation potentials of 2 , 8^{Br} and 15 – 17 against σ_m values of the R group.	101

LIST OF SCHEMES

<u>Scheme 1.1:</u> Production of oligo(thiophenes) by chemical synthesis.....	2
<u>Scheme 1.2:</u> Proposed reaction scheme for the cathodic electrochemical synthesis of poly(<i>p</i> -phenylene).	3
<u>Scheme 1.3:</u> Mechanism of electropolymerization of five-membered heterocycles.	5
<u>Scheme 1.4:</u> General scheme for dendrimer synthesis <i>via</i> (i) divergent method and (ii) convergent method.	7
<u>Scheme 2.1:</u> General syntheses of thienylbenzene “monomers” using Pd-catalyzed coupling reactions.	33
<u>Scheme 2.2:</u> General reaction scheme for the syntheses of 9 – 17	43
<u>Scheme 3.1:</u> Synthetic approaches to <i>C</i> ₃ -symmetric thienyl benzenes. a) Pd-catalyzed cross coupling reaction: <i>n</i> = 0 or 1, <i>R</i> = H or alkyl, <i>R'</i> = coupling reaction precursor, <i>X</i> = Br or I; b) Cyclotrimerization reaction: <i>n</i> = 0 or 1, <i>R</i> = Br or alkyl, <i>R'</i> = acetyl, nitrovinyl or ethynyl.	57
<u>Scheme 3.2:</u> Pd-catalyzed cross-coupling reactions to obtain compounds 1 – 4	59
<u>Scheme 3.3:</u> Pd-catalyzed coupling of 2-thienylmagnesium bromide and 1,3,5-triiodobenzene to give 3 , 5^I and 7^I	62
<u>Scheme 3.4:</u> Pd-catalyzed coupling of 2-thienylmagnesium bromide and 1,3,5-triiodobenzene to give 3 , 5^{Br} and 7^{Br}	63
<u>Scheme 3.5:</u> Pd-catalyzed coupling of 5'-tributylstannyl-2,2'-bithiophene and 1,3,5-triiodothiophene to give 4 , 6^I , 8^I and tetrathiophene.	67
<u>Scheme 3.6:</u> Pd-catalyzed coupling of 5'-tributylstannyl-2,2'-bithiophene and 1,3,5-tribromothiophene to give 4 , 6^{Br} , 8^{Br} and tetrathiophene.	68

<u>Scheme 4.1:</u> Syntheses of 9 – 12 and 14 – 17 by reaction of bromothienyl compounds with RMgX or RSnBu ₃	93
<u>Scheme 4.2:</u> Pd-catalyzed Kumada coupling of 7^{Br} with MeMgI to give 9 and the homocoupled by-product, 18	94

LIST OF APPENDICES

Appendix 1. Crystal Structure Data for 2	106
Appendix 2. Crystal Structure Data for 4	108

LIST OF ABBREVIATIONS

BT	2,2'-bithiophene
Cp	cyclopentadienyl
CV	cyclic voltammogram
d	doublet
δ	chemical shift in parts per million
dd	doublet of doublets
DMA	<i>N,N</i> -dimethylacetamide
DMF	dimethyl formamide
DMSO	dimethyl sulfoxide
dppf	1,1'-bis(diphenylphosphino)ferrocene
dppp	1,3-bis(diphenylphosphino)propane
E_{pa}	anodic peak potential
Fc/Fc ⁺	ferrocene/ferrocenium
FET	Field Effect Transistor
G0	dendrimer core
G1	first generation dendrimer
G2	second generation dendrimer
HRMS	High Resolution Mass Spectrometry
ITO	Indium Tin Oxide
<i>m</i> -	<i>meta</i>
m	multiplet
MRI	Magnetic Resonance Imaging
NBS	N-bromosuccinamide
NLO	Non Linear Optic
<i>o</i> -	<i>ortho</i>
OAc ⁻	acetate
OLED	Organic Light Emitting Diode
OPV	Organic Photovoltaic
OTf	triflate
p	pseudo
<i>p</i> -	<i>para</i>
PBT	5-phenyl-2,2'-bithiophene
PCMB	[6,6]-phenyl C60 butyric acid methyl ester
PT	poly(thiophene)
PMT	photomultiplier tube
R_f	distance traveled up a TLC plate relative to the total distance traveled by the solvent
s	singlet
SCE	standard calomel electrode
σ_I	sigma-inductive contribution
σ_m	sigma- <i>meta</i>

σ_p	sigma- <i>para</i>
σ_R	sigma-resonance contribution
T	thiophene
t	triplet
TBAP	tetrabutylammonium perchlorate
TBAPF ₆	tetrabutylammonium hexafluorophosphate
TCS	tetrachlorosilane
TT	2,2'-5',2''-terthiophene
$^zJ_{xy}$	coupling constant between x&y over z bonds

1 General Introduction

1.1 Conjugated Polymers

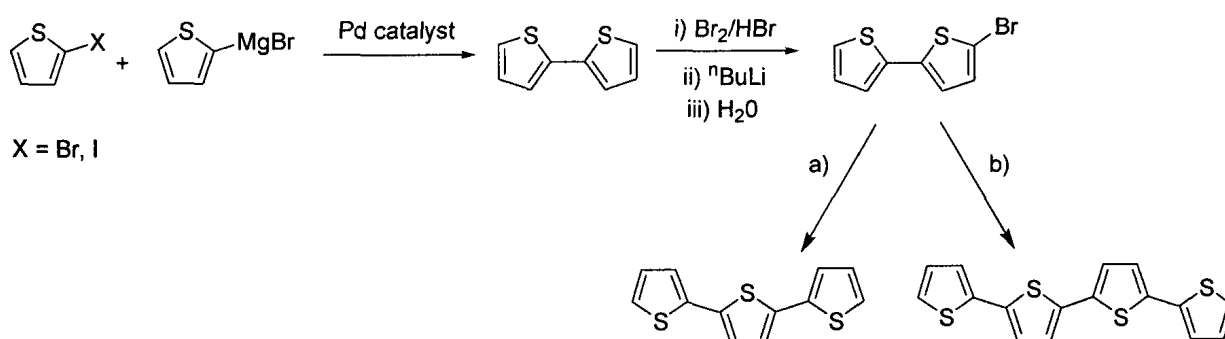
The modern era of conducting organic polymers began in 1977 when Heeger and MacDiarmid discovered that n-doped poly(acetylene) was significantly more conducting than the undoped material.¹ Prior to this discovery, electrical conductivity had only been observed in metals in their standard states, inorganic polymers and molecular crystals.²

In 1979, an important milestone in the development of conjugated poly(heterocycles) was achieved – the production of highly conductive and homogeneous films of poly(pyrrole) *via* oxidative electropolymerization of pyrrole using a platinum electrode.³ Prior electrochemical syntheses of poly(pyrrole) from aqueous H₂SO₄ solution had produced material with poor mechanical and electrical properties and did not give rise to further developments. With the successful synthesis of poly(pyrrole), electropolymerization was rapidly extended to a variety of aromatic compounds including thiophene, furan, indole, carbazole, azulene, pyrene, benzene and fluorene.⁴

Of the many systems studied, poly(thiophene) (**PT**) offered the significant advantages of high stability in its doped and undoped states, and high structural versatility (by elaboration of the 3- and 4-position of the thiophene ring). There has been considerable research directed to the development of **PT** and its potential applications. These applications can be divided into three main categories: (i) application of the doped, conducting state (*e.g.*, **PT**-based gas sensors); (ii) of the neutral, semiconducting state (*e.g.*, in nonlinear optics (NLO)); and (iii) electrochemical applications (*e.g.*, energy storage devices).⁴

1.1.1 Syntheses of Poly(thiophenes) (PT)s

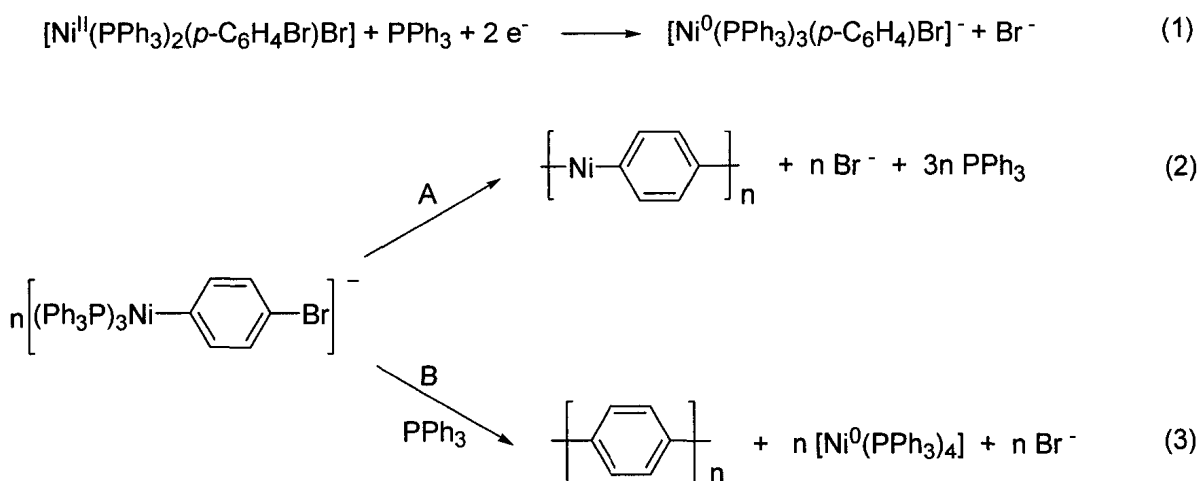
Poly(thiophenes) are prepared either *chemically* or *electrochemically*. Although chemical syntheses are the best for the preparation of thiophene oligomers of controlled structure, their application in the preparation of polymers is less common due to the low solubility and conductivity of the polymers produced.⁴ Chemical syntheses generally entail a series of stepwise lengthening of oligomers by coupling reactions, *e.g.*, the reaction of 2-thienylmagnesium bromide and 2-halothiophene under Kumada coupling conditions, followed by bromination of the 2,2'-bithiophene product and reaction with a second equivalent of 2-thienylmagnesium bromide would give 2,2':5',2''-terthiophene (a, Scheme 1.1) and/or 2,2'-5',2''-5'',2'''-quaterthiophene (b) by a homocoupling mechanism.



Scheme 1.1: Production of oligo(thiophenes) by chemical synthesis.

Electrochemical synthesis can be conducted using either an *anodic* or a *cathodic route*. The latter produces **PT** by the electroreduction of a metal complex, *e.g.*, Ni^{II}Br(PPh₃)₂(2-bromo-5-thienyl) in CH₃CN solution.⁵ This method was initially proposed for the synthesis of poly(*p*-phenylene).⁶ In this reaction, the Ni complex,

$[\text{Ni}(\text{PPh}_3)_2(p\text{-C}_6\text{H}_4\text{Br})\text{Br}]$, first undergoes a two electron reduction to give a nucleophilic species (1, Scheme 1.2), which can then attack the C-Br bond on an adjacent molecule in two different ways: pathway (A), through the metal atom to give $(\text{-Ni-C}_6\text{H}_4)_n$; or pathway (B), through the carbon atom to give poly(*p*-phenylene). The latter is similar to the mechanism proposed for the synthesis of poly(*p*-phenylene) *via* a Ni-catalyzed polymerization of Grignard reagents.⁷



Scheme 1.2: Proposed reaction scheme for the cathodic electrochemical synthesis of poly(*p*-phenylene).⁶

The polymer produced by this cathodic route possesses properties of both pathways, which has lead the authors to believe that equations (1) and (2) occur concurrently during the reaction. The drawback to this method, however, is that the polymer is produced in a neutral, insulating form; this leads to the rapid passivation of the electrode and confines film thickness to *ca.* 100 nm.

Anodic electropolymerization has several advantages over chemical and cathodic electrochemical syntheses of poly(heterocycles): *i*) a catalyst is not required; *ii*) the

polymer produced is grafted directly onto the surface of the electrode; *iii*) the film thickness can be controlled easily by varying the deposition charge; and *iv*) the growing polymer can be characterized by electrochemical and/or spectroscopic techniques.⁴

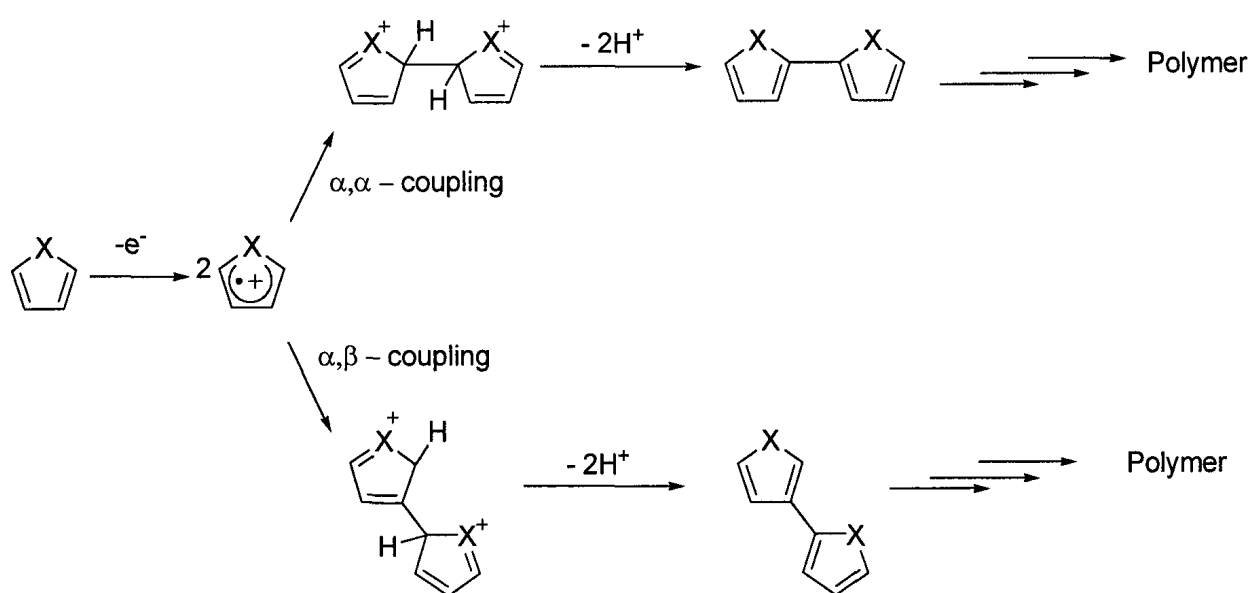
The electropolymerization of bithiophene was first reported in 1980.⁸ This was followed in 1982 by the first report of electropolymerization of thiophene.⁹ Since these initial reports, there have been a number of studies aimed at the optimization of electrosynthetic conditions for improving the quality of polymer films produced.⁴

1.1.1.1 Mechanism of Anodic Electropolymerization of Heterocycles

The electropolymerization of heterocycles occurs *via* a well understood radical cation pathway which can be applied to thiophene, pyrrole and furan (Scheme 1.3; X = S, NH and O, respectively).

In the first step, the monomer is oxidized to its radical cation. Given that the electron transfer reaction is much faster than the diffusion of the monomer into the bulk solution, a high concentration of radicals exist near the electrode surface. The second step involves the coupling of two radical cations to yield a dication that gives way to the neutral dimer with the loss of two protons. Coupling can occur at either the α or β position; however, α coupling is favored over β because this position is approximately 20 times more reactive⁴ and because coupling at the α position leads to longer conjugation lengths.¹⁰ As a result of the applied potential, the dimer and subsequent oligomers, which are more easily oxidized than the monomer, undergo oxidation and further coupling with monomeric radicals to form the growing polymer. The oxidation potential of thiophene is 1.65 V (*vs.* SCE) while that of **PT** is only 1.1 V. Electropolymerization will continue

until all the monomer in solution is consumed or until the deposition charge is discontinued. Oligomers will continue to grow in solution until they become insoluble and deposit on the electrode surface. The ratio of α - β to α - α coupling in the polymer is unknown but an increase in the number of α - α couplings in the starting monomer (*e.g.*, by use of 2,2'-bithiophene instead of thiophene) will lead to a higher number of the preferred α - α coupling in the polymer.



Scheme 1.3: Mechanism of electropolymerization of five-membered heterocycles.¹⁰

1.2 Dendrimers

The successful synthesis of dendritic structures by Vögtle and co-workers¹¹ in 1978 has led to an exponential increase in the design and use of dendrimers in chemistry and in biology. Dendrimers, also known as arborols or cascade, cauliflower or starburst polymers, are attractive molecules due to their unique structures and physico-chemical

properties. Unlike traditional polymers, dendrimers are monodispersed and have a well-defined molecular structure characterized by a series of branching units that extend outward from a central core (Figure 1.1).

Dendrimers are built using a sequence of reaction steps with each step leading to an additional layer, creating a higher generation of dendrimer with a greater number peripheral of groups. The dendrimer core is referred to as generation 0 (G0). Each successive branch point designates another generation (*e.g.*, the first branch point is the first generation, or G1).

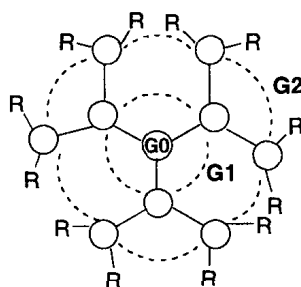
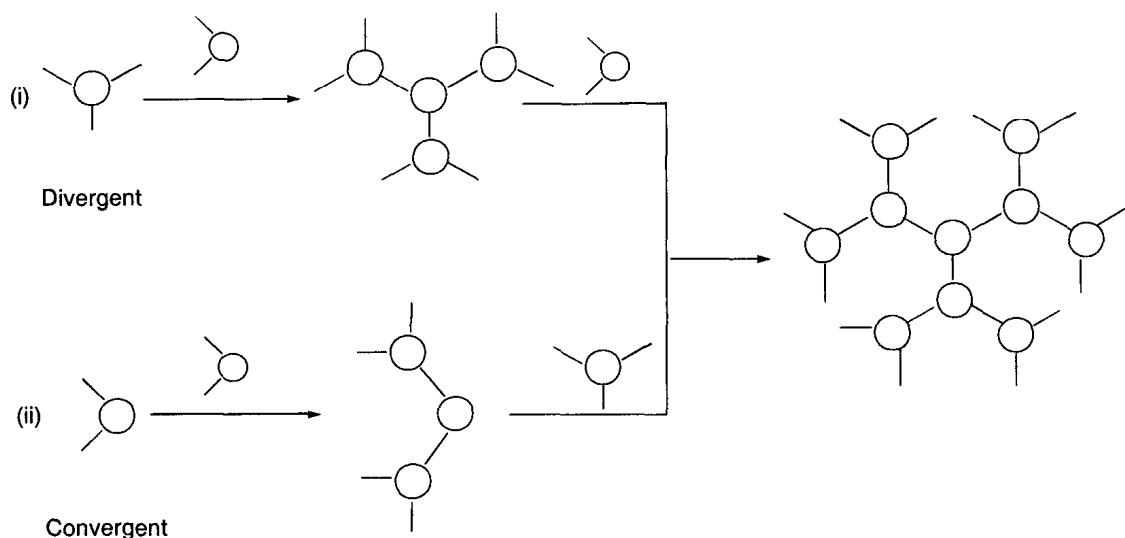


Figure 1.1: Schematic diagram of a G2 dendrimer, where R = peripheral functional group.

Dendrimers can be synthesized *via* two different routes: (i) *Divergent*, where the macromolecule is built from the core outward or, (ii) *Convergent*, in which the macromolecule is built from the periphery inward (Scheme 1.4). The disadvantage to a divergent synthesis is that the number of reactions occurring at the core increases exponentially with successive generations. This may create a large number of products that are difficult to separate. A convergent route eliminates this problem because there are a limited number of reactions that occur at each step. However, the final coupling reaction of the branched unit to the core is often difficult due to steric hindrance.¹²



Scheme 1.4: General scheme for dendrimer synthesis *via* (i) divergent method and (ii) convergent method.

Dendrimers can be tailored for a variety of applications by varying their periphery groups, branching units or core. Due to their structural flexibility, dendrimers have been used in a wide range of applications such as drug delivery systems, contrast agents in magnetic resonance imaging (MRI), or carriers in gene therapy.¹³

1.2.1 Previous Work with Star-Shaped Oligothiophenes Dendrimers

Star-shaped oligothiophenes (Figure 1.2) have come to the fore over the last several years both as monomers in cross-linked semiconducting polymers and as the cores of conjugated dendrimers. These materials have potential application in a wide range of devices that exploit the unique optical and electronic properties of thiophenes. The general structure of these dendrimers consists of conjugated linker oligomers attached to branching nodes. Variation in the length of the linkers as well as variation in the number

of generations should produce dendrimers with tunable optical properties (*e.g.*, higher conjugation produces red-shifted excitation and emission spectra). Furthermore, peripheral functional groups can be modified in order to adjust the solubility of the material, or they can be conjugated to targeting groups to generate sensors for biological applications. These materials could also be polymerized and used in electroluminescence and photovoltaic applications.

Pappenfus and Mann¹⁴ reported the synthesis of a series of thiophene-based homologues with aromatic cores (*i.e.*, benzene or thiophene) linked to terthiophene “arms” *via* acetylene linkages (A, Figure 1.2). Ethynyl linkages were used to achieve coplanarity between the oligothiophene units and the aromatic core and enhance conjugation. These compounds were produced in modest yields (3 – 4 %) over 10 steps using Sonogashira coupling methods. It should be noted, however, that large excesses (9 – 36 molar equiv.) of the ethynyl-derived terthiophene were required to force the complete substitution of the appropriate aryl halide.

Spectroscopic and electrochemical measurements revealed a bathochromic shift in the absorption and emission maxima with increased substitution around the aromatic core.¹⁴ Furthermore, these compounds displayed oxidation potentials in the range of 0.88 V to 0.93 V, with compounds possessing higher degrees of substitution being easier to oxidize.

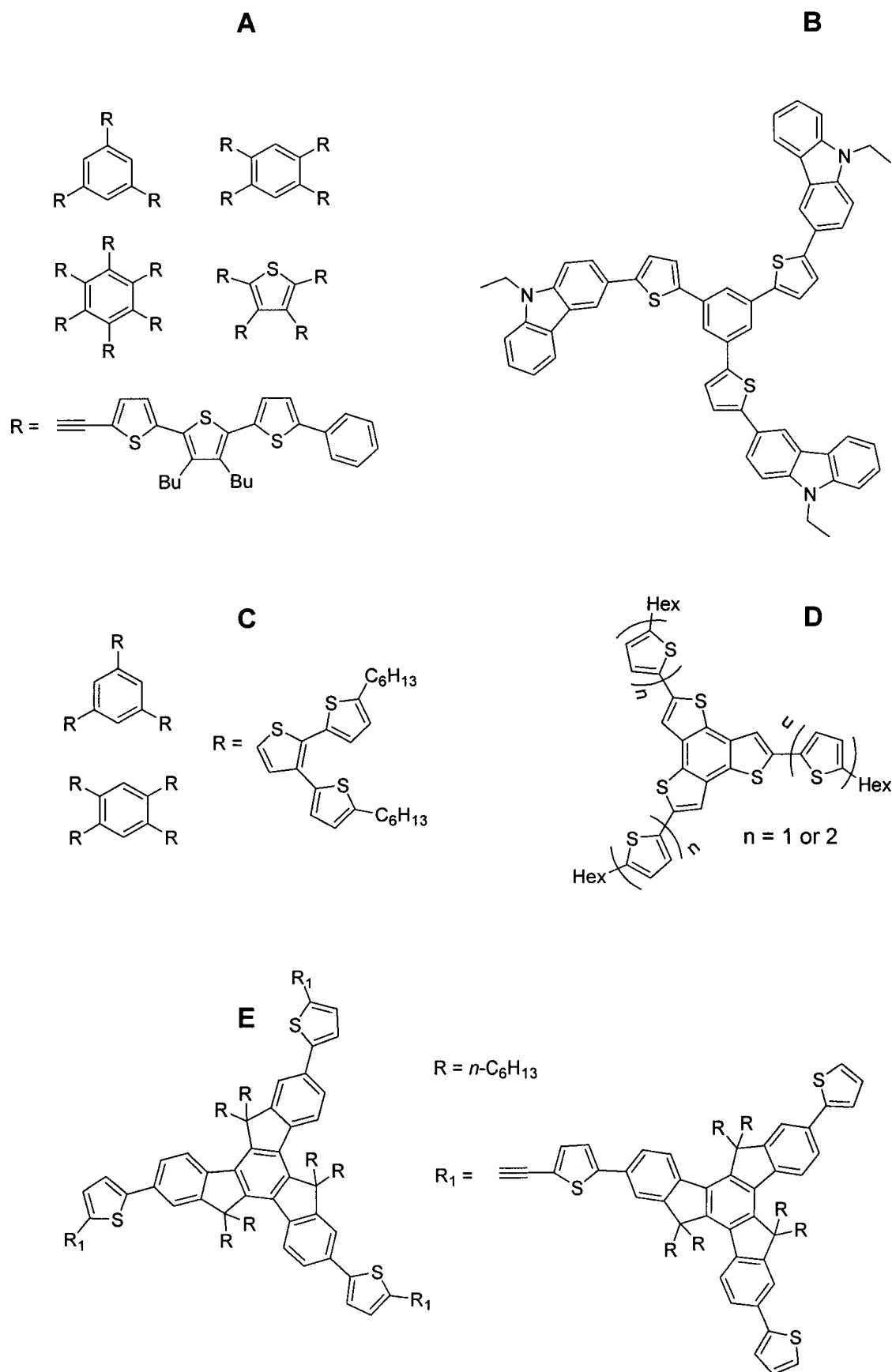


Figure 1.2: Reported star-shaped benzene-cored thienyl dendrimers ($\leq G2$).

Tomas *et al.*¹⁵ reported the synthesis of a series of star-shaped, benzene and carbazole core compounds similar to **B** (Figure 1.2). These compounds were made using a convergent synthetic strategy based on Stille coupling conditions. They exhibited strong blue emissions and were very promising for organic light-emitting diode (OLED) applications.

Mitchell *et al.*¹⁶ reported the synthesis of G1 (**C**, Figure 1.2) and G2 (not shown) C_3 - and C_4 -symmetric benzene core thiophene dendrimers. These compounds could be made straightforwardly using a convergent synthesis and Kumada coupling conditions. Most compounds were obtained in good yields (*ca.* 15 % over 5 – 7 steps); however, due to difficulties in purification, the G2 C_4 -symmetric dendrimer was obtained in low yield (1 % over 7 steps).

The application of these materials in organic photovoltaic (OPV) devices was also investigated.¹⁷ The materials were blended with [6,6]-phenyl C60 butyric acid methyl ester (PCBM) to fabricate the photovoltaic devices. It was determined that the C_3 -symmetric materials possessed better charge transport than the analogous C_4 -symmetric compounds. Furthermore, increasing the length of the C_4 -symmetric compounds resulted in an increase in device performance, which was attributed to an increase in carrier mobility. Poor solubility of the G2 C_3 -symmetric compound prevented further investigation of its properties.

Roncali *et al.*¹⁸ reported the synthesis of a C_3 -symmetric thienyl compound with a planar central core involving three thiophene rings fused to a benzene ring (**D**, Figure 1.2) for use in photovoltaic applications. These compounds were made in low yields using a mixed convergent/divergent synthesis involving Stille coupling reactions (*ca.* 3 % over 9

($n = 1$) or 11 ($n = 2$) steps). The rigid trithienobenzene core was used to improve conjugation; molecular models and experimental data have shown that benzene cores bearing pendent thienyl substituents (as in **A – C**) had greater steric hinderance, which limited their effective conjugation, than benzene cores fused to thiophene rings.

Finally, Pei *et al.*¹⁹ reported the synthesis and investigation of a family of π -conjugated dendrimers based on truxene and thienylethynylene (**E**, Figure 1.2). The compounds were synthesized using a mixed convergent/divergent route based on Sonogashira and Wittig reactions. The materials were particularly attractive for use in light harvesting applications because they displayed high molar extinction coefficients (*e.g.*, $2.7 \times 10^8 \text{ M}^{-1} \text{ cm}^{-1}$) and broad UV-visible absorption bands.

1.3 Cross-Coupling Reactions

Carbon-carbon bond forming reactions are important in academic laboratories as well as in pharmaceutical and fine chemical industries because they allow the synthesis of large complex molecules from simple, inexpensive starting materials. In this thesis, the syntheses of C_2 - and C_3 -symmetric thienylbenzene compounds are investigated using a series of metal-catalyzed cross-coupling reactions (*e.g.*, Kumada, Stille or Suzuki reactions; Table 1.1). A general catalytic cycle for this type of reaction (Figure 1.3) involves an oxidation addition, a transmetallation and a reductive elimination step.²⁰

The first step in the catalytic cycle is the oxidative addition of the 1-alkenyl, 1-alkynyl, allyl, benzyl or aryl halide to the Pd(0) catalyst to form a stable trans-palladium(II) complex **I**. Oxidative addition is commonly the rate-determining step and the relative reactivity decreases in the order of $\text{I} > \text{OTf} > \text{Br} \gg \text{Cl}$. The coupling of aryl

chlorides, which are generally inexpensive and readily available, is not effected by most catalysts and therefore aryl iodides and bromides, which are more costly, are typically used.

Table 1.1: Reactants and catalysts for various cross-coupling reactions.

Cross-Coupling Reaction	Reactant A (Hybridization at carbon center)	Reactant B (Hybridization at carbon center)	Catalyst
Stille	R-SnR ₃ (sp ²)	R-X (sp ² or sp ³)	Pd
Suzuki	R-B(OR) ₃ (sp ²)	R-X (sp ² or sp ³)	Pd
Kumada	R-MgX (sp ² or sp ³)	R-X (sp ²)	Pd or Ni
Sonogashira	RC≡CH (sp)	R-X (sp ² or sp ³)	Pd and Cu
Negishi	R-ZnX (sp ²)	R-X (sp ² or sp ³)	Pd or Ni

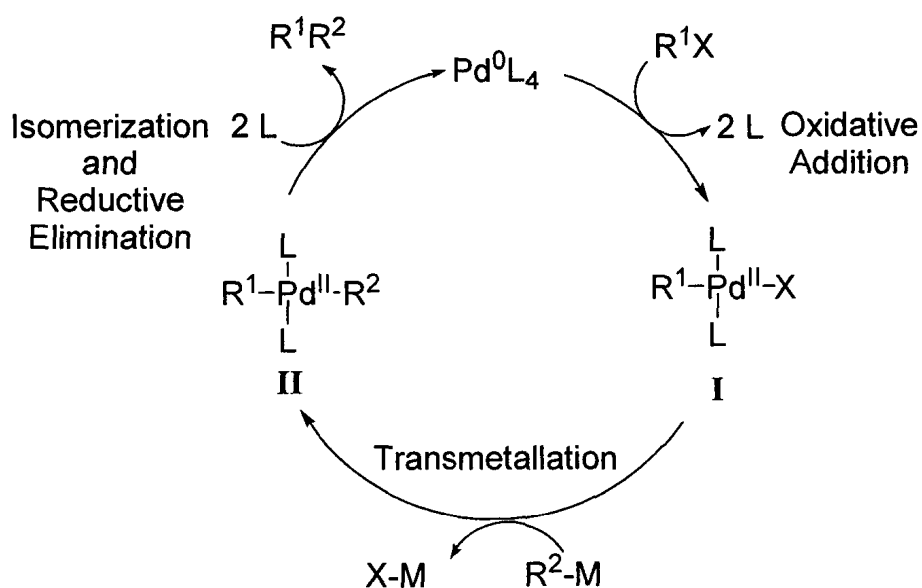


Figure 1.3: General catalytic cycle for a Pd-catalyzed cross-coupling reactions.

Of the wide variety of Pd catalysts, the most common is Pd(PPh₃)₄. Other complexes such as PdCl₂(PPh₃)₂ or Pd(OAc)₂ coupled with a phosphine ligand or N-heterocyclic carbene, may also be used as efficient catalyst precursors because they are stable to air and can easily be reduced to active Pd(0) complexes *in situ*. Palladium complexes of bulky phosphine ligands (*e.g.*, tris(2,4,6-trimethoxyphenyl)phosphine) are generally reactive toward oxidative addition because they readily form coordinatively unsaturated species.²⁰

In the transmetalation step, the R² group of the prefunctionalized starting material is exchanged for the coordinated halide (X) on the Pd center. Reductive elimination of the R¹ and R² groups from the Pd complex **II** regenerates the Pd(0) catalyst. For reductive elimination to occur, the two R groups must be *cis* to each other. If these groups are in a *trans* configuration, they will need to undergo isomerization to the *cis* configuration before reductive elimination can occur. The order of reactivity of some typical R groups is diaryl- > (alkyl)aryl- > dipropyl- > diethyl- > dimethylpalladium(II), which suggests the participation of the π -orbitals of the aryl group during bond formation.²⁰

1.4 Goals and Scope of this Thesis

The goal of this project was to develop a series of general, high yielding synthetic strategies to obtain star-shaped thienylbenzene compounds for use as monomers in conducting polymers and as building blocks in star-shaped conducting dendrimers. Our motivation stemmed from the growing interest in the use of these materials (whose physical properties are readily tuned) as the active elements in various optoelectronic

devices such as organic light emitting diodes (OLEDs), field effect transistors (FETs), *etc.*

In this work, we systematically compared the use of Suzuki, Stille and Kumada coupling approaches for the syntheses of both C_2 - and C_3 -symmetric species (**1** – **4**, Figure 1.4). Although a selection of these methods has been used in the past to generate compounds of the same general structure, these syntheses are typically hampered by long reaction times, arduous separations of partially-substituted products, and low isolated yields. Herein we present improved syntheses for the known compounds **3** and **4** using straightforward Kumada and Stille coupling reactions, respectively. Electrochemical and spectroscopic measurements were conducted, and the physical and optical properties of phenyl compounds containing either two (**1** and **2**) or three (**3** and **4**) thiophene substituents were compared. Moreover, we report and discuss solid-state X-ray crystallographic data for compounds **2** and **4**.

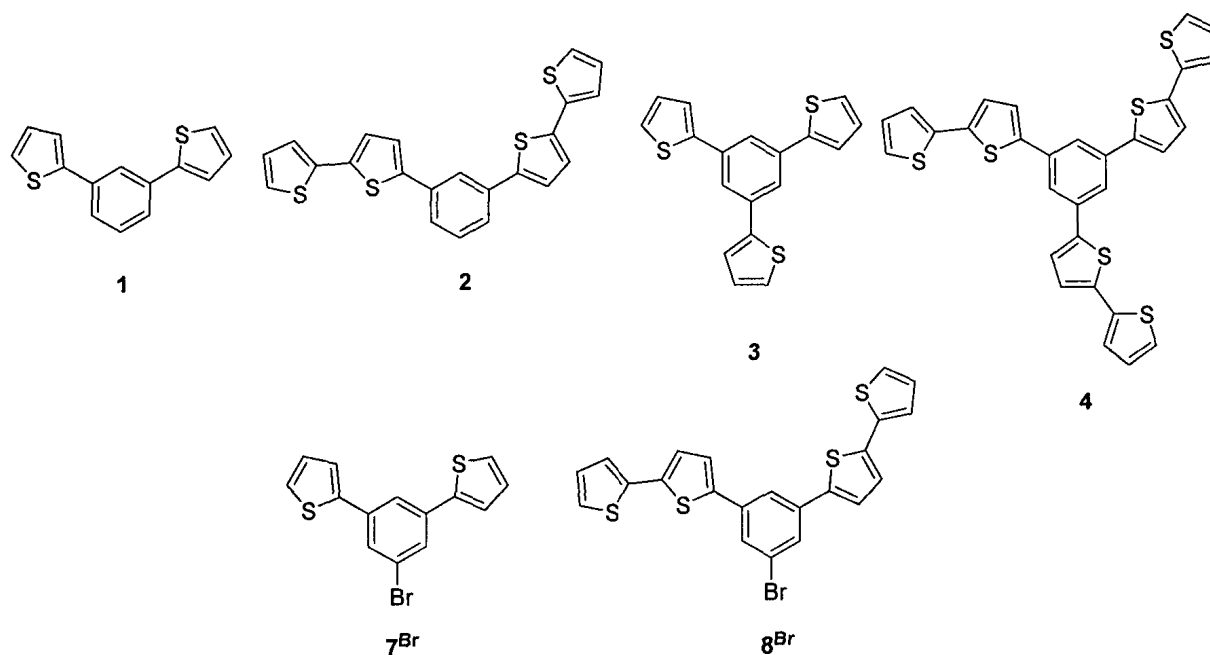


Figure 1.4: Target Compounds.

Furthermore, rational and high-yielding methods to make valuable meta-substituted benzenes that bear both thiophene and halogen groups (*e.g.*, **7^{Br}** and **8^{Br}**; Figure 1.4) were determined. These materials are particularly interesting as they allow both electrochemical (*e.g.*, through thiophene) and chemical elaboration (*e.g.*, through Br). Moreover, we demonstrate how the chemical handles in these compounds may be used to give a family of elaborated C_2 -symmetric compounds of the general structure 1,3-bis(thienyl)-5-R-benzene, whose optoelectronic properties varied depending on the nature of the R group (Figure 1.5).

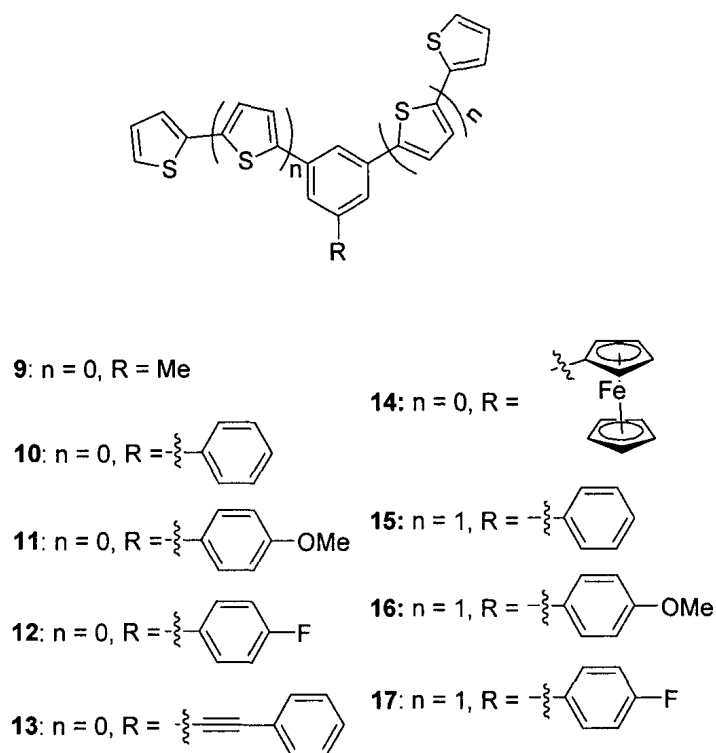


Figure 1.5: C_2 -Symmetric Target Compounds.

References

- (1) Shirakawa, H.; Louis, E. J.; MacDiarmid, A. G.; Chiang, C. K.; Heeger, J. *J. Chem. Soc., Chem Commun.* **1977**, 16, 578.
- (2) Stubb, H.; Punkka, E.; Paloheimo, J. *Mater. Sci. Eng.* **1993**, 10, 85.
- (3) Diaz, A. F.; Kanazawa, K. K. *J. Chem. Soc., Chem. Commun.* **1979**, 635.
- (4) Roncali, J. *Chem. Rev.* **1992**, 92, 711.
- (5) Zotti, G.; Schiavon, G. *J. Electroanal. Chem.* **1984**, 163, 385.
- (6) Schiavon, G.; Zotti, G.; Bontempelli, G. *J. Electroanal. Chem.* **1984**, 161, 323.
- (7) Yamamoto, T.; Hayashi, Y.; Yamamoto, A. *Bull. Chem. Soc. Jpn.* **1978**, 51, 2091.
- (8) Diaz, A. F. *Chem. Scr.* **1981**, 17, 142.
- (9) Tourillon, G.; Garnier, F. *J. Electroanal. Chem.* **1982**, 135, 173.
- (10) Wolf, M. O. *Adv. Mater.* **2001**, 13, 545.
- (11) Buhleier, E.; Wehner, W.; Vögtle, F. *Synthesis* **1978**, 155.
- (12) Boas, U.; Christensen, J. B.; Heegaard, P. M. H. *Dendrimers in Medicine and Biotechnology, New Molecular Tools*; The Royal Society of Chemistry: Cambridge, UK, 2006.
- (13) Klajnert, B.; Bryszewska, M. *Acta. Biochim. Pol.* **2001**, 48, 199.
- (14) Pappenfus, T. M.; Mann, K. R. *Org. Lett.* **2002**, 4, 3043.
- (15) Thomas, J. K. R.; Lin, J. T.; Tao, Y.-T.; Ko, C.-W. *Chem. Mater.* **2002**, 14, 1354.
- (16) Mitchell, W. J.; Kopidakis, N.; Rumbles, G.; Ginley, D. S.; Shaheen, S. E.

- J. Mater. Chem.* **2005**, *15*, 4518.
- (17) Kopidakis, N.; Mitchell, W. J.; van de Lagemaat, J.; Ginley, D. S.; Rumbles, G.; Shaheen, S. E.; Rance, W. L. *Appl. Phys. Lett.* **2006**, *89*, 103524.
- (18) Nicolas, Y.; Blanchard, P.; Levillain, E.; Allain, M.; Mercier, N.; Roncali, J. *Org. Lett.* **2004**, *6*, 276.
- (19) Wang, J.-L.; Luo, J.; Liu, L.-H.; Zhou, Q.-F.; Ma, Y.; Pei, J. *Org. Lett.* **2006**, *8*, 2281.
- (20) Meijere, A. d.; Diederich, F. *Metal-Catalyzed Cross-Coupling Reactions*; 2nd. ed.; Wiley: New York, NY, 2004.

2 Experimental Details

2.1 General Considerations

Unless otherwise indicated, reagents were obtained from commercial sources and used as supplied. The catalyst $\text{NiCl}_2(\text{dppp})$ was a gift from Prof. James Wisner (UWO). Glassware was flame-dried before use, and all reactions were conducted under Ar using standard Schlenk techniques, unless stated otherwise. Solvents were dried and deoxygenated either by thorough N_2 purge followed by passage through columns of alumina (Innovative Technology or MBraun solvent purification systems), or by distillation under Ar from the appropriate drying agent.

UV-visible absorption and emission spectra were recorded over the range of 200 – 800 nm using a Photon Technology International Quanta Master (QM7/2005) scanning spectrofluorometer with a xenon flash lamp and PMT detector (190 – 680 nm) interfaced to a computer work station (Section 3.3) or a Molecular Kinetics MOS-250 spectrofluorometer with a xenon lamp and PMT detector (Section 4.3). Solutions were diluted to a concentration of *ca.* 0.05 μM using CH_2Cl_2 and analyzed in quartz cuvettes. High-resolution mass spectrometry data were collected by Mr. Doug Harisine using a Finnigan MAT 8400 instrument. Melting points were obtained using a Fisher-John melting point apparatus and reported uncorrected.

Unless otherwise indicated, NMR spectra were recorded using a Varian Mercury 400 spectrometer (400.089 MHz for ^1H and 100.613 for ^{13}C) at 293 K in CDCl_3 using residual solvent proton (relative to external SiMe_4 , δ 0.00) or solvent carbon (relative to external SiMe_4 , δ 77.0) as internal reference. Downfield shifts were taken as positive. All coupling constants are given in Hz; s = singlet, d = doublet, t = triplet, m = multiplet, p =

pseudo, br = broad. Where appropriate, ^1H NMR data are correlated to the molecule under consideration by way of a ChemDraw image.

Thin-layer chromatography was performed using 250 μm silica gel glass plates with florescent indicator (254 nm Rose Scientific, Edmonton, Alberta) and viewed by exposure to UV light. Flash column chromatography was conducted using ACP ultra pure silica gel, 60 Å, 230 – 400 mesh (Silicycle, Québec, Quebec), using the eluent(s) specified. All solvent mixtures are reported as volume ratios.

2.2 Electrochemical Experiments

Electrochemical experiments were conducted according to three different methods: (i) Method A. Polymers were synthesized using a Princeton Applied Research (PAR) 263A potentiostat/galvanostat interfaced to a personal computer with Scribner version 2.8 Corrware/Corrview electrochemistry software. Solutions were prepared in air and contained 0.002 M monomer and 0.1 M tetrabutylammonium hexafluorophosphate (TBAPF_6) in CH_2Cl_2 (5 mL). They were purged with Ar for 5 min before experiments were conducted. A 2.0 mm diameter Pt disk inlaid in Teflon was used as the working electrode and Ag wire was used as the reference electrode. Cyclic voltammogram measurements were carried out in 0.1 M TBAPF_6 CH_3CN solutions at a scan rate of 100 mV/s; (ii) Method B. Polymers were synthesized using potentiodynamic synthesis on transparent Indium-Tin Oxide (ITO)-coated glass electrodes. Again, CH_2Cl_2 solutions containing 0.002 M monomer and 0.1 M TBAPF_6 were used for the polymerization. Spectroelectrochemical experiments were carried out in 0.1 M TBAPF_6 CH_3CN solutions using an Oceans Optics spectrophotometer over the spectral range of 400 – 1000 nm; (iii)

Method C. Electrochemical experiments were conducted using a coiled Pt wire as the counter electrode, a Ag wire as a quasi reference electrode and a 0.5 mm diameter Pt disk inlaid in glass as the working electrode. After each experiment, the Pt electrode was polished on a felt pad with 0.3 μm alumina (Buehler, Ltd., Lake Bluff, IL) and cleaned electrochemically using a 0.1 M aqueous solution of H_2SO_4 for 5 – 10 min. All solutions were prepared in a drybox using anhydrous solvent in an airtight vessel equipped with a Teflon cap through which the electrodes were inserted. Cyclic voltammograms were recorded on a CH Instruments (Austin, TX) model 610A Electrochemical Workstation. Solutions for each voltammogram were made of 0.001 g of compound and 3 mL of either CH_3CN or CH_2Cl_2 ; the supporting electrolyte was 0.1 M tetrabutylammonium perchlorate (TBAP). After each experiment, the potentials obtained were calibrated using ferrocene as an internal standard ($E^\circ (\text{Fc}/\text{Fc}^+) = 0.424 \text{ V vs. SCE}^1$)

2.3 Syntheses of Coordination Complexes

2.3.1 *trans*- $\text{PdCl}_2(\text{PhCN})_2$

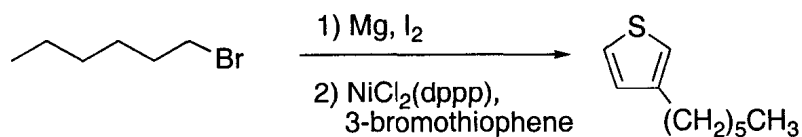
The title compound was made according to a published procedure.² A 50 mL two-neck round-bottom flask equipped with a condenser was charged with PdCl_2 (1.26 g, 7.09 mmol) and benzonitrile (1.3 mL). The red suspension was heated to 130 $^\circ\text{C}$ overnight to give an orange solution. This solution was allowed to cool to r.t. and Et_2O (10 mL) was added, which caused an orange precipitate to form. This was collected by filtration, washed with Et_2O (10 mL) and dried *in vacuo*. Yield: 1.92 g (70 %).

2.3.2 PdCl₂(dppf)

In a 25 mL round-bottom flask, *trans*-PdCl₂(PhCN)₂ (0.28 g, 0.72 mmol) was dissolved in the minimum CH₂Cl₂. To this solution, 1,1'-bis(diphenylphosphino)ferrocene (dppf) (0.40 g, 0.72 mmol) in CH₂Cl₂ (20 mL) was added dropwise. This resulted in a black solution that rapidly changed color to orange and finally deep red. The volume was reduced to *ca.* 5 mL and Et₂O (30 mL) was added to give an orange precipitate. This was isolated by filtration, washed with Et₂O (2 × 10 mL) and dried *in vacuo*. Yield: 0.512 g (55 %). ¹H NMR: δ 4.19 (ps, 4H, Cp), 4.40 (ps, 4H, Cp), 7.40 (pt, 8H, Ph), 7.49 (pt, 4H, Ph), 7.89 (pt, 8H, Ph). ³¹P NMR: δ -26.7 (s). The spectroscopic data for this compound are better resolved than those reported in the literature.³

2.4 Syntheses of Precursors to Coupling Reactions

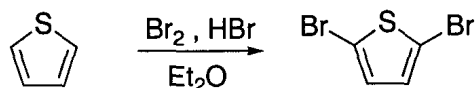
2.4.1 3-hexylthiophene



This compound was made according to a published procedure.^{4,5} A solution of 1-bromohexane (5.11 g, 0.031 mol) in Et₂O (40 mL) was added dropwise to a 100 mL three-neck round-bottom flask containing an ice cold orange mixture of magnesium turnings (0.822 g, 0.034 mmol), Et₂O (10 mL) and a few iodine crystals. This gave a white-grey suspension almost immediately. The suspension was stirred for 3 h on ice before 3-bromothiophene (5.0 g, 0.031 mol) in Et₂O (20 mL) and solid NiCl₂(dppp) (0.017 g,

0.031 mmol) were added. The resulting orange mixture was brought to reflux for 15 h to give a dark brown solution that was cooled using a flow of Ar before being quenched with 1 M HCL (15 mL). The organic layer was isolated and the aqueous layer was extracted with Et₂O (3 × 15 mL). The combined organic layers were washed with H₂O (15 mL), dried with MgSO₄ and the volume was reduced to give a dark brown viscous liquid. Purification by vacuum distillation gave the desired product as a colorless liquid (bp: 25 °C, 1 mm Hg). Yield: 1.75 g (17 %). ¹H NMR: δ 0.87 (pt, 3H, CH₃), 1.28 (m, 4H, CH₂), 1.61 (m, 4H, CH₂), 2.62 (t, 2H, CH₂, ³J_{HH} = 7.6), 6.92 (m, 2H), 7.23 (m, 1H). The spectroscopic data for this compound were the same as those reported in the literature.^{5,6}

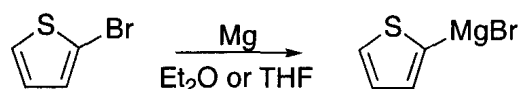
2.4.2 2,5-dibromothiophene



This compound was made according to a published procedure.⁷ A 25 mL round-bottom flask was charged with thiophene (1.88 mL, 23.8 mmol), HBr (6.7 mL) and Et₂O (4.5 mL). The colorless solution was cooled to –10 °C using an ethylene glycol/CO_{2(s)} bath. A solution of Br₂ (47.6 mmol, 2.44 mL) in HBr (2.3 mL) was added dropwise with vigorous stirring over 15 min using an addition funnel. After 30 min, the cooling bath was removed and the solution allowed to warm to r.t.. The aqueous layer was extracted with CH₂Cl₂ (3 × 10 mL). The organic fractions were combined and a large volume of H₂O was added. This caused the following color changes: the organic layer turned from dark purple to colorless and the aqueous layer turned from colorless to yellow. The organic layer was isolated, dried over MgSO₄ and reduced to give a viscous yellow

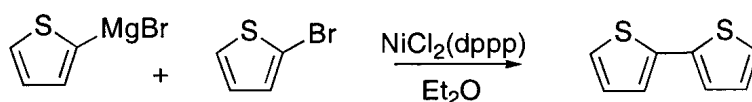
liquid. The desired product, a yellow liquid, was obtained by vacuum distillation (bp: 30 °C, 1 mm Hg). Yield: 0.233 g (73 %). ^1H NMR: δ 6.85 (s, 2H, CH). $^{13}\text{C}\{^1\text{H}\}$ NMR: δ 111.8, 130.6. HRMS $\text{C}_4\text{H}_2\text{Br}_2\text{S}$ calcd (found): 239.8244 (239.8251). Spectroscopic data were not given in the literature.⁷

2.4.3 2-thienylmagnesium bromide

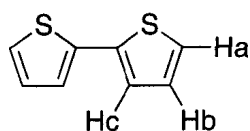


This compound was made by a slight modification to a reported procedure.⁸ In a typical synthesis, a three-neck round-bottom flask equipped with a condenser was charged with Mg turnings (1.1 equiv., 0.267 – 1.64 g), Et₂O (6 % w/v) and a few iodine crystals. The mixture was cooled to 0 °C using an ice bath and a solution of 2-bromothiophene (1.0 equiv., 1.63 – 10.0 g) in the same solvent (4 % w/v) was added slowly using a cannula. The ice bath was removed and the mixture was allowed to warm to r.t. at which point there was a rapid color change from brown-orange to grey. Solutions of 2-thienylmagnesium bromide were used without further workup after an additional 3 h of stirring at r.t.. This procedure was successfully applied to the synthesis of up to 350 mL of 0.15 M reagent.

2.4.4 2,2'-bithiophene

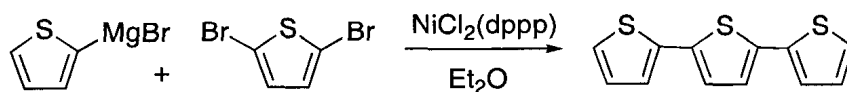


This compound was made using a published procedure.⁹ A solution of 2-bromothiophene (5.90 mL, 61.3 mmol) in Et₂O (175 mL) was added to 2-thienylmagnesium bromide (430 mL, 0.14 M). The catalyst, NiCl₂(dppp) (0.332 g, 0.613 mmol), was then added. After 3 d at reflux, the mixture was cooled on ice before being hydrolyzed with ice cold 1 M HCl (250 mL). The organic layer was isolated and the aqueous layer was extracted with Et₂O (2 × 200 mL). The organic fractions were combined, dried over MgSO₄ and reduced *in vacuo* to give a dark brown liquid. Distillation under vacuum yielded the pale blue-green product (bp: 55 – 60 °C, 1 mm Hg), which solidified at r.t. Yield: 9.14 g (90 %). This solid was further purified by sublimation at 80 °C overnight to give colorless crystals.



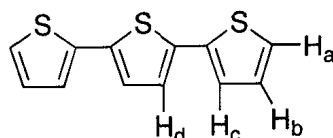
¹H NMR: δ 7.03 (dd, 2H, H_b, ³J_{HH} = 3.4, ³J_{HH} = 5.6), 7.19 (dd, 2H, H_a/H_c, ³J_{HH} = 3.4, ⁴J_{HH} = 1.2), 7.22 (dd, 2H, H_a/H_c, ³J_{HH} = 5.6, ⁴J_{HH} = 1.2). ¹³C{¹H} NMR: δ 124.0, 124.6, 128.0, 137.6. HRMS C₈H₆S₂ calcd (found): 165.9911 (165.9915). The spectroscopic data for this compound are better resolved than those reported in the literature.⁹

2.4.5 2,2':5',2''-terthiophene



2,2':5',2''-terthiophene is a known photosensitizer.¹⁰ Care should be taken to prevent skin exposure and inhalation of this compound. Photosensitizing effects last for ca. 3 wk. during which time solar UV irradiation of 2,2':5',2''-terthiophene-exposed areas may result in local skin irritation and, if exposure has been by inhalation, a full-body reaction may occur.

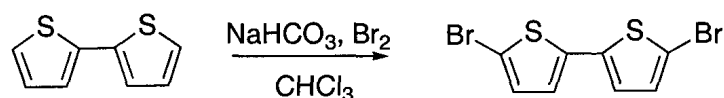
This compound was made using a published procedure.⁹ In a 250 mL three-neck flask equipped with a condenser, a solution of 2,5-dibromothiophene (0.823 g, 3.40 mmol) in Et₂O (4% w/v) and NiCl₂(dppp) (0.024 g, 0.044 mmol) were added to a solution containing 2-thienylmagnesium bromide (50 mL, 0.06 M) to give an orange-brown mixture that was brought to reflux for 19 h. The reaction mixture was then cooled and quenched on ice with 1 M HCl (50 mL). The aqueous layer was extracted with Et₂O (3 × 20 mL). The organic fractions were combined, dried over MgSO₄, and reduced *in vacuo*, to give a brown oil. This was purified by recrystallization from hexanes followed by sublimation at 96 °C (1 mm Hg). The final product was a fluffy yellow powder. Yield: 0.104 g (12 %).



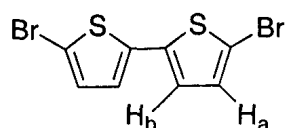
¹H NMR: δ 7.03 (dd, 2H, H_b, ³J_{HH} = 3.6, ³J_{HH} = 5.1), 7.08 (s, 2H, H_d), 7.18 (dd, 2H, H_a/H_c, ³J_{HH} = 3.6, ⁴J_{HH} = 0.8), 7.22 (dd, 2H, H_a/H_c, ³J_{HH} = 5.1, ⁴J_{HH} = 0.8). ¹³C{¹H} NMR:

δ 123.9, 124.5, 124.7, 128.1, 129.0, 131.1. HRMS $C_{12}H_8S_3$ calcd (found): 247.9788 (247.9779). The spectroscopic data for this compound were not given in the literature.⁹

2.4.6 5,5'-dibromo-2,2'-bithiophene

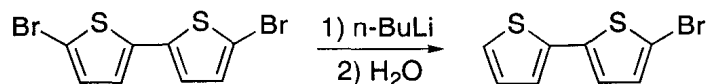


This compound was made according to a published procedure.⁹ In a 50 mL two neck round-bottom flask, 2,2'-bithiophene (0.80 g, 4.8 mmol) was dissolved in $CHCl_3$ (10 mL). Solid $NaHCO_3$ (0.344 g, 4.09 mmol) was added to give a white suspension. Liquid Br_2 (0.49 mL, 9.62 mmol) in $CHCl_3$ (2 mL) was added dropwise *via* an addition funnel to produce a green suspension. After being stirred for 1 h at r.t., the suspension was filtered to remove all solids and concentrated to give a yellow powder. Recrystallization from hexanes gave a fluffy yellow powder. Yield: 0.77 g (49 %).

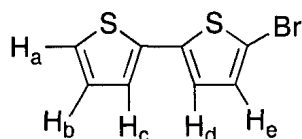


1H NMR: δ 6.85 (d, 2H, H_a/H_b , $^3J_{HH} = 3.8$), 6.96 (d, 2H, H_a/H_b , $^3J_{HH} = 3.8$).
 $^{13}C\{^1H\}$ NMR: δ 124.4, 130.9 (quaternary carbon atoms not observed). HRMS: $C_8H_4Br_2S_2$ calcd (found) 321.8121 (321.8120). 1H NMR data for this compound were the same as those reported in the literature.⁹ The $^{13}C\{^1H\}$ NMR data were not reported, however.

2.4.7 5'-bromo-2,2'-bithiophene



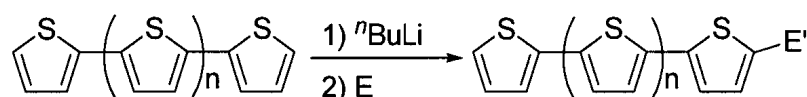
This compound was made using a published procedure.⁹ In a 50 mL Schlenk flask, 5,5'-dibromo-2,2'-bithiophene (1.10 g, 3.33 mmol) was dissolved in dry THF (10 mL). The yellow solution was cooled to $-78\text{ }^{\circ}\text{C}$ using an acetone/CO_{2(s)} bath and a 1.6 M solution of *n*BuLi in hexanes (2.08 mL, 3.33 mmol) was added *via* cannula. After 30 min, the cooling bath was removed and the reaction mixture was allowed to warm to r.t.. The yellow solution was stirred for another 30 min at r.t. before being hydrolyzed with H₂O. The organic layer was separated and its volume was reduced almost to dryness. The final product, a colorless liquid, was obtained by flash column chromatography using pure hexanes (*R*_f = 0.6). Yield 0.36 g (43 %).



¹H NMR: δ 6.92 (d, 1H, H_d/H_e, ³*J*_{HH} = 4.0), 6.97 (d, 1H, H_d/H_e, ³*J*_{HH} = 4.0), 7.01 (dd, 1H, H_b, ³*J*_{HH} = 3.6, ³*J*_{HH} = 5.2), 7.11 (dd, 1H, H_a/H_c, ³*J*_{HH} = 3.6, ⁴*J*_{HH} = 1.2), 7.23 (dd, 1H, H_a/H_c, ³*J*_{HH} = 5.2, ⁴*J*_{HH} = 1.2). The spectroscopic data are better resolved than those reported in the literature.⁹

2.4.8 Syntheses of 5'-substituted bithiophenes and a 2''-substituted terthiophene

The compounds reported in Sections 2.4.8.1 – 2.4.8.4 were made according to the general scheme shown below.



2.4.8.1 2,2'-bithienyl-5'-boronic acid

This compound was made by a reported procedure;¹¹ in the general scheme $n = 0$, $E = \text{B(OMe)}_3$ and $E' = \text{B(OH)}_2$. In a 50 mL Schlenk flask, 2,2'-bithiophene (0.537 g, 3.23 mmol) was dissolved in THF (5 mL) to give a colorless solution. This was cooled to $-10\text{ }^\circ\text{C}$ on an ethylene glycol/ $\text{CO}_{2(\text{s})}$ bath and a 1.6 M solution of $n\text{BuLi}$ in hexanes (2.08 mL, 3.23 mmol) was added dropwise. After 30 min at this temperature, the cooling bath was removed and the solution was stirred for another 30 min at r.t.. The yellow solution was then cooled to $-78\text{ }^\circ\text{C}$ using an acetone/ $\text{CO}_{2(\text{s})}$ bath, and a solution of trimethoxyborane (1.10 mL, 9.69 mmol) in THF (2 mL) was added slowly over several min. After 1 h, the cooling bath was removed and the solution was allowed to warm to r.t.. The solution was then quenched on ice using a 10 % aqueous solution of H_2SO_4 (15 mL). The aqueous layer was discarded and the organic layer was washed with brine ($3 \times 20\text{ mL}$). Chloroform was added to the organic layer in order to increase the volume. This was extracted with a 10 % aqueous solution of NaOH ($3 \times 20\text{ mL}$). The aqueous fractions were combined and concentrated HCl was added to achieve a pH of 1. At this point, a precipitate formed and was recovered by filtration. The grey solid product was used without further purification. Yield: 0.312 g (46 %). ^1H NMR ($\text{DMSO}-d_6$): δ 7.07

(pdd, 1H, CH), 7.30 (m, 2H, CH), 7.50 (d, 1H, CH, $^3J_{\text{HH}} = 5.2$), 7.57 (d, 1H, CH, $^3J_{\text{HH}} = 3.2$), 8.30 (s, 2H, B-OH). ^1H NMR data for this compound were the same as those reported in the literature.¹¹ The $^{13}\text{C}\{^1\text{H}\}$ NMR data were not reported, however.

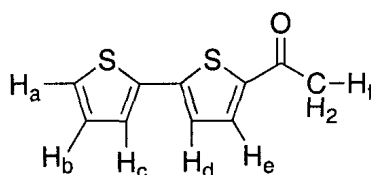
2.4.8.2 2,2':5',2''-terthienylboronic acid

This compound was made in a manner similar to the protocol outlined in Section 2.4.8.1; here $n = 1$, $\text{E} = \text{B}(\text{OMe})_3$ and $\text{E}' = \text{B}(\text{OH})_2$. Thus, the intermediate lithium salt that was generated by the reaction of 2,2':5',2''-terthiophene (0.270 g, 1.09 mmol) and $^n\text{BuLi}$ (0.70 mL, 1.09 mmol) was quenched by the dropwise addition of a solution of trimethoxyborane (0.37 mL, 3.26 mmol) in THF (2 mL). This formed a brown solid. The cooling bath was removed and the solution was allowed to warm to r.t.. Stirring was continued at this temperature for 2.5 h. Workup was the same as in Section 2.4.8.1. The desired product was recovered by filtration and used without further purification. Yield: 0.132 g (42 %). ^1H NMR ($\text{DMSO}-d_6$): δ 7.08 (dd, 1H, CH, $^3J_{\text{HH}} = 4.0$, $^3J_{\text{HH}} = 4.0$), 7.28 (pd, 1H, CH), 7.28 (pd, 1H, CH), 7.33 (m, 2H, CH), 7.51 (pdd, 1H, CH), 7.59 (d, 1H, CH, $^3J_{\text{HH}} = 4.0$), 8.30 (br, 2H, B-OH). HRMS $\text{C}_{12}\text{H}_9\text{BO}_2\text{S}_3$ calcd (found): 291.9858 (291.0239).

2.4.8.3 5'-acetyl-2,2'-bithiophene

This compound was made according to a published procedure¹² and in a manner similar to the protocol outlined in Section 2.4.8.1; here $n = 0$, $\text{E} = \text{DMA}$ and $\text{E}' = \text{C}(\text{O})\text{CH}_3$. Thus, the intermediate lithium salt that was generated by the reaction of 2,2'-bithiophene

(0.333 g, 2.00 mmol) and n BuLi (1.25 mL, 2.00 mmol) was quenched with DMA (0.186 mL, 2.00 mmol). After stirring for 2 h at r.t., the yellow solution was cooled on ice and hydrolyzed with H₂O (50 mL). The aqueous layer was extracted with CH₂Cl₂ (2 × 50 mL). The organic fractions were combined, dried over Na₂SO₄ and reduced to yield a yellow-brown residue. This was purified by flash column chromatography (1:5 hexanes:CH₂Cl₂) to give the desired product as a fluffy yellow powder (R_f = 0.4). Yield: 2.36 g (94 %).

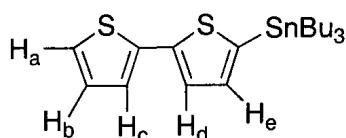


^1H NMR: δ 2.56 (s, 3H, H_f), 7.06 (dd, 1H, H_b, $^3J_{\text{HH}} = 4.5$, $^3J_{\text{HH}} = 5.6$), 7.18 (d, 1H, H_d/H_e, $^3J_{\text{HH}} = 4.5$), 7.33 (m, 2H, H_a and H_c), 7.59 (d, 1H, H_d/H_e, $^3J_{\text{HH}} = 4.5$). $^{13}\text{C}\{^1\text{H}\}$ NMR: δ 26.8, 124.4, 125.9, 126.7, 128.5, 133.5, 136.6, 142.6, 146.0. HRMS C₁₀H₈OS₂ calcd (found): 208.0017 (208.0020). The spectroscopic data for this compound were the same as those reported in the literature.¹²

2.4.8.4 5'-tributylstannyl-2,2'-bithiophene

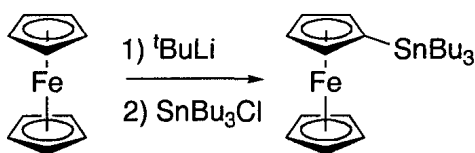
This compound was made¹³ and purified¹⁴ according to a published procedure and in a manner similar to the protocol outlined in Section 2.4.8.1; here $n = 0$, E = Bu₃SnCl and E' = SnBu₃. Thus, the intermediate lithium salt that was generated by the reaction of 2,2'-bithiophene (3.00 g, 18.0 mmol) and n BuLi (11.3 mL, 18.0 mmol) was quenched by the dropwise addition of n Bu₃SnCl (4.87 mL, 18.0 mmol). The cooling bath was removed and the yellow suspension was heated to reflux overnight. The resulting yellow

suspension was cooled and KF (1.05 g, 18.0 mmol) was added. The slurry was stirred for 1 h before the solids were removed by filtration. The filtrate was reduced to a viscous yellow liquid, which was purified by vacuum distillation (bp: 190 – 200 °C, 1 mm Hg) to give the desired product as a yellow liquid. Yield: 2.08 g (76 %).



^1H NMR: δ 0.91 (t, 9H, CH_3 , $^3J_{\text{HH}} = 8.0$), 1.12 (t, 6H, CH_2 , $^3J_{\text{HH}} = 8.0$), 1.35 (m, 6H, CH_2), 1.58 (m, 6H, CH_2), 7.00 (dd, 1H, H_b , $^3J_{\text{HH}} = 3.8$, $^3J_{\text{HH}} = 5.0$), 7.07 (d, 1H, H_d/H_e , $^3J_{\text{HH}} = 3.2$), 7.18 (m, 2H, H_a/H_c), 7.30 (d, 1H, H_d/H_e , $^3J_{\text{HH}} = 3.2$). $^{13}\text{C}\{^1\text{H}\}$ NMR: δ 11.0, 13.9, 27.5, 29.2, 123.7, 124.2, 125.2, 128.0, 136.3, 136.9, 137.9, 143.0. HRMS: $\text{C}_{20}\text{H}_{32}\text{S}_2\text{Sn}$ calcd (found): 456.0967 (456.0974). The spectroscopic data for this compound were the same as those reported in the literature.¹³

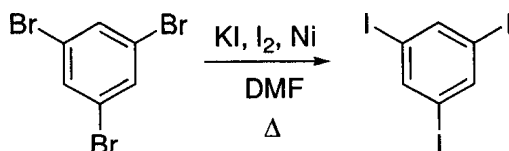
2.4.9 Tri(*n*-butyl)stannylderivative



This compound was made according to a published procedure.¹⁵ In a 100 mL Schlenk flask, a 1.7 M solution of $t\text{BuLi}$ (6.32 mL, 10.7 mmol) was added dropwise over 15 min to an ice cold, orange solution of ferrocene (1.00 g, 5.37 mmol) dissolved in a 1:1 mixture of THF:hexanes (50 mL). The resulting red suspension was stirred vigorously for 30 min. The mixture was brought to r.t. and $n\text{Bu}_3\text{SnCl}$ (2.62 g, 8.05 mmol) was added dropwise over 5 min to give a bright orange suspension. After 90 min at r.t., the reaction

was quenched using a 10 % aqueous solution of NaOH (10 mL). The aqueous layer was extracted with Et₂O (3 × 15 mL). The combined organic fractions were washed with H₂O (15 mL), dried over MgSO₄, and reduced *in vacuo* to give a dark red liquid. Purification by vacuum distillation gave the desired product as a dark red liquid (bp: 155 – 160 °C, 1 mm Hg). Yield: 1.41 g (56 %). ¹H NMR: δ 0.85 – 1.12 (m, 15H, CH₂ and CH₃), 1.34 (m, 6H, CH₂), 1.58 (m, 6H, CH₂), 4.02 (t, 2H, CH, ³J_{HH} = 1.6), 4.10 (s, 5H, Cp), 4.33 (t, 2H, CH, ³J_{HH} = 1.6). The spectroscopic data for this compound were the same as those reported in the literature.¹⁵

2.4.10 1,3,5-triiodobenzene

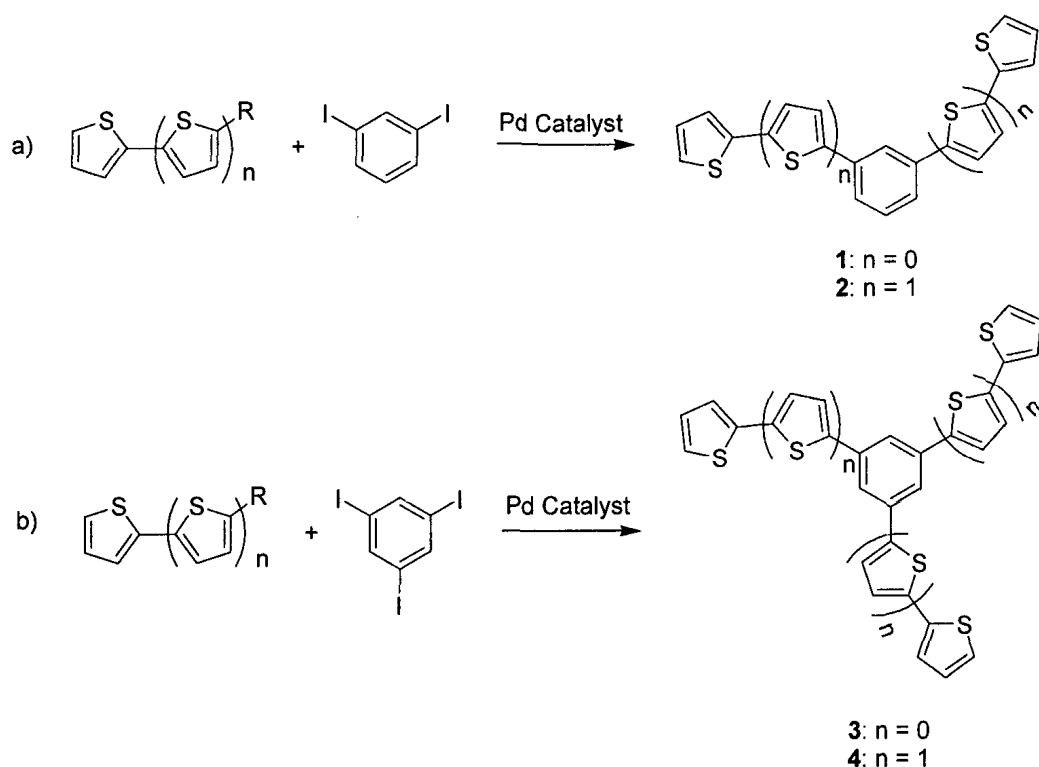


This compound was made using a published procedure.¹⁶ In a 50 mL two-neck round-bottom flask equipped with a condenser, 1,3,5-tribromobenzene (3.30 g, 10.5 mmol), KI (10.38 g, 62.0 mmol) and I₂ (15.2 g, 59.7 mmol) were dissolved in DMF (40 mL) to give a dark orange solution. Nickel powder (5.97 g, 101.7 mmol) was then added and the flask was purged with Ar for 15 min before being heated to reflux for 3 h. Upon cooling to r.t., the purple-green suspension solidified. This was transferred to a separatory funnel using alternating portions of a 3 % aqueous solution of HCl (200 mL) and CH₂Cl₂ (200 mL), without transferring any nickel metal. The aqueous layer was extracted with CH₂Cl₂ (3 × 50 mL). The organic layers were combined, washed with H₂O, dried over MgSO₄ and reduced to a tan colored powder. Sublimation at 60 °C (1 mm Hg) overnight removed the

contaminating 1,3-dibromo-5-iodobenzene and 1-bromo-3,5-diiodobenzene. A second sublimation at 120 – 130 °C (1 mm Hg) gave the desired product as a pale yellow powder. Yield: 2.80 g (59 %). ^1H NMR: δ 8.00 (s, 3H, CH). $^{13}\text{C}\{^1\text{H}\}$ NMR: δ 95.4, 144.6. HRMS $\text{C}_6\text{H}_3\text{I}_3$ calcd (found): 455.7369 (455.7375). The spectroscopic data for this compound were the same as those reported in the literature.¹⁶

2.5 Cross-Coupling Reactions to Yield Thienylbenzene “Monomers”

Di - (a) and trisubstituted (b) benzene compounds were prepared according to the general Pd-catalyzed scheme shown below by three different routes: Kumada, Stille and Suzuki.

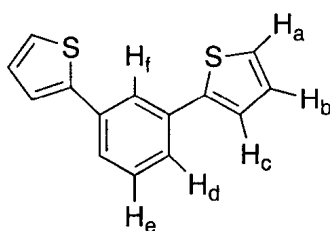


Scheme 2.1: General syntheses of thienylbenzene “monomers” using Pd-catalyzed coupling reactions.

2.5.1 Kumada Couplings

2.5.1.1 1,3-bis(2'-thienyl)benzene (1)

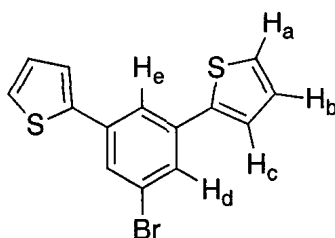
This compound was made according to Scheme 2.1 (a) ($E' = \text{MgBr}$; $n = 0$). In a 500 mL three-neck flask equipped with a bubbler, an orange suspension of 1,3-diiodobenzene (1.50 g, 4.55 mmol) and $\text{PdCl}_2(\text{dppf})$ (0.099 g, 0.137 mmol) in THF (15 mL) was added dropwise to an ice cold suspension of 2-thienylmagnesium bromide (0.17 M, 160 mL) in the same solvent to give a yellow slurry. This mixture was magnetically stirred at r.t. for 2 d before being hydrolyzed on ice with 1 M HCl (200 mL), followed by H_2O (100 mL). The aqueous layer was extracted with Et_2O (3×100 mL). The combined organic fractions were washed with saturated NaHCO_3 (50 mL), followed by H_2O (50 mL) before being dried over MgSO_4 and reduced to a dark brown liquid by rotatory evaporation. The desired product, a white microcrystalline solid, was obtained by flash column chromatography using petroleum ether as eluent ($R_f = 0.4$). mp. (lit) 83 – 85 °C (85 – 86 °C). Yield: 0.880 g (73 %).



^1H NMR: δ 7.13 (dd, 2H, H_b , $^3J_{\text{HH}} = 3.5$, $^3J_{\text{HH}} = 5.1$), 7.34 (dd, 2H, H_a/H_c , $^3J_{\text{HH}} = 5.1$, $^4J_{\text{HH}} = 1.2$), 7.40 (dd, 2H, H_a/H_c , $^3J_{\text{HH}} = 3.5$, $^4J_{\text{HH}} = 1.2$), 7.42 (d, 1H, H_e , $^3J_{\text{HH}} = 7.9$), 7.56 (dd, 2H, H_d , $^3J_{\text{HH}} = 7.9$, $^4J_{\text{HH}} = 1.6$), 7.88 (pt, 1H, H_f). $^{13}\text{C}\{^1\text{H}\}$ NMR: δ 123.7, 123.8, 125.4, 128.3, 129.7, 135.3, 144.2 (one quaternary carbon atom not observed). HRMS: $\text{C}_{14}\text{H}_{10}\text{S}_2$ calcd (found): 242.0224 (242.0223). ^1H NMR data for this compound were the same as those reported in the literature.¹⁷ The $^{13}\text{C}\{^1\text{H}\}$ NMR data were not reported, however.

2.5.1.2 1-bromo-3,5-bis(2'-thienyl)benzene (**7^{Br}**)

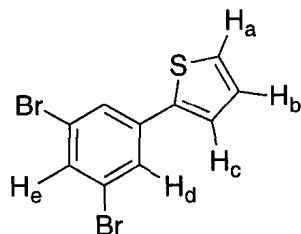
This compound was made in a manner similar to the protocol outlined in Section 2.5.1.1, with a slight modification - the reaction mixture was heated to 60 °C overnight. Thus, an orange solution containing 1,3,5-tribromobenzene (3.90 g, 0.129 mol) in dry THF (100 mL) and solid PdCl₂(dppf) (0.09 g, 0.124 mmol) were added to a suspension of 2-thienylmagnesium bromide (0.08 M, 330 mL) in the same solvent. Following work-up, the desired product, a white fluffy solid (mp. 73 – 74°C), was obtained by flash column chromatography (neat hexanes, R_f = 0.2). Yield 1.85 g (46 %).



¹H NMR: δ 7.11 (dd, 2H, H_b, ³J_{HH} = 3.6, ³J_{HH} = 4.8), 7.35 (m, 4H, H_a and H_c), 7.66 (pd, 2H, H_d), 7.73 (pt, 1H, H_e). ¹³C{¹H} NMR: δ 122.4, 123.6, 124.5, 126.1, 127.8, 128.4, 137.0, 142.5. HRMS: C₁₄H₉BrS₂ calcd (found): 319.9329 (319.9332).

2.5.1.3 1,3-dibromo-5-(2'-thienyl)benzene (**5^{Br}**)

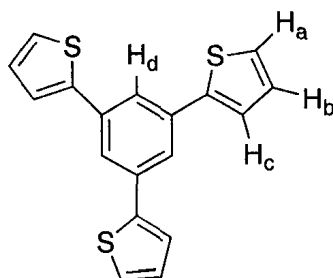
This compound, a white crystalline material (mp. 56 – 59 °C), was isolated using column chromatography (neat hexanes, R_f = 0.6) as a byproduct of the synthesis of 1-bromo-3,5-bis(2'-thienyl)benzene (Section 2.5.1.2). Yield: 0.38 g (10 %).



^1H NMR: δ 7.09 (dd, 1H, H_b , $^3J_{\text{HH}} = 3.8$, $^3J_{\text{HH}} = 5.0$), 7.31 (pdd, 1H, H_a/H_c), 7.35 (pdd, 1H, H_a/H_c), 7.56 (pt, 1H, H_e), 7.67 (pd, 2H, H_d). $^{13}\text{C}\{^1\text{H}\}$ NMR: δ 123.6, 124.9, 126.7, 127.7, 128.5, 132.8, 138.0, 141.2. HRMS: $\text{C}_{10}\text{H}_6\text{Br}_2\text{S}$ calcd (found): 315.8557 (315.8567).

2.5.1.4 1,3,5-tris(2'-thienyl)benzene (3)

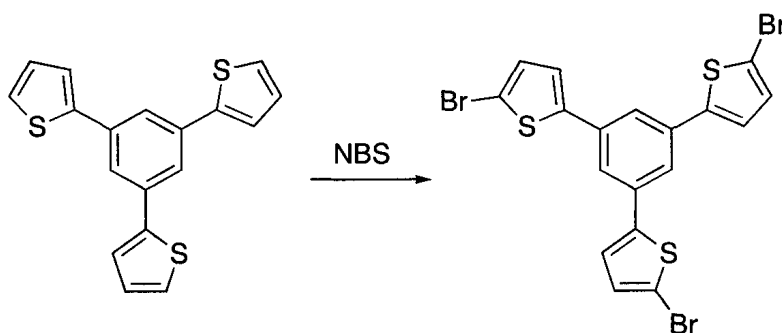
This compound was made in a manner similar to the protocol outlined in Section 2.5.1.1 and according to Scheme 2.1 (b) ($\text{E}' = \text{MgBr}$; $n = 0$). Thus, reaction of a THF (100 mL) solution of 1,3,5-triiodobenzene (1.34 g, 2.94 mmol) and solid $\text{PdCl}_2(\text{dppf})$ (0.064 g, 0.088 mmol) with a suspension of 2-thienylmagnesium bromide (0.117 M, 150 mL) in the same solvent gave, after workup and purification by flash column chromatography (20:1 hexanes: CHCl_3 , $R_f = 0.3$), the desired product as a white crystalline solid, mp. (lit.) 160 – 162 $^\circ\text{C}$ (156 – 158 $^\circ\text{C}$). Yield: 0.820 g (86 %).



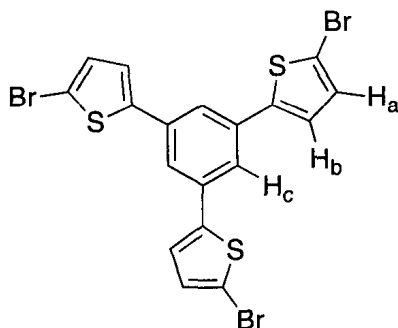
^1H NMR: δ 7.15 (dd, 3H, H_b , $^3J_{\text{HH}} = 3.6$, $^3J_{\text{HH}} = 5.1$), 7.36 (dd, 3H, H_a/H_c , $^3J_{\text{HH}} = 5.1$, $^4J_{\text{HH}} = 1.2$), 7.43 (dd, 3H, H_a/H_c , $^3J_{\text{HH}} = 3.6$, $^4J_{\text{HH}} = 1.2$), 7.76 (s, 3H, H_d). $^{13}\text{C}\{^1\text{H}\}$ NMR:

δ 123.0, 124.1, 125.7, 128.4, 135.9, 143.8. HRMS: $C_{18}H_{12}S_3$ calcd (found): 324.0101 (324.0112). The spectroscopic data for this compound were the same as those reported in the literature.¹⁷

2.5.1.5 1,3,5-tris(2'-bromo-5'-thienyl)benzene



This compound was made according to published procedure.¹⁸ In a 10 mL round bottom flask, *N*-bromosuccinamide was added portion-wise over 30 min to an ice-cold solution of 1,3,5-tris(2'-thienyl)benzene (0.100 g, 0.309 mmol) dissolved in a 1:1 mixture of $CHCl_3$:HOAc (8 mL). Once the addition was complete, the ice bath was removed and the mixture was stirred overnight at r.t.. The volume of the crude reaction mixture was reduced to *ca.* 2 mL and hexanes (10 mL) were added to give the desired product as a white solid. This was filtered and washed with H_2O (10 mL) and acetone (10 mL). Yield: 0.093 g (54 %).



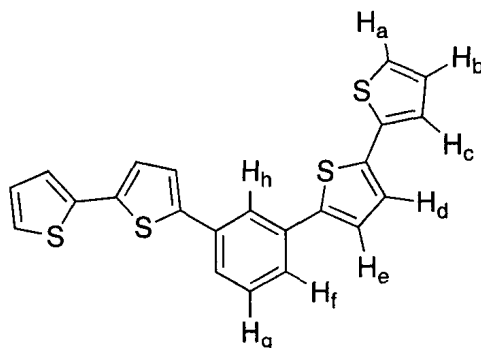
^1H NMR: δ 7.08 (pdd, 3H, H_a/H_b), 7.13 (pdd, 3H, H_a/H_b), 7.53 (ps, 3H, H_c).

$^{13}\text{C}\{^1\text{H}\}$ NMR: δ 112.7, 122.4, 124.5, 131.2, 135.5, 144.6. HRMS: $\text{C}_{18}\text{H}_9\text{Br}_3\text{S}_3$ calcd (found): 557.7417 (557.7412). ^1H NMR data for this compound were the same as those reported in the literature.¹⁸ The $^{13}\text{C}\{^1\text{H}\}$ NMR data were not reported, however.

2.5.2 Stille Couplings

2.5.2.1 1,3-bis{5'-(2',2''-bithienyl)}benzene (2)

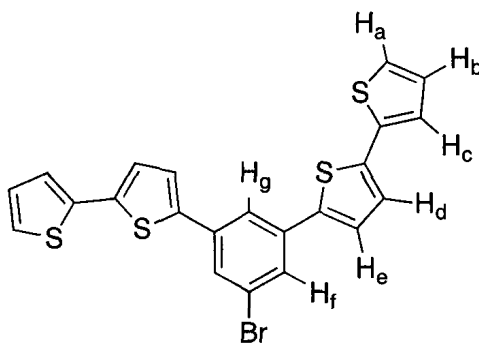
This compound was made according to Scheme 2.1 (a) ($\text{E}' = \text{SnBu}_3$, $n = 1$). In a 250 mL three-neck flask equipped with a condenser, a yellow solution of 5'-tributylstannyl-2,2'-bithiophene (2.08 g, 4.58 mmol) in toluene (5 mL) was added to an orange suspension containing 1,3-diiodobenzene (0.504 g, 1.53 mmol) and $\text{PdCl}_2(\text{dppf})$ (0.100 g, 0.777 mmol) in the same solvent (50 mL). This gave a pale brown suspension, which was brought to reflux for 3 d. The dark brown reaction mixture was then cooled under a slow flow of Ar and hydrolyzed with H_2O (50 mL). The aqueous layer was extracted with Et_2O (3×50 mL). The combined organic fractions were washed with an aqueous solution of KF (3×50 mL), dried over MgSO_4 and evaporated to dryness to give a yellow solid. The desired product, a yellow powder, was obtained by flash column chromatography using petroleum ether as eluent ($R_f = 0.2$), mp. 168 – 172 °C. Yield: 0.528 g (71 %).



^1H NMR: δ 7.05 (dd, 2H, H_b , $^3J_{\text{HH}} = 3.6$, $^3J_{\text{HH}} = 5.0$), 7.18 (d, 2H, H_d/H_e , $^3J_{\text{HH}} = 3.6$), 7.24 (m, 4H, H_a and H_c), 7.30 (d, 2H, H_d/H_e , $^3J_{\text{HH}} = 3.6$), 7.40 (t, 1H, H_g , $^3J_{\text{HH}} = 6.8$), 7.52 (dd, 2H, H_f , $^3J_{\text{HH}} = 7.2$, $^4J_{\text{HH}} = 2.0$), 7.8 (pt, 1H, H_h). $^{13}\text{C}\{^1\text{H}\}$ NMR: δ 122.97, 123.99, 124.39, 124.753, 125.01, 128.13, 129.78, 135.00, 137.33, 137.54, 142.69. HRMS: $\text{C}_{22}\text{H}_{14}\text{S}_4$ calcd (found): 405.9978 (405.9968). The spectroscopic data for this compound were the same as those reported in the literature.¹⁸ Crystals of this compound suitable for X-ray diffraction analysis were grown at 4 °C from CH_2Cl_2 /hexane over a period of two weeks.

2.5.2.2 1-bromo-3,5-bis{5'-(2',2''-bithienyl)}benzene (8^{Br})

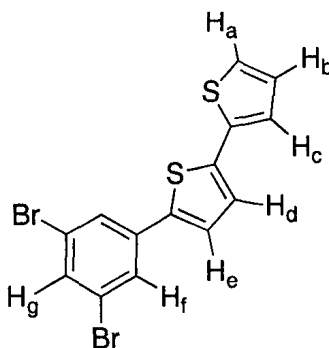
This compound was made in a manner similar to the protocol outlined in Section 2.5.2.1. Thus, 5'-tributylstannyl-2,2'-bithiophene (3.26 g, 7.17 mmol) was dissolved in the minimum toluene and added to an orange solution of 1,3,5-tribromobenzene (1.12 g, 3.58 mmol) in the same solvent (75 mL). The catalyst, $\text{PdCl}_2(\text{dppf})$ (0.079 g, 0.107 mmol), was then added to give a brown mixture. Work up and purification by flash column chromatography (neat hexanes, $R_f = 0.1$), gave the desired product as a fluffy yellow solid (mp. 175 – 179 °C). Yield: 0.302 g (27 %).



^1H NMR: δ 7.05 (dd, 2H, H_b , $^3J_{\text{HH}} = 3.6$, $^3J_{\text{HH}} = 5.2$), 7.18 (d, 2H, H_d/H_e , $^3J_{\text{HH}} = 3.8$), 7.24 (m, 4H, H_a and H_c), 7.29 (d, 2H, H_d/H_e , $^3J_{\text{HH}} = 3.8$), 7.64, (pd, 2H, H_f), 7.69 (pt, 1H, H_g). $^{13}\text{C}\{^1\text{H}\}$ NMR: δ 101.5, 110.0, 124.3, 124.8, 125.1, 125.2, 127.4, 128.2, 132.4 (3 quaternary carbon atoms not observed). HRMS: $\text{C}_{22}\text{H}_{13}\text{BrS}_4$ calcd (found): 483.9083 (483.9082).

2.5.2.3 1,3-dibromo-5-{5'-(2',2''-bithienyl)}benzene (6^{Br})

This compound, a pale yellow solid (mp. 139 – 143 °C), was isolated using column chromatography (neat hexanes, $R_f = 0.4$), as a byproduct of the synthesis of 1-bromo-3,5-bis{5'-(2',2''-bithienyl)}benzene (Section 2.4.2.2). Yield: 0.038 g (4 %).

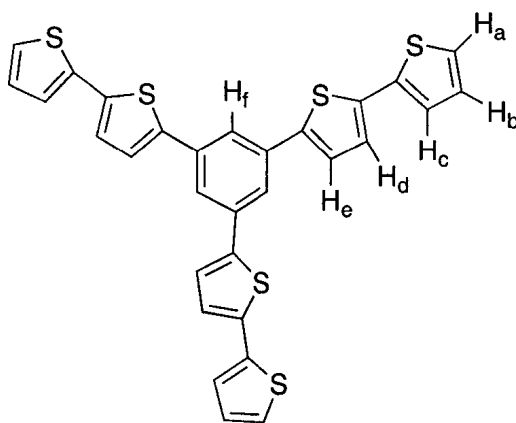


^1H NMR: δ 7.05 (pt, 1H, H_b), 7.15 (d, 1H, H_d/H_e , $^3J_{\text{HH}} = 3.2$), 7.23 (m, 3H, H_a and H_c and H_d/H_e), 7.55 (pd, 1H, H_g), 7.65 (pd, 2H, H_f). $^{13}\text{C}\{^1\text{H}\}$ NMR: δ 123.6, 124.4, 124.9, 125.2, 125.6, 127.3, 128.2, 132.8, 137.6 (4 quaternary carbon atoms not observed). HRMS:

C₁₀H₆Br₂S₂ calcd (found): 397.8434 (397.8433). ¹H NMR data for this compound were the same as those reported in the literature.¹¹ The ¹³C{¹H} NMR data were not reported, however.

2.5.2.4 1,3,5-tris{5'-(2',2''-bithienyl)}benzene (4)

This compound was made in a manner similar to the protocol outlined in Section 2.5.2.1 and according to Scheme 2.1 (b) (E' = SnBu₃; n = 1). In a 100 mL three-neck flask equipped with a condenser, 1,3,5-triiodobenzene (0.184 g, 0.402 mmol) and PdCl₂(dppf) (0.062 g, 0.048 mmol) were dissolved in toluene (25 mL) prior to the dropwise addition of 5'-tributylstannyl-2,2'-bithiophene (1.10 g, 2.42 mmol) in toluene (15 mL). Following work-up, the desired product, a yellow powder, was obtained by purification using flash column chromatography (neat hexanes, R_f = 0.1). mp. (lit) 210 – 214 °C (136 °C). Yield: 0.92 g (18 %).



¹H NMR: δ 7.06 (dd, 3H, H_b, ³J_{HH} = 5.0, ³J_{HH} = 3.6), 7.20 (dd, 3H, H_d/H_e, ³J_{HH} = 3.4, ³J_{HH} = 1.0), 7.25 (m, 6H, H_a/H_c), 7.34 (dd, 3H, H_d/H_e, ³J_{HH} = 3.4, ³J_{HH} = 1.0), 7.71 (s, 3H, H_f). ¹³C{¹H} NMR: δ 122.1, 124.1, 124.8, 124.8, 128.2, 135.7, 137.5, 137.7, 142.2. HRMS: C₃₀H₁₈S₆ calcd (found): 569.9733 (569.9740). ¹H NMR (DMSO-*d*₆,

399.76 MHz): δ 7.09 (dd, 1H, H_b, $^3J_{\text{HH}} = 3.6$, $^3J_{\text{HH}} = 5.0$), 7.36 (d, 1H, H_e, $^3J_{\text{HH}} = 3.9$), 7.38 (dd, 1H, H_d, $^3J_{\text{HH}} = 3.9$, $^5J_{\text{HH}} = 1.2$), 7.52 (dd, 1H, H_c, $^3J_{\text{HH}} = 5.0$, $^5J_{\text{HH}} = 1.2$), 7.77 (d, 1H, H_a, $^3J_{\text{HH}} = 3.6$), 7.79 (s, 1H, H_f). ^1H NMR data for this compound were the same as those reported in the literature.¹⁷ The $^{13}\text{C}\{^1\text{H}\}$ NMR data were not reported, however. Crystals of this compound suitable for X-ray diffraction analysis were grown at 4 °C from CH_2Cl_2 /hexane over a period of two weeks.

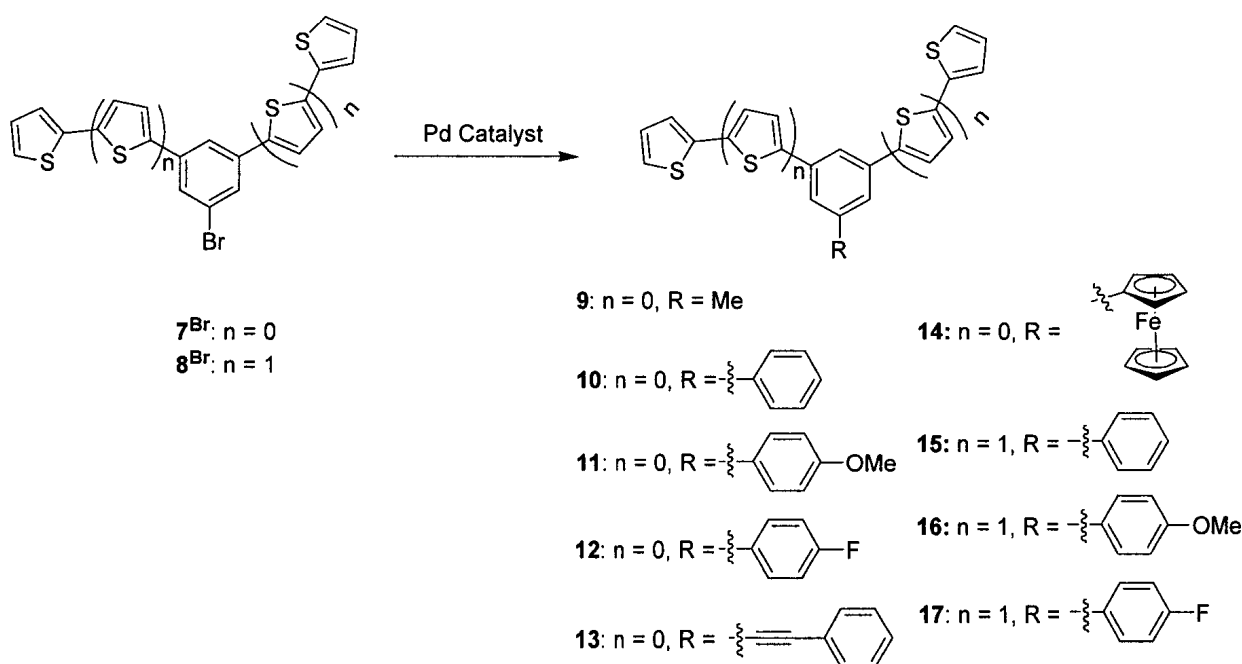
2.5.3 Suzuki Coupling

2.5.3.1 1,3,5-tris{5'-(2',2''-bithienyl)}benzene (4)

The title compound was also made according to Scheme 2.1 (b) ($\text{E}' = \text{B}(\text{OH})_2$; $n = 1$). In a 250 mL three-neck flask equipped with a condenser, $\text{Pd}(\text{OAc})_2$ (0.014 g, 0.063 mmol), PPh_3 (0.050 g, 0.190 mmol) and an aqueous solution of Na_2CO_3 (1 M, 3.6 mL) were added to a pale yellow solution of 2,2'-bithienyl-5'-boronic acid (0.381 g, 1.81 mmol) and 1,3,5-triiodobenzene (0.207 g, 0.453 mmol) in THF (100 mL). The resulting green solution was brought to reflux for 3 d. The brown solution was removed from heat, cooled under a slow flow of N_2 and quenched on ice with H_2O (100 mL). Dichloromethane (50 mL) was added and the aqueous layer was extracted with the same solvent (3×50 mL). The organic layers were combined, dried over MgSO_4 and the solvent was evaporated to give a light brown solid. The desired product, a yellow powder, was obtained *via* flash column chromatography (98:2 hexanes: CH_2Cl_2 , $R_f = 0.1$). Yield: 0.234 g (90 %). ^1H and $^{13}\text{C}\{^1\text{H}\}$ NMR data were the same as those reported in Section 2.5.2.4.

2.6 Onward Reaction of Bromothienylbenzene Monomers

The bromothienylbenzene compounds **7^{Br}** and **8^{Br}** were further reacted with various electron donating and withdrawing groups (Scheme 2.2) using Kumada, Stille or Sonogashira coupling reactions.



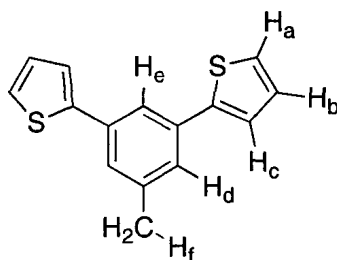
Scheme 2.2: General reaction scheme for the syntheses of **9** – **17**.

2.6.1 Kumada Coupling

2.6.1.1 1-methyl-3,5-bis(2'-thienyl)benzene (**9**)

The title compound was made in a manner similar to the protocol outlined in Section 2.5.1.2 and according to Scheme 2.2 ($n = 0$; $R = \text{Me}$). Thus, a 3.0 M solution of methylmagnesium bromide (0.621 mL, 1.86 mmol) in Et_2O and solid $\text{PdCl}_2(\text{dppf})$ (0.027 g, 0.037 mmol) were added to an ice cold solution of 1-bromo-3,5-bis(2'-thienyl)benzene in the same solvent (100 mL) to give an orange solution. Work-up and

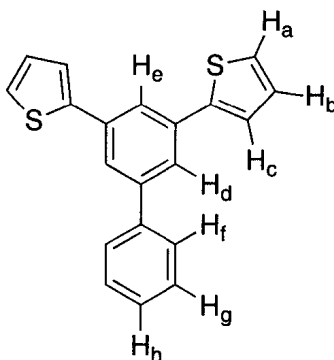
purification by flash column chromatography (neat hexanes, $R_f = 0.2$) gave the desired product as a white solid (mp. 55 – 57 °C). Yield: 0.0824 g (52 %).



^1H NMR: δ 2.44 (s, 3H, H_f), 7.11 (dd, 2H, H_b , $^3J_{HH} = 3.6$, $^3J_{HH} = 5.2$), 7.31 (d, 2H, H_a/H_c , $^3J_{HH} = 5.2$), 7.37 (m, 4H, H_a/H_c and H_d), 7.67 (s, 1H, H_e). $^{13}\text{C}\{^1\text{H}\}$ NMR: δ 21.7, 121.1, 123.61, 125.2, 126.2, 128.2, 135.2, 139.4, 144.3. HRMS: $\text{C}_{15}\text{H}_{12}\text{S}_2$ calcd (found): 256.0380 (256.0376).

2.6.1.2 1-phenyl-3,5-bis(2'-thienyl)benzene (10)

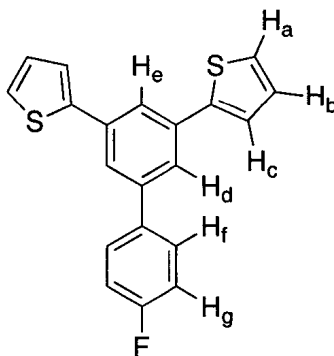
This compound was made in a manner similar to the protocol outlined in Section 2.5.1.2 and according to Scheme 2.2 ($n = 0$; $R = \text{phenyl}$). Thus, a 3.0 M solution of phenylmagnesium bromide (0.775 mL, 2.32 mmol) in THF and solid $\text{PdCl}_2(\text{dppf})$ (0.034 g, 0.047 mmol) were added to an ice cold solution of 1-bromo-3,5-bis(2'-thienyl)benzene (0.500 g, 1.55 mmol) in the same solvent (100 mL) to give an orange solution. The desired product was isolated as a white solid (mp. 133 – 135 °C), following work-up and purification by flash column chromatography (neat hexanes, $R_f = 0.1$). Yield: 0.334 g (68 %).



^1H NMR: δ 7.13 (dd, 2H, H_b , $^3J_{\text{HH}} = 3.6$, $^3J_{\text{HH}} = 4.8$), 7.34 (dd, 2H, H_a/H_c , $^3J_{\text{HH}} = 4.8$, $^4J_{\text{HH}} = 1.0$), 7.43 (m, 3H, H_h and H_a/H_c), 7.50 (t, 2H, H_g , $^3J_{\text{HH}} = 7.6$), 7.67 (dd, 2H, H_f , $^3J_{\text{HH}} = 7.6$, $^4J_{\text{HH}} = 1.6$), 7.74 (pd, 2H, H_d), 7.83 (pt, 1H, H_e). $^{13}\text{C}\{^1\text{H}\}$ NMR: δ 122.8, 123.9, 124.36, 125.5, 127.5, 128.0, 128.3, 129.1, 135.8, 140.9, 142.9, 144.1. HRMS: $\text{C}_{20}\text{H}_{14}\text{S}_2$ calcd (found): 318.0537 (318.0536).

2.6.1.3 1,1'-(4'-fluorophenyl)-3,5-bis(2''-thienyl)benzene (12)

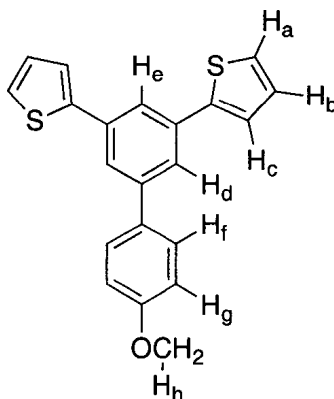
This compound was made in a manner similar to the protocol outlined in Section 2.5.1.2 and according to Scheme 2.2 ($n = 0$; $\text{R} = 4\text{-fluorophenyl}$). Thus, a 0.5 M THF solution of 4-fluorophenylmagnesium bromide (1.89 mL, 1.87 mmol) and solid $\text{PdCl}_2(\text{dppf})$ (0.027 g, 0.037 mmol) were added to an ice cold solution of 1-bromo-3,5-bis(2'-thienyl)benzene (0.400 g, 1.24 mmol) in THF (100 mL) to give an orange solution. Work-up and purification by flash column chromatography (20:1 hexanes: CH_2Cl_2 , $R_f = 0.2$) gave the desired product as a white solid (mp. 95 – 98 °C). Yield: 0.350 g (84 %).



^1H NMR: δ 7.16 (m, 4H, H_b and H_f/H_g), 7.35 (dd, 2H, H_a/H_c , $^3J_{\text{HH}} = 5.2$, $^4J_{\text{HH}} = 1.2$), 7.43 (dd, 2H, H_a/H_c , $^3J_{\text{HH}} = 3.6$, $^4J_{\text{HH}} = 1.2$), 7.63 (m, 2H, H_f/H_g), 7.67 (pd, 2H, H_d), 7.82 (pt, 1H, H_e). $^{13}\text{C}\{^1\text{H}\}$ NMR: δ 116.0, 122.7, 124.1, 125.6, 128.4, 129.1, 135.9, 136.9, 141.9, 144.0, 161.7, 164.2. HRMS: $\text{C}_{20}\text{H}_{13}\text{FS}_2$ calcd (found): 336.0443 (336.0437).

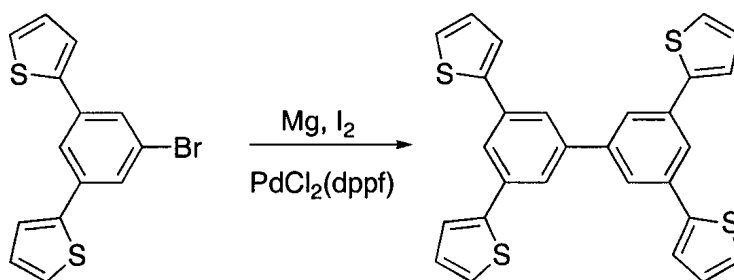
2.6.1.4 1,1'-(4'-methoxyphenyl)-3,5-bis(2''-thienyl)benzene (11)

This compound was made in a manner similar to the protocol outlined in Section 2.5.1.2 and according to Scheme 2.2 ($n = 0$; $\text{R} = 4\text{-methoxyphenyl}$). To a colorless ice-cold solution of 1-bromo-3,5-bis(2'-thienyl)benzene (0.400 g, 1.24 mmol) in THF (100 mL), a 0.5 M THF solution of 4-methoxyphenylmagnesium bromide (3.72 mL, 1.87 mmol) and solid $\text{PdCl}_2(\text{dppf})$ (0.027 g, 0.037 mmol) were added to give a bright red solution. Following work-up and purification by flash column chromatography (5:2 hexanes: CH_2Cl_2 , $R_f = 0.4$), the desired product was isolated as a white solid (mp. 121 – 123 $^\circ\text{C}$). Yield: 0.225 g (52 %).



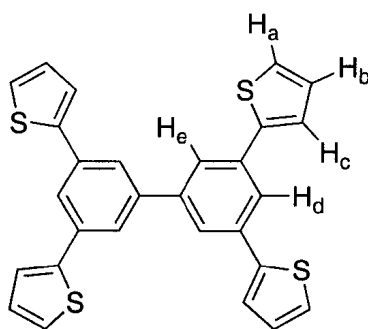
^1H NMR: δ 3.88 (s, 3H, H_h), 7.03 (m, 2H, H_f/H_g), 7.13 (dd, 2H, H_b, $^3J_{\text{HH}} = 5.2$, $^3J_{\text{HH}} = 3.6$), 7.34 (dd, 2H, H_a/H_c, $^3J_{\text{HH}} = 1.2$, $^3J_{\text{HH}} = 5.2$), 7.42 (dd, 2H, H_a/H_c, $^3J_{\text{HH}} = 1.2$, $^3J_{\text{HH}} = 3.6$), 7.61 (m, 2H, H_f/H_g), 7.69 (pd, 2H, H_d), 7.78 (pt, 1H, H_e). $^{13}\text{C}\{^1\text{H}\}$ NMR: δ 55.6, 114.5, 122.2, 123.8, 124.0, 125.4, 128.3, 128.6, 133.3, 135.7, 142.5, 144.2, 159.8. HRMS: C₂₁H₁₆OS₂ calcd (found): 348.0643 (348.0644).

2.6.1.5 1,1',5,5'-tetra(2''-thienyl)-3,3'-biphenyl (18)



In a flame-dried 50 mL, 3-neck round bottom flask, 1-bromo-3,5-di(2'-thienyl)benzene (0.600 g, 1.86 mmol) was dissolved in THF (20 mL) and solid Pd(dppf)Cl₂ (0.014 g, 0.019 mmol) was added to give an orange mixture. Magnesium turnings (0.022 g, 0.931 mmol) and a few iodine crystals were then added. After holding the mixture at reflux overnight, there was no visible reaction. Therefore, MeI (100 μL , 0.309 mmol)

was added, and the Mg dissolved within minutes. The reaction mixture was heated to reflux for 18 h before being quenched on ice with H₂O (10 mL). Workup was the same as outlined Section 2.5.1.1. The desired product, a white solid (mp. 148 – 155 °C) was obtained following flash column chromatography (neat hexanes, R_f = 0.1). Yield: 0.112 g (25 %).

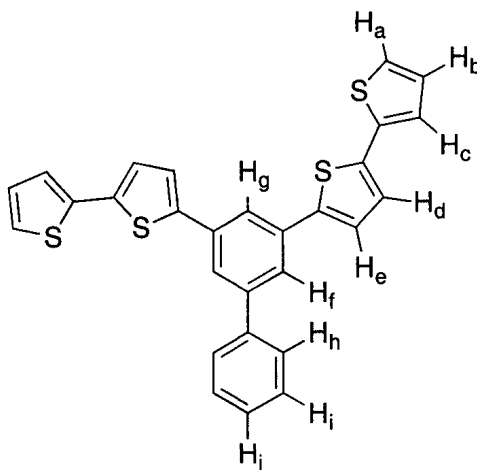


¹H NMR: δ 7.15 (dd, 4H, H_b, ³J_{HH} = 5.0, ³J_{HH} = 3.6), 7.36 (dd, 4H, H_a/H_c, ³J_{HH} = 5.0, ⁴J_{HH} = 1.0), 7.45 (dd, 4H, H_a/H_c, ³J_{HH} = 3.6, ⁴J_{HH} = 1.0), 7.77 (pd, 4H, H_d), 7.90 (pt, 2H, H_e).
¹³C{¹H} NMR: δ 123.2, 124.1, 124.4, 125.7, 128.4, 135.9, 142.4, 143.9. HRMS: C₂₈H₁₈S₄ calcd (found): 482.0291 (482.0290).

2.6.1.6 1-phenyl-3,5-bis{5'-(2',2''-bithienyl)}benzene (15)

This compound was made in a manner similar to the protocol outlined in Section 2.5.1.2 and according to Scheme 2.2 (n = 1; R = phenyl). A 3.0 M solution of phenylmagnesium bromide (0.173 mL, 0.519 mmol) and solid PdCl₂(dppf) (0.008 g, 0.010 mmol) were added to an ice-cold solution yellow solution of 1-bromo-3,5-bis{5'-(2',2''-bithienyl)}benzene (0.100 g, 0.346 mmol) in THF (20 mL) to give an orange mixture.

Workup and purification by flash column chromatography (neat hexanes, $R_f = 0.1$) gave the desired product as a pale yellow solid (mp. 134 – 138 °C). Yield: 0.109 g (68 %).



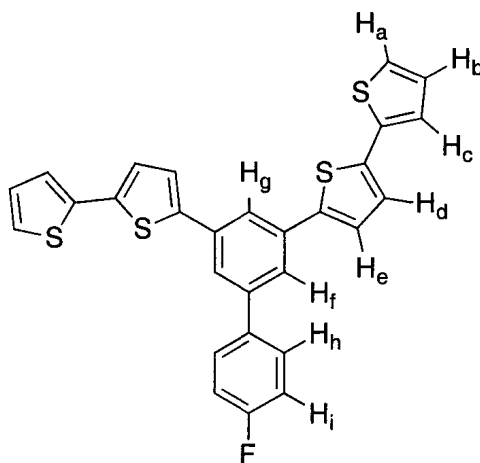
^1H NMR: δ 7.05 (dd, 2H, H_b , $^3J_{\text{HH}} = 5.2$, $^3J_{\text{HH}} = 3.6$), 7.20 (d, 2H, H_d/H_e , $^3J_{\text{HH}} = 3.6$), 7.24 (m, 4H, H_a and H_c), 7.35 (d, 2H, H_d/H_e , $^3J_{\text{HH}} = 3.6$), 7.42 (t, 1H, H_j , $^3J_{\text{HH}} = 7.2$), 7.50 (t, 2H, H_h , $^3J_{\text{HH}} = 7.2$), 7.67 (d, 2H, H_i , $^3J_{\text{HH}} = 7.2$), 7.71 (pd, 2H, H_f), 7.79 (pt, 1H, H_g).
 $^{13}\text{C}\{^1\text{H}\}$ NMR: δ 121.9, 124.0, 124.1, 124.6, 124.7, 124.8, 127.5, 128.1, 128.2, 129.1, 135.5, 137.4, 137.5, 140.7, 142.6, 143.1. HRMS: $\text{C}_{28}\text{H}_{18}\text{S}_4$ calcd (found): 482.0291 (482.0285).

2.6.1.7 1,1'-(4'-fluorophenyl)-3,5-bis{5''-(2'',2'''-bithienyl)}benzene (17)

This compound was made in a manner similar to the protocol outlined in Section 2.5.1.2 and according to Scheme 2.2 ($n = 1$; $\text{R} = 4\text{-fluorophenyl}$). To an ice cold yellow solution of 1-bromo-3,5-bis{5''-(2'',2'''-bithienyl)}benzene (0.100 g, 0.346 mmol) in THF (20 mL), a 0.5 M solution of 4-fluorophenylmagnesium bromide (1.04 mL, 0.519 mmol) and $\text{PdCl}_2(\text{dppf})$ (0.008 g, 0.010 mmol) were added to give an orange solution. The desired product, a pale yellow solid (mp. 154 – 157°C), was obtained following workup

and purification by flash column chromatography (10:1 hexanes:CH₂Cl₂, R_f = 0.3).

Yield: 0.123 g (71 %).

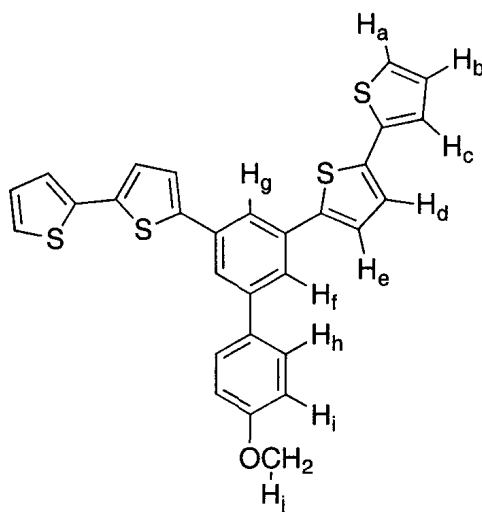


¹H NMR: δ 7.05 (dd, 2H, H_b, ³J_{HH} = 5.2, ³J_{HH} = 3.6), 7.19 (d, 4H, H_d/H_e and H_h/H_i), 7.26 (m, 4H, H_a and H_c), 7.34 (d, 2H, H_d/H_e, ³J_{HH} = 3.6), 7.64 (m, 4H, H_d/H_e and H_f), 7.77, (pt, 1H, H_g). ¹³C{¹H} NMR: δ 115.9, 116.1, 121.9, 123.8, 124.1, 124.7, 124.8, 128.2, 129.1, 129.2, 135.6, 136.8, 137.5, 137.6, 142.1, 142.4. HRMS: C₂₈H₁₇FS₄ calcd (found): 500.0197 (500.0208).

2.6.1.8 1,1'-(4'-methoxyphenyl)-3,5-bis{5''-(2'',2'''-bithienyl)}benzene (16)

This compound was made in a manner similar to the protocol outlined in Section 2.5.1.2 and according to Scheme 2.2 (n = 1; R = 4-methoxyphenyl). To an ice cold yellow solution of 1-bromo-3,5-bis{5'- (2'',2'''-bithienyl)}benzene (0.146 g, 0.5 mmol) in THF (20 mL), a 0.5 M solution of 4-methoxyphenylmagnesium bromide (1.52 mL, 0.758 mmol) and PdCl₂(dppf) (0.011 g, 0.015 mmol) were added to give a bright red solution. The desired product, a light yellow solid (mp. 144 – 147 °C), was obtained

following workup and purification by flash column chromatography (3:1 hexanes:CH₂Cl₂, R_f = 0.2). Yield: 0.090 g (35 %).



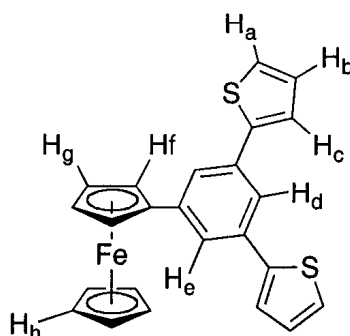
¹H NMR: δ 3.89 (s, 3H, H_j), 7.04 (m, 4H, H_b and H_h/H_i), 7.19 (d, 2H, H_d/H_e, ³J_{HH} = 3.8), 7.24 (m, 4H, H_a/H_c), 7.33 (d, 2H, H_d/H_e, ³J_{HH} = 3.8), 7.61 (m, 2H, H_h/H_i), 7.67 (pd, 2H, H_f), 7.74 (pt, 1H, H_g). ¹³C{¹H} NMR: δ 55.6, 110.0, 114.6, 121.4, 123.6, 124.0, 124.5, 124.7, 124.8, 128.1, 128.5, 133.1, 135.4, 137.4, 137.6, 142.6, 142.7. HRMS: C₂₉H₂₀OS₄ calcd (found): 512.0397 (512.0390).

2.6.2 Stille Coupling

2.6.2.1 1-ferrocenyl-3,5-bis(2'-thienyl)benzene (14)

The title compound was made according to Scheme 2.2 (n = 0; R = ferrocenyl). In a 100 mL, flame-dried three neck flask, a dark red solution of tributylstannylferrocene (0.612 g, 1.3 mmol) in THF (2 mL) was added to a colorless solution of 1-bromo-3,5-bis(2'-thienyl)benzene (0.278 g, 0.865 mmol) in THF (30 mL) to give an orange mixture. Following the addition of PdCl₂(dppf) (0.018 g, 0.026 mmol), the mixture was brought to reflux for 2 d. The resulting dark brown solution was cooled under a stream of Ar. The

reaction was quenched with H₂O (10 mL), solid KF (2 eq) was added, and the mixture was stirred for 2 h. Ether (15 mL) was then added and the aqueous layer was extracted with the same solvent (2 × 15 mL). The combined organic fractions were washed with H₂O (10 mL), dried over MgSO₄, and reduced to give a dark red liquid. The crude product was purified by flash column chromatography (20:1 hexanes:CH₂Cl₂) to obtain the desired product as a dark orange liquid. Yield: 0.033 g (8 %).



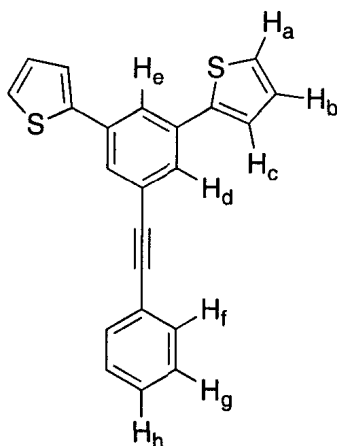
¹H NMR: δ 4.10 (s, 5H, H_h), 4.37 (pt, 2H, H_g/H_f), 4.72 (pt, 2H, H_g/H_f), 7.14 (dd, 2H, H_b, ³J_{HH} = 3.6, ³J_{HH} = 5.2), 7.34 (dd, 2H, H_a/H_c, ³J_{HH} = 5.2, ⁴J_{HH} = 1.2), 7.41 (dd, 2H, H_e, ³J_{HH} = 3.6, ⁴J_{HH} = 1.2), 7.63 (pd, 2H, H_e), 7.67 (pt, 1H, H_d). ¹³C{¹H} NMR: δ 67.1, 69.4, 70.0, 85.0, 121.7, 123.3, 123.7, 125.3, 128.3, 135.3, 141.2, 144.3 (two quaternary carbon atoms not observed). HRMS: C₂₄H₁₈FeS₂ calcd (found): 426.0199 (426.0189).

2.6.3 Sonogashira Coupling

2.6.3.1 1,1'-(2'-phenylacetylene)-3,5-bis(2''-thienyl)benzene (13)

In a 50 mL three-neck flask equipped with a condenser and bubbler, 1-bromo-3,5-bis(2'-thienyl)benzene (0.253 g, 0.786 mmol) was dissolved in a 1:1 mixture of THF:Et₃N (10 mL). The catalyst mixture, Pd(PPh₃)₂Cl₂ (0.028 g, 0.039 mmol) and CuI (0.015 g, 0.008 mmol), was added to this solution to give an orange suspension. Phenylacetylene

(0.120 g, 1.18 mmol) was added dropwise over 5 min to give a dark brown mixture. Once the addition was complete, the mixture was heated to 60 °C for 24 h. The dark brown suspension was cooled, CH₂Cl₂ was added and the mixture was filtered through Celite. The filtrate was reduced to give a black viscous liquid. The product, a white solid (mp. 118 – 120 °C), was isolated by flash column chromatography (neat hexanes, R_f = 0.3). Yield: 0.227 g (68 %).



¹H NMR: δ 7.13 (dd, 2H, H_b, ³J_{HH} = 3.6, ³J_{HH} = 5.0), 7.35 (dd, 2H, H_a/H_c, ³J_{HH} = 5.0), 7.41 (m, 5H, H_a/H_c, H_f/H_g and H_h), 7.63 (m, 2H, H_f/H_g), 7.70 (pd, 2H, H_d), 7.80 (pt, 1H, H_e). ¹³C{¹H} NMR: δ 88.9, 90.3, 123.2, 123.5, 124.1, 124.8, 125.7, 128.1, 128.4, 128.6, 128.8, 132.0, 135.5, 143.3. HRMS: C₂₂H₁₄S₂ calcd (found): 426.0199 (426.0189).

2.7 References

- (1) Debad, J. D.; Morris, J. C.; Magnus, P.; Bard, A. J. *J. Org. Chem.* **1997**, *62*, 530.
- (2) Hartley, F. R. *Organomet. Rev. A* **1976**, *6*, 119.
- (3) Hayashi, T.; Konishi, M.; Kobori, Y.; Kumada, M.; Higuchi, T.; Hirotsu, K. *J. Am. Chem. Soc.* **1984**, *106*, 158.
- (4) Lin, P.-Y.; Shi, S.-J.; Hsu, F.-L. *Syn. Comm.* **1999**, *29*, 1911.
- (5) Pham, C. H.; Mark Jr., H. B.; Zimmer, H. *Syn. Comm.* **1986**, *16*, 689.
- (6) Hagemann, O.; Jorgensen, M.; Krebs, F. C. *J. Org. Chem.* **2006**, *71*, 5546.
- (7) Keegstra, M. A.; Brandsma, L. *Synthesis* **1988**, 890.
- (8) Tamao, K.; Kodama, S.; Nakajima, I.; Kumada, M.; Minato, A.; Suzuki, K. *Tetrahedron* **1982**, *38*, 3347.
- (9) Pham, C. V.; Burkhardt, A.; Shabana, R.; Cunningham, D. D.; Mark Jr., H. B.; Zimmer, H. *Phosphorus, Sulfur and Silicon* **1989**, *46*, 153.
- (10) Friedman, D. C. S.; Friedman, F. *J. Mol. Struc.-Theochem* **1995**, *33*, 71.
- (11) Obara, S.; Tada, K. 2004; WO 2004/009669 A1.
- (12) Cherioux, F.; Guyard, L. *Adv. Funct. Mater.* **2001**, *11*, 305.
- (13) Pinault, T.; Cherioux, F.; Therrien, B.; Suss-Fink, G. *Heteroatom Chemistry* **2004**, *15*, 121.
- (14) Hark, R. R.; Hauze, D. H.; Petrovskaja, O.; Joullie, M. M. *Can. J. Chem.* **2001**, *79*, 1632.
- (15) Guillaneux, D.; Kagan, H. B. *J. Org. Chem.* **1995**, *60*, 2502.
- (16) Gan, Z.; Roy, R. *Can. J. Chem.* **2002**, *80*, 908.

- (17) Pelter, A.; Jenkins, I.; Jones, D. E. *Tetrahedron* **1997**, *53*, 10357.
- (18) Mitchell, W. J.; Kopidakis, N.; Rumbles, G.; Ginley, D. S.; Shaheen, S. E.
J. Mater. Chem. **2005**, *15*, 4518.

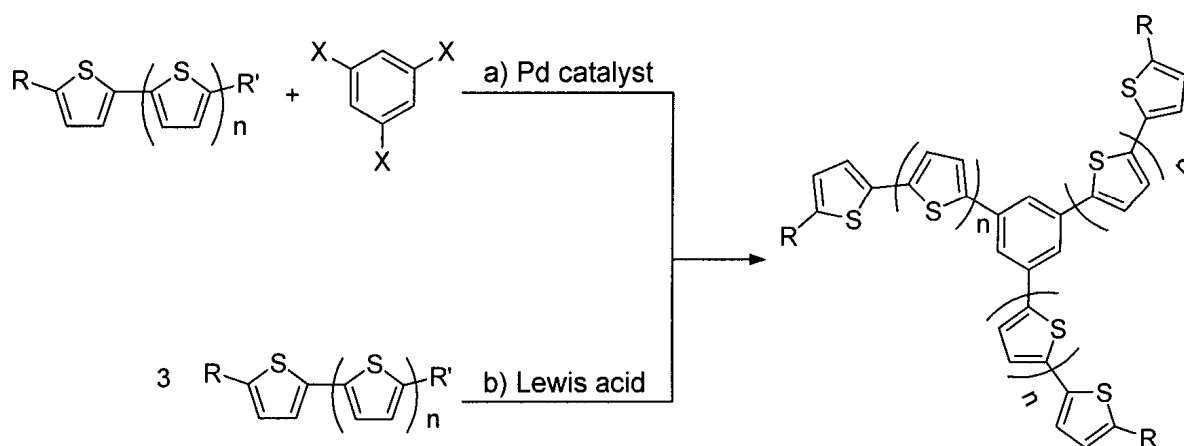
3 C₃ – Symmetric Thienyl Benzenes and Related Compounds

3.1 General Introduction

Star-shaped, benzene core conjugated dendrimers ($\leq G_2$) containing thiophene repeating units have slowly emerged in the literature over the last decade. These materials are potentially very useful because they possess both the attractive structural characteristics unique to dendrimers (Section 1.2, p.5) and the optoelectronic properties of thiophenes. Similar to linear oligothiophenes, the electronic and spectroscopic properties of these materials can, in principle, be tuned either by the introduction of substituents into the oligothiophene linker (*e.g.*, a metal or another aromatic group) or by variation of the linker's length. An increase in length would result in enhanced conjugation and a bathochromic shift in the absorption and emission maxima. In contrast to the synthesis of poly(thiophene), which is generally made by electropolymerization, these dendrimeric materials can be synthesized with size reproducibility using synthetic organic techniques to produce well-defined and monodispersed macromolecules.

Although these materials are potentially very useful, there have been few reports of conjugated thiophene dendrimers due to the difficulty of their synthetic preparation. Star-shaped, 1,3,5-tri(oligothienyl)benzenes have conventionally been made *via* two general synthetic routes: (i) Pd-catalyzed cross-coupling reactions between 1,3,5-tribromobenzene and a substituted oligothiophene; and (ii) cyclotrimerization reactions (*e.g.*, of 5'-acetylthiophene) (Scheme 3.1). The main advantage of the latter type of reaction is that fewer products are formed (*i.e.*, the intended 1,3,5-tri(thienyl)benzene and the dimerized intermediate, (*E*)- β -methylchalcone, when 5'-acetylthiophene is used). Therefore, purification of the crude reaction mixture by column chromatography would

be simpler in principle than that of the crude mixture of a coupling reaction where the production of three different compounds (mono-, di- and tri-substituted benzenes) is possible. The cyclotrimerization reaction has, however, been reported for the synthesis of the core (G0). Elaboration of this core would be increasingly difficult as successive generations were added. A higher yielding, reliable route to these materials is therefore desired.



Scheme 3.1: Synthetic approaches to C_3 -symmetric thienyl benzenes. a) Pd-catalyzed cross coupling reaction: $n = 0$ or 1 , $R = H$ or alkyl, $R' =$ coupling reaction precursor, $X = Br$ or I ; b) Cyclotrimerization reaction: $n = 0$ or 1 , $R = Br$ or alkyl, $R' =$ acetyl, nitrovinyl or ethynyl.

The syntheses of 1,3-bis- (**1**) and 1,3,5-tris(2'-thienyl)benzene (**3**), and 1,3-bis- (**2**) and 1,3,5-tris{5'-(2',2''-thienyl)benzene (**4**) (Chart 3.1) have been reported previously using various Pd-catalyzed coupling reactions and, in the case of **3** and **4**, cyclotrimerization reactions (*vide infra*). Reported synthetic routes generally use high catalyst loadings, harsh reaction conditions and sometimes require starting materials that are not easily synthesized (*e.g.*, 2-thienyl-5-boronic acid). Thus, our motivation was to develop a novel, high yielding synthetic route to obtain **1** – **4**. Ideally, this route would

require low catalyst loadings, mild reaction conditions and use commercially available starting materials. Although compounds **1** and **2** are not C_3 -symmetric, they were synthesized in order to compare the physical and optical properties of phenyl compounds containing either two (**1** and **2**) or three (**3** and **4**) thiophene substituents.

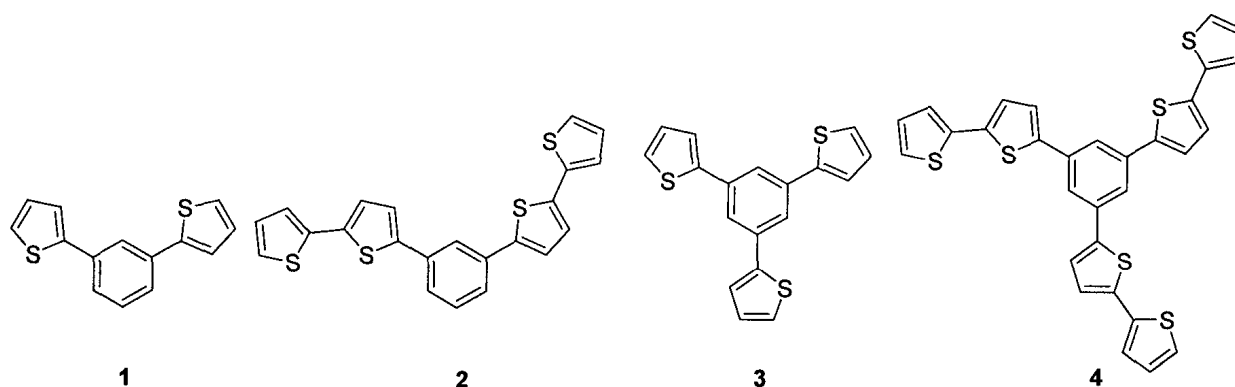


Chart 3.1: Target thienylbenzene compounds.

3.2 Syntheses of Compounds **1**, **2**, **3** and **4**

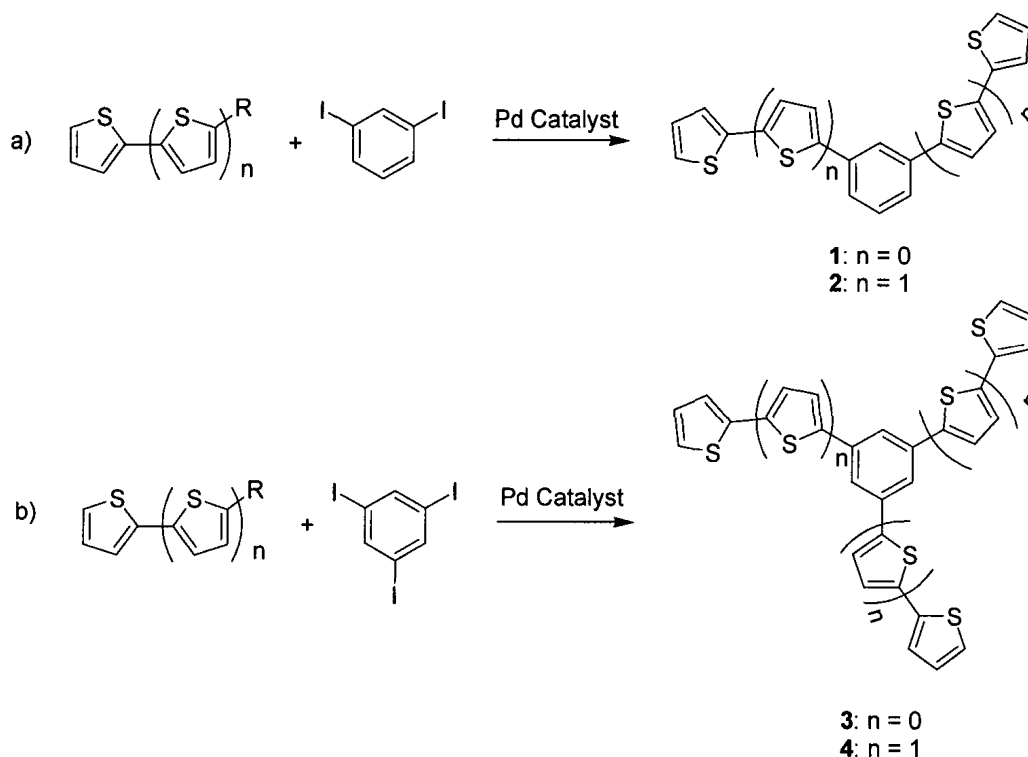
See Experimental Section 2.5, p. 33.

3.3 Results and Discussion

3.3.1 Syntheses of 1,3-bis- and 1,3,5-tris(2'-thienyl)benzene

We found that Kumada cross-coupling reactions between either 1,3-di- or 1,3,5-triiodobenzene and 2-thienylmagnesium bromide using $\text{PdCl}_2(\text{dppf})$ (dppf = 1,1'-bis(diphenylphosphino)ferrocene) as catalyst gave 1,3-bis(2'-thienyl)benzene (**1**) or 1,3,5-tris(2'-thienyl)benzene (**3**) in 80 % or 86 % yield, respectively (Scheme 3.2). These reactions used only slight excesses of the thienyl starting material (5:1 Grignard

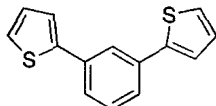
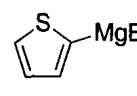
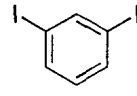
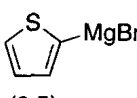
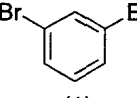
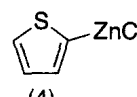
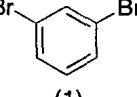
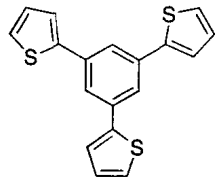
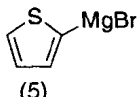
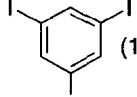
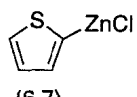
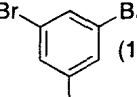
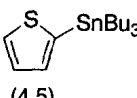
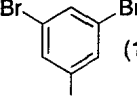
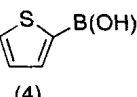
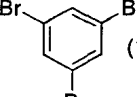
reagent:triiodobenzene) and low catalyst loadings (3 mol %), and were conducted under mild synthetic conditions (r.t. for 48 h). Furthermore, the Grignard reagent, 2-thienylmagnesium bromide, was easily obtained from the reaction of 2-bromothiophene and Mg turnings and could be used without purification.



Scheme 3.2: Pd-catalyzed cross-coupling reactions to obtain compounds **1** – **4**.

Other reported Pd-catalyzed syntheses of **1** and **3** involved the coupling of 1,3-diiodo- or 1,3,5-tribromobenzene and 2-thienyl zinc, boron or tin reagents in Negishi, Suzuki and Stille reactions, respectively. A summary of the reagents, reaction conditions and isolated yields are given in Table 3.1. In almost every case, the metallated coupling reagent was relatively straightforward to prepare, but always required a pre-lithiation step (*e.g.*, 2-tributylstannylthiophene was generated from 2-lithiothiophene and tributylstannyl chloride).

Table 3.1: Syntheses of 1,3-bis- (1) and 1,3,5-tris(2'-thienyl)benzene (3) via Ni- or Pd-catalyzed cross-coupling reactions.

Target	Reaction Type	Reagents (equiv.)	Catalyst (loading/mol %)	Reaction Conditions	Isolated Yields (%)	Reference
 1	Kumada	 	PdCl ₂ (dppf) (3)	r.t., 48 h	80	This work
	Kumada	 	NiCl ₂ (dppp) ^a (2)	reflux, 24 h	81	2
	Negishi	 	Ni(PPh ₃) ₂ Cl ₂ (10)	50 °C, 12h	65	3
 3	Kumada	 	PdCl ₂ (dppf) (3)	r.t., 48 h	86	This work
	Negishi	 	Pd(PPh ₃) ₄ (1)	50 °C, 48 h	60	3
	Stille	 	PdCl ₂ (PPh ₃) ₂ (6.5)	90 °C, 65 h	47	4
	Suzuki	 	Pd(OAc) ₂ / PPh ₃ (2/6)	85 °C, 1.3 h	90	5

^adppp = 1,3-bis(diphenylphosphino)propane

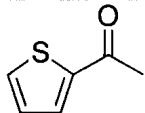
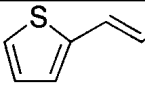
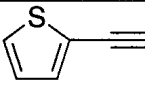
Sato *et al.*² obtained **1** in a yield comparable to that reported for our Kumada reaction (81 % vs. 80%, respectively). However in their synthesis, 2-thienylmagnesium bromide was coupled to 1,3-dibromobenzene and NiCl₂(dppp) was used as catalyst. Furthermore, the reported Kumada coupling involved refluxing an ethereal solution over 24 h whereas our coupling reaction involved milder reaction conditions and longer reaction times (r.t., 48 h). Our Kumada coupling reaction has not been attempted under these reaction conditions; however, it is believed that higher reaction temperatures could lead to a more efficient coupling reaction and to higher yields for this synthesis.

The Suzuki cross-coupling reaction reported by Obara and Tada⁶ gave the highest known yield of **3** (90 %) in the shortest reaction time. It should be noted, however, that in our hands the synthesis of 2-thienyl-5-boronic acid was very unreliable. We attempted to make this starting material several times but could never isolate it. Similar results were found with the synthesis of 2,2'-dithienyl-5'-boronic acid (Section 3.3.2, p.64).

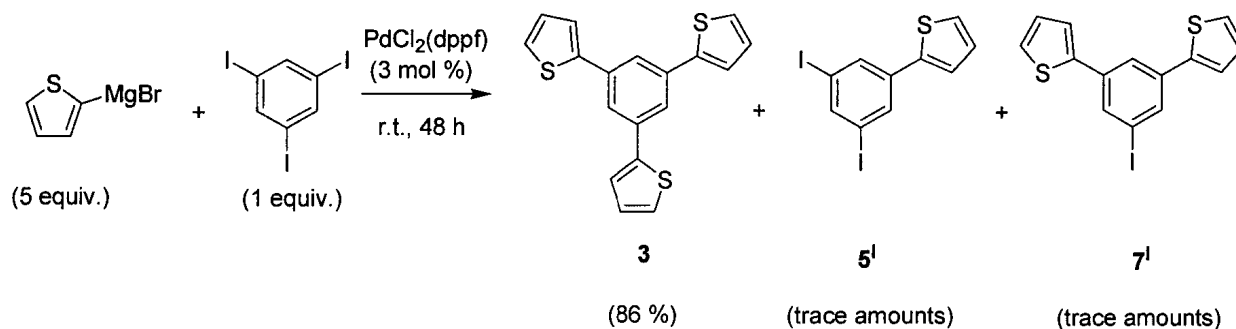
The synthesis of **3** has also been reported using various types of cyclotrimerization reactions (Table 3.2). For example, Cherioux *et al.*¹ have reported the triple ketolization and dehydration of 2-acetylthiophene (and of 5'-acetyl-2,2'-bithiophene, Section 3.3.2, p.64) in the presence of a mixture of tetrachlorosilane (TCS) and ethanol (5:1) to obtain **3** in 70% yield (Table 3.2, entry 1). The overall yield (starting from thiophene) of our Kumada coupling reaction was significantly higher than that of this cyclotrimerization (86 % vs. 56 %). Variations on this synthesis have also been reported by other groups.^{7,8} These include cyclotrimerization reactions of trans-2-(2'-nitrovinyl)thiophene in the presence of an initiator (*e.g.*, NaOAc) or of 2-

ethynylthiophene in the presence of TaCl₅ and CCl₄, which gave **3** in moderate (66%) and poor (15%) yields (Table 3.2, entries 2 and 3).^{9,10}

Table 3.2: Syntheses of 1,3,5-tris(2'-thienyl)benzene (**3**) *via* cyclotrimerization reactions.

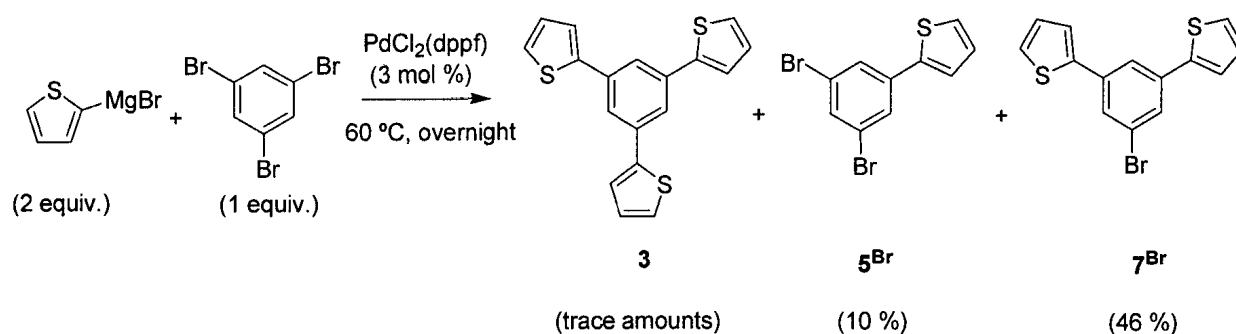
Entry	Reagents	Reaction Conditions	Yield (%)	Reference
1	 TCS/EtOH	r.t., 18 h	70	1,11,12
2	 NaOAc	90 °C, 20 h	66	9,10
3	 TaCl ₅ /CCl ₄	r.t., 1 h	15	13

Our Pd-catalyzed synthesis of **3** gave predominantly the intended product, but also trace quantities of 1,3-diiodo-5-(2'-thienyl)benzene (**5^I**) and 1-iodo-3,5-bis(2'-thienyl)benzene (**7^I**) (Scheme 3.3). The reaction mixture was separated by flash column chromatography using neat hexanes as the eluent. This separation was extremely time consuming; efforts to decrease time requirements by increasing the polarity of the eluent (*i.e.*, 5 % CH₂Cl₂ in hexanes) led to streaking of the compounds and poor separation of the intended product.



Scheme 3.3: Pd-catalyzed coupling of 2-thienylmagnesium bromide and 1,3,5-triiodobenzene to give **3**, **5^I** and **7^I**.

Compound **7^I**, which has previously been considered only as an unwanted side-product, is potentially a very useful compound in its own right because it offers both chemical (*i.e.*, I) and electrochemical handles (*i.e.*, thiophene) for onward manipulation (Chapter 4, p.90). Therefore, the Kumada reaction was optimized to favor the production of the disubstituted product. We reasoned that 1,3,5-tribromobenzene would be a better starting material than 1,3,5-triiodobenzene for the production of mixed (halo)(thienyl)benzenes because arylbromides generally react more sluggishly than aryl iodides in Pd-catalyzed coupling reactions and would therefore make controlled partial substitution more feasible. Thus, **7^{Br}** was produced in the highest yield (46 %) when a 2:1 ratio of 2-thienylmagnesium bromide and 1,3,5-tribromobenzene was used, and the reaction mixture was heated gently overnight (60 °C) in the presence of PdCl₂(dppf) catalyst (Scheme 3.4). Compounds **3** and **5^{Br}** were also formed in this reaction and their presence was confirmed by TLC. However, due to the difficulty associated with separation of these products, only **5^{Br}** was also isolated as a pure compound (10 % yield).



Scheme 3.4: Pd-catalyzed coupling of 2-thienylmagnesium bromide and 1,3,5-triiodobenzene to give **3**, **5^{Br}** and **7^{Br}**.

3.3.2 Syntheses of 1,3-bis- and 1,3,5-tris{5'-(2',2''-bithienyl)}benzene

The Stille cross-coupling reactions between either 1,3-di- or 1,3,5-triiodobenzene and 5'-tributylstannyl-2,2'-bithiophene using PdCl₂(dppf) as the catalyst gave 1,3-bis{5'-(2',2''-bithienyl)}benzene (**2**) and 1,3,5-tris{5'-(2',2''-bithienyl)}benzene (**4**) in 83 % and 18 % yield, respectively (Scheme 3.2). These reactions used slight excesses of the bithienyl starting materials (3:1 5'-tributylstannyl-2,2'-bithiophene:1,3-diiodobenzene and 4.5:1 5'-tributylstannyl-2,2'-bithiophene:1,3,5-triiodobenzene) and low catalyst loadings (3 mol %). Although the stannyl reagent was straightforward to synthesize, purification by vacuum distillation required high temperature (~ 450 °C), and resulted in only moderate yields (76 %). Because the isolated yield of **4** was low, we investigated other possible synthetic routes to obtain this product (Table 3.3).

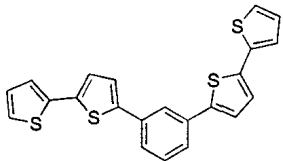
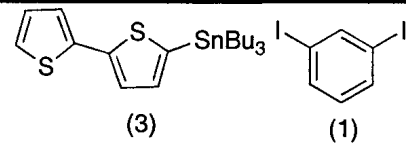
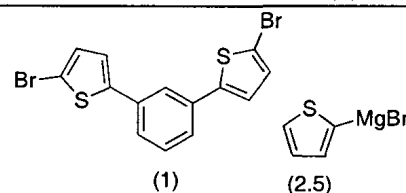
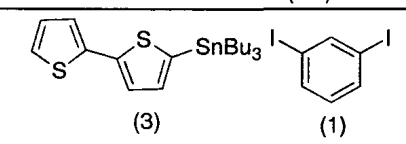
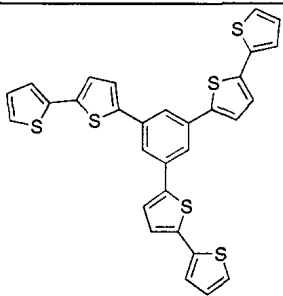
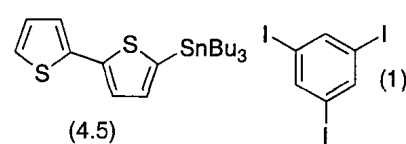
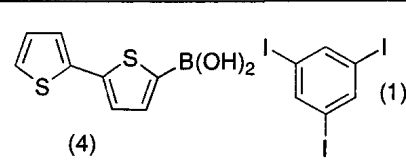
Inspired by the reported synthesis of 1,3,5-tris(2'-thienyl)benzene (**3**) by Obara and Tada,⁶ we applied the Suzuki cross-coupling reaction to the synthesis of **4**. In this reaction, 2,2'-dithienyl-5-boronic acid was coupled with 1,3,5-triiodobenzene in the presence of Pd(OAc)₂ (5 mol %) and PPh₃ to afford **4** in high yield (90 %). A novel modification to Obara and Tada's procedure was our use of 1,3,5-triiodobenzene instead of 1,3,5-tribromobenzene. This was thought to facilitate the reaction because oxidative addition of aryl iodides to Pd(0) is typically quicker than that of aryl bromides. Furthermore, the synthesis of 1,3,5-triiodobenzene was straightforward¹⁴ and gave reasonable yields (*ca.* 60 %). The disadvantage to this approach was that the synthesis of the boronic acid starting material proved to be very unreliable; on some occasions, no product was formed. Moreover, there was no reported method of purification of the acid. The crude mixture was therefore used in the Suzuki coupling reaction; this gave a

reaction mixture that was difficult to purify using flash chromatography. Although the Stille reaction was very low yielding by contrast, the metallated coupling reagent, 5'-tributylstannyl-2,2'-bithiophene, could be obtained relatively easily.

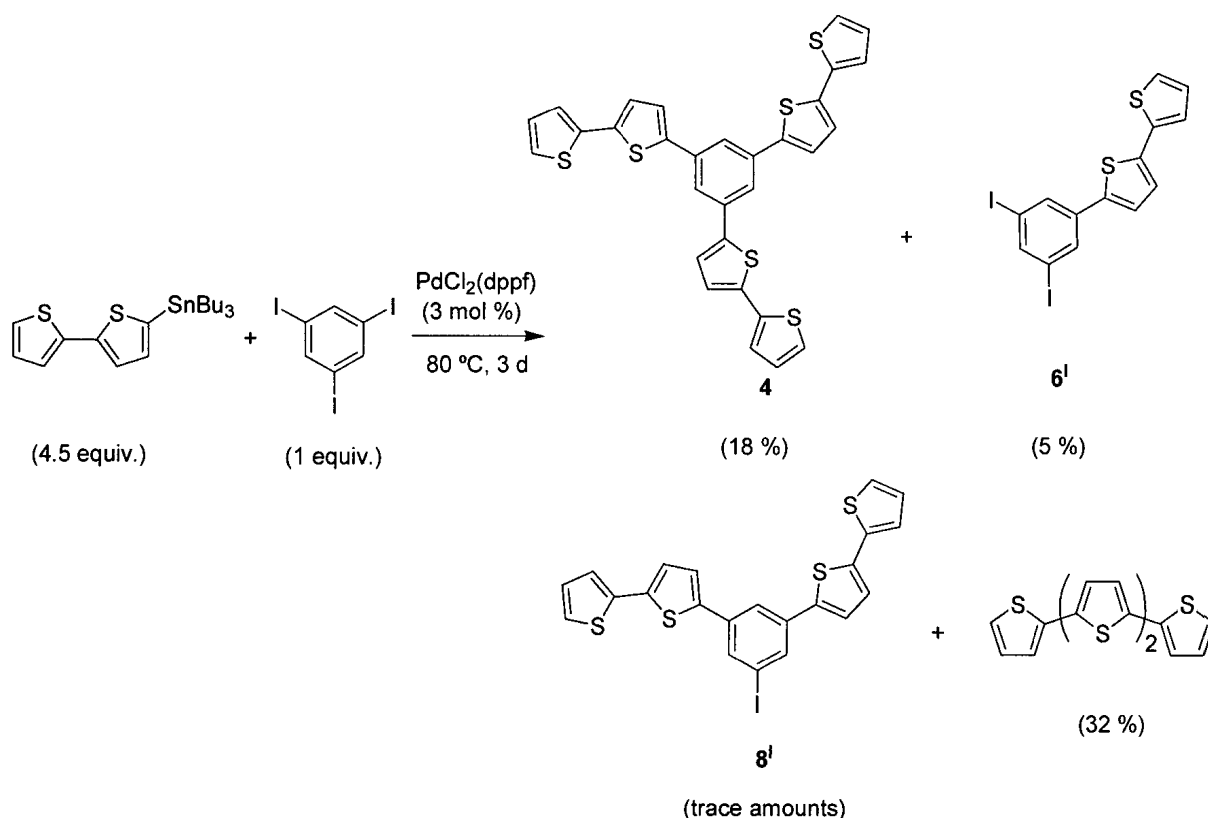
The synthesis of **4** has also been reported using cyclotrimerization reactions.^{1,8} It should be noted that this is the only reported synthetic route to obtain **4**. As stated previously, the advantage to this approach was that fewer products are formed. However, this cyclotrimerization reaction gave only moderate reported yields (56 – 65 %), and in our hands was wholly irreproducible. Various conditions were assayed but only starting material was isolated from the reaction mixtures.

As expected, the Stille coupling synthesis of **4** gave a mixture of products from which 1,3-diiodo-5-{5'-(2',2''-bithienyl)}benzene (**6^I**) and 1-iodo-3,5-bis{5'-(2',2''-bithienyl)}benzene (**8^I**) were also isolated in trace amounts (Scheme 3.5). Purification of **4** by flash column chromatography in neat hexanes was even more tedious than the purification of **3**. Efforts to decrease purification time by increasing eluent polarity (5 % CH₂Cl₂ in hexanes) led to contamination of all products with tetrathiophene, a by-product of the reaction, which appeared as yellow fluorescent streak overlapping the bands of **6^I** and **8^I** (purple fluorescent) on the TLC plate of the reaction mixture.

Table 3.3: Syntheses of 1,3-bis- (2) and 1,3,5-tris{5'-(2',2''-bithienyl)}benzene (4) *via* Ni- and Pd-catalyzed cross coupling reactions.

Target	Reaction Type	Reagents (equiv.)	Catalyst (loading/mol %)	Reaction Conditions	Isolated Yields (%)	Reference
 2	Stille	 (3) (1)	PdCl ₂ (dppf) (3)	80 °C, 3 d	83	This work
	Kumada	 (1) (2.5)	NiCl ₂ (dppp) ^a (2)	40 °C, 24 h	9	2
	Stille	 (3) (1)	PdCl ₂ (PPh ₃) ₂ (5)	80 °C, overnight	86	15
 4	Stille	 (4.5) (1)	PdCl ₂ (dppf) (3)	80 °C, 3 d	18	This work
	Suzuki	 (4) (1)	Pd(OAc) ₂ / PPh ₃ (8.5/25.5)	90 °C, 63 h	90	This work

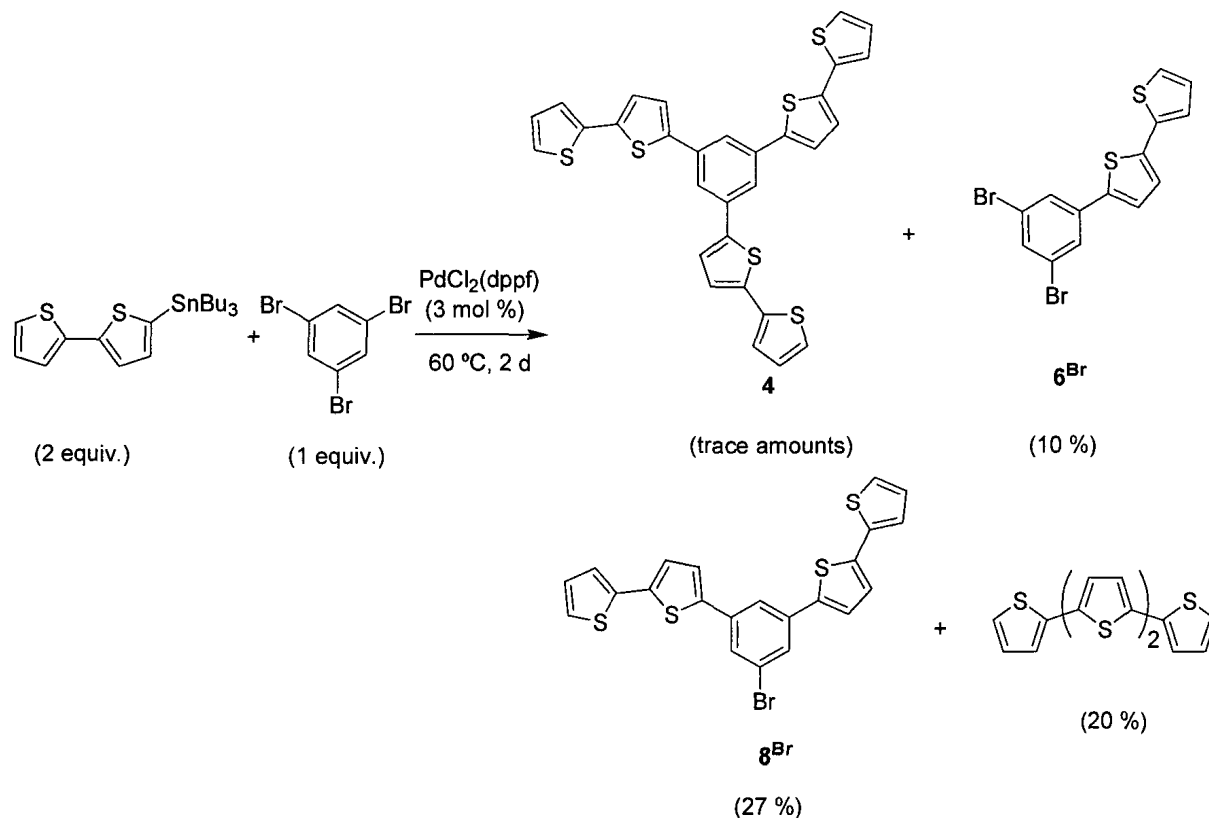
^adppp = 1,3-bis(diphenylphosphino)propane



Scheme 3.5: Pd-catalyzed coupling of 5'-tributylstannyl-2,2'-bithiophene and 1,3,5-triiodothiophene to give **4**, **6^I**, **8^I** and tetrathiophene.

Once again, the mixed (halo)(thienyl)benzenes are very useful compounds in their own rights. Therefore, the synthesis was optimized in order to favor the production of either **6** or **8**. When a 2:1 ratio of 5'-tributylstannyl-2,2'-bithiophene:1,3,5-tribromobenzene was used and the reaction mixture heated to 60°C for 48 h in the presence of $\text{PdCl}_2(\text{dppf})$ (3 mol %), the desired products were obtained in modest yields (**6^{Br}**, 10 % and **8^{Br}**, 27 %; Scheme 3.6). Again, 1,3,5-tribromobenzene was used in the optimization of these reactions, as it allowed for better control over the degree of substitution in the final product. The low isolated yields obtained for **4**, **6^{Br}** and **8^{Br}** were due to difficulty in separation of these compounds from tetrathiophene. No matter the

reaction conditions, all three substitution products were observed in the reaction mixture by TLC.



Scheme 3.6: Pd-catalyzed coupling of 5'-tributylstannyl-2,2'-bithiophene and 1,3,5-tribromothiophene to give **4**, **6^{Br}**, **8^{Br}** and tetrathiophene.

3.3.3 Crystal Structures

3.3.3.1 1,3-bis{5'-(2',2''-bithienyl)}benzene (**2**)

Crystals of **2** suitable for X-ray diffraction analysis were grown at $4\text{ }^\circ\text{C}$ from CH_2Cl_2 /hexanes over a period of two weeks. The solid-state structure of **2** was reasonably well defined, although the terminal thiophene rings on each bithiophene substituent were disordered. This was modeled by two coplanar rings (the major components were 0.759 and 0.885, respectively) with approximately the α C and S

being exchanged (Figure 3.1). The molecule was not planar and therefore did not possess extended conjugation in the solid state (Figure 3.2). In one of the two bithiophene substituents the torsion angle between the thiophene rings was 177° but in the other it was 153° . Selected bond distances and torsion angles are given in Table 3.4.

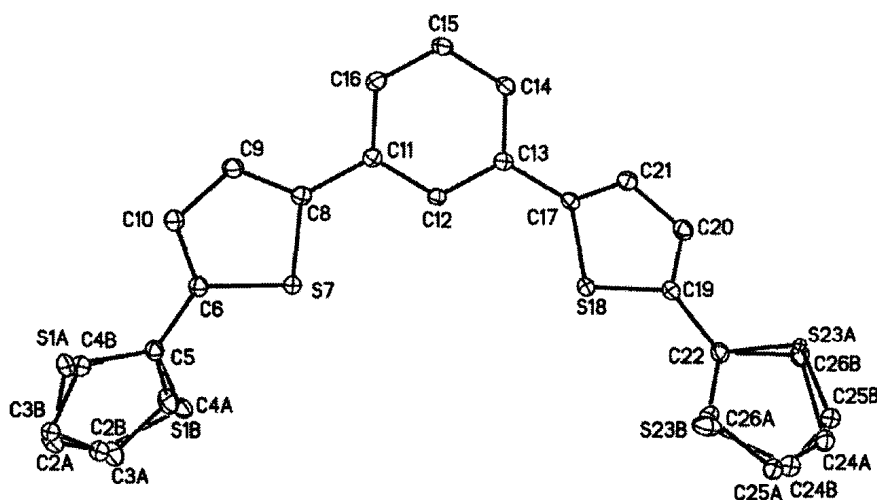


Figure 3.1: ORTEP representation of **2** (20 % ellipsoids). Hydrogen atoms have been omitted for clarity.

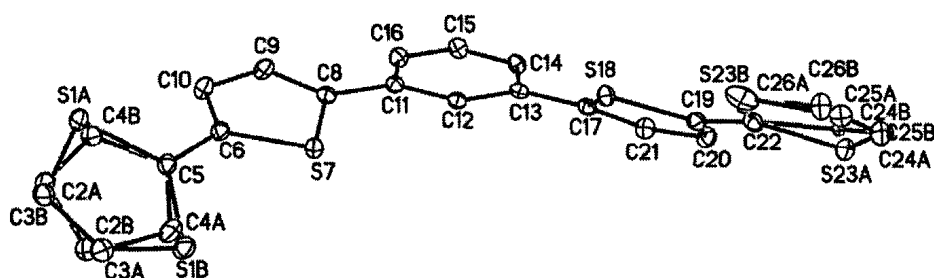


Figure 3.2: Alternative view of **2**.

Table 3.4: Selected bond distances (Å) and torsion angles ($^\circ$) for **2** with estimated standard deviations in parentheses.

C(3A)-C(4A)	1.416(12)	C20-C21	1.408(3)
C5-C6	1.462(3)	C(25A)-C(26A)	1.461(9)
C8-C11	1.468(3)	C(4A)-C5-C6-C10	152.7(8)
C10-C9	1.408(4)	S7-C8-C11-C12	-14.8(4)
C13-C17	1.463(3)	C12-C13-C17-S18	-34.4(4)
C19-C22	1.456(3)	C20-C19-C22-C(26A)	176.5(8)

3.3.3.2 1,3,5-tris{5'-(2',2''-bithienyl)}benzene (**4**)

Crystals of **4** suitable for X-ray diffraction analysis were likewise grown at 4 °C from CH₂Cl₂/hexanes over a period of two weeks. The solid-state structure of **4** had two crystallographically independent, but very similar, molecules in its unit cell. These differed in the orientation of one of the bithiophene substituents (Figure 3.3). Alternative views of molecules A and B are shown in Figure 3.4. Selected bond distances and torsion angles are found in Table 3.5.

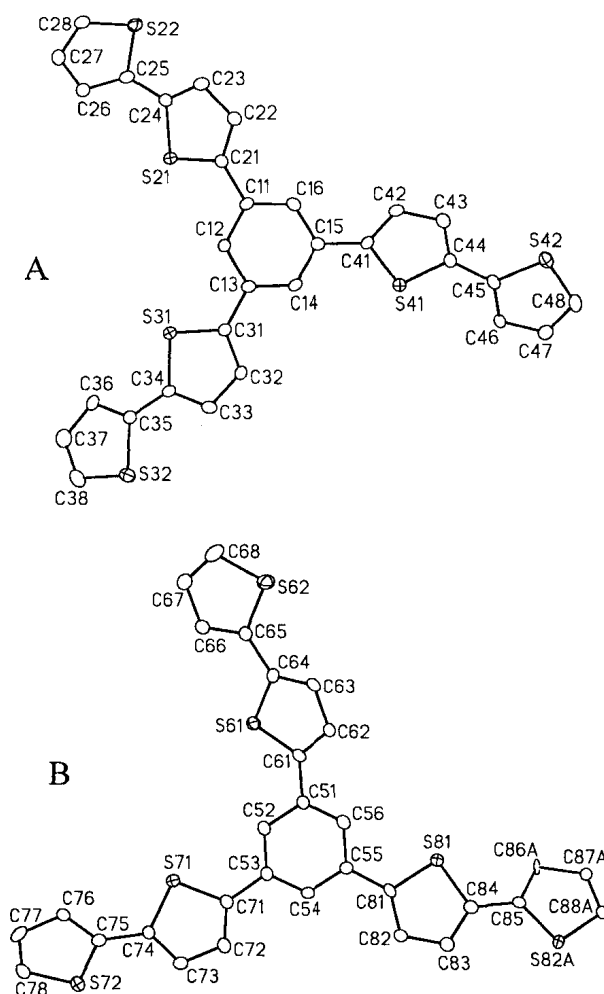


Figure 3.3: ORTEP representations of the two crystallographically independent molecules of **4** (20% ellipsoids). Hydrogen atoms have been omitted for clarity.

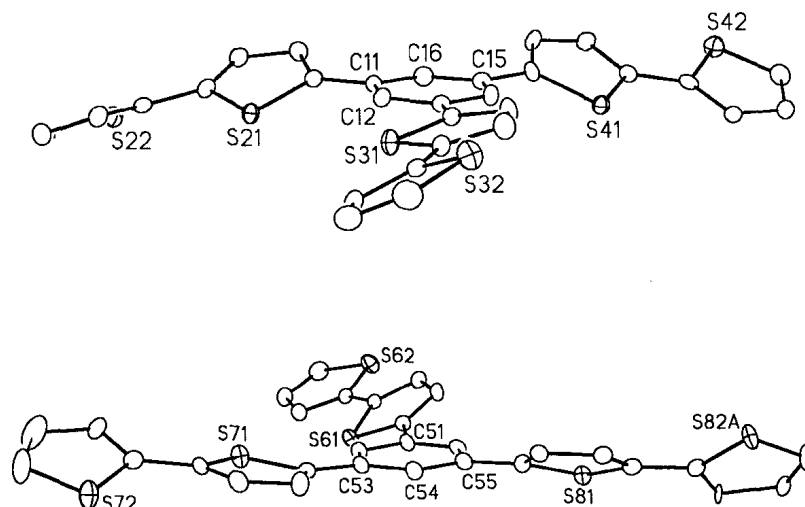


Figure 3.4: Alternative views of molecules A and B.

Table 3.5: Selected bond distances (Å) and torsion angles (°) for **4** with estimated standard deviations in parentheses.

C11-C21	1.466(8)	C42-C43	1.384(9)
C13-C31	1.461(8)	C44-C45	1.459(8)
C15-C41	1.467(9)	C46-C47	1.403(8)
C22-C23	1.414(9)	C12-C11-C21-S21	-24.1(9)
C24-C25	1.467(9)	C12-C13-C31-S31	14.2(9)
C26-C27	1.417(9)	C14-C15-C41-S41	26.5(9)
C32-C33	1.403(9)	C23-C24-C25-C26	-149.3(8)
C34-C35	1.451(8)	C33-C34-C35-C36	-166.3(7)
C36-C37	1.404(9)	C43-C44-C45-C46	178.8(7)

The solid-state structures of **2** and **4** shared some similarities: (i) neither of these molecules was planar overall; however, they both possessed one planar bithiophene substituent; (ii) they had similar bond lengths and angles; and (iii) the bithienyl units in **2** crystallized in essentially the same orientation as the invariable bithienyl units in **4**. However, in contrast to the structures of **2**, **4** contained two crystallographically independent molecules in its unit cell; only one of these showed disorder in the terminal

thiophene ring of one of the bithiophene substituents. Furthermore, there were 8 (4 sets of 2) molecules in the unit cell of **4** whereas the unit cell of **2** contained two molecules.

3.3.4 Electronic Spectroscopy

The mono-, di- and trisubstituted thienyl compounds were colourless (**3**, **5^{Br}** and **7^{Br}**) or very pale yellow (**4**, **6^{Br}** and **8^{Br}**), and displayed intensely blue-purple fluorescence. The absorption and fluorescence spectra of **3** and **4** are shown as examples in Figure 3.5, and the pertinent absorption and fluorescence data are given in Table 3.6.

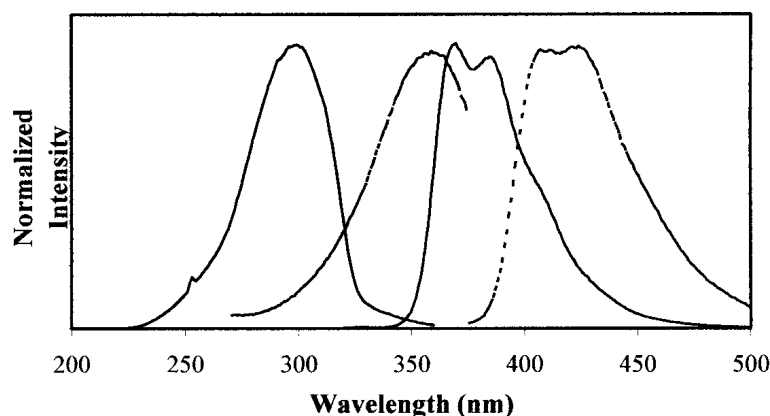
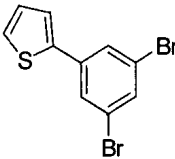
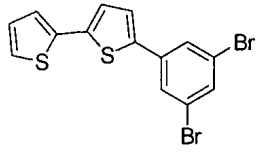
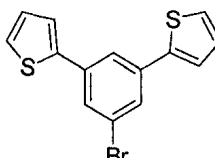
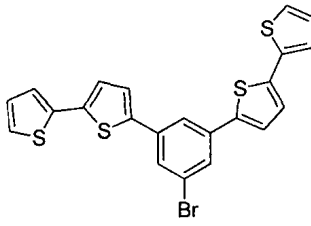
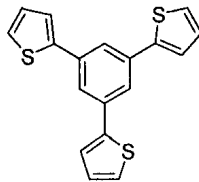
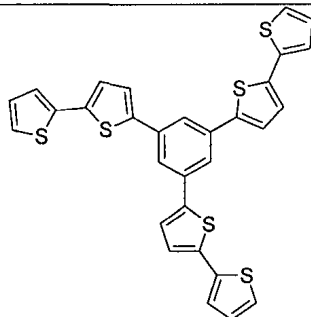


Figure 3.5: Absorption (blue) and fluorescence (red) spectra for **3** (—) and **4** (---).

Structureless absorption bands were observed for compounds **3**–**8** and are assigned to the π - π^* transition. In general, the absorption maxima for the “monothienyl” compounds were observed at higher energies than those of the “bithienyl” compounds (*ca.* 300 vs. 350 nm). Becker *et al.*¹⁶ investigated the optical properties of a series of α -oligothiophenes with one to seven rings and reported an inverse relationship between the change in energy of the absorption maxima and the conjugation length of these

compounds. Thus, the energy of the absorption maxima of these compounds can be thought of as a measurement of the spatial extent of π -conjugation.²

Table 3.6: Absorption and fluorescence data for compounds **3** – **8**.

Compound	Absorption (λ_{max} /nm)	Fluorescence (λ_{max} /nm)	Compound	Absorption (λ_{max} /nm)	Fluorescence ^a (λ_{max} /nm)
 5^{Br}	286	354	 6^{Br}	355	408
 7^{Br}	298	360	 8^{Br}	358	408
 3	300	370	 4	360	408

^aThe absorption λ_{max} was used as the excitation wavelength.

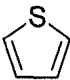
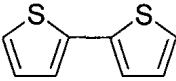
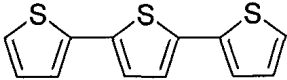
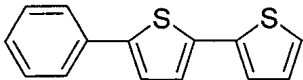
The absorption maxima for the “monothienyl” compounds **3**, **5^{Br}** and **7^{Br}** (300, 286 and 298 nm, respectively) lay between those of thiophene (**T**) (231 nm) and 2,2':5',2''-terthiophene (**TT**), but were comparable to that of 2,2'-bithiophene (**BT**) (303

nm) (Table 3.7). This indicated some degree of conjugation between the thienyl and phenyl rings. Sato *et. al*² calculated the approximate conjugation length as represented by the number of double bonds (*n*) in a series of *ortho*-, *meta*-, and *para*-bis(bithienyl) phenyl compounds using equation 3.1, where E is the peak energy in eV.

$$E = (7.32/n) = 2.26 \quad (3.1)$$

Using equation 3.1, the *n* values for **5^{Br}**, **7^{Br}** and **3** were calculated as 3.6, 3.8 and 4.0. This indicated that there was not a significant increase in conjugation with increased substitution around the phenyl ring. By comparison, the calculated *n* values for **T**, **BT** and **TT** were 2.4, 4.0 and 5.9, respectively.

Table 3.7: Absorption and fluorescence maxima for selected oligothiophenes.¹⁶

Compound	Acronym	Absorption (λ_{max} /nm)	Fluorescence (λ_{max} /nm)
 Thiophene	T	231	---
 2,2'-Bithiophene	BT	303	362
 2,2'-5',2''-Terthiophene	TT	354	426
 5-phenyl-2,2'-bithiophene ²	PBT	---	413

The absorption maxima of the “bithienyl” compounds **4**, **6^{Br}**, and **8^{Br}** (360, 355, 358 nm) were closest to that of **TT** (354 nm). This indicated once again a degree of conjugation between the bithienyl and the phenyl rings. Calculation of the conjugation length of these systems gave the following n values: **6^{Br}**, 5.9; **8^{Br}**, 6.0; and **4**, 6.2. Consequently, as observed with the monothienyl systems, there was not a significant increase in conjugation with increased substitution on the phenyl ring.

In contrast to the absorption spectra, the fluorescence spectra of compounds **3** – **8** showed structured bands (Figure 3.5). In general, the shapes of the fluorescence bands of oligothiophenes, depend on the number of thiophene rings.² Therefore, this can also be used as a tool to compare the degree of conjugation of these compounds. The fluorescence band of the monothienyl compounds showed two overlapped peaks. The fluorescence bands of **4**, **6^{Br}** and **8^{Br}** resembled those of **TT**, which was consistent with the degree of conjugation determined from the absorption spectra of these systems.

Sato *et al.*² reported the fluorescence maximum of 5-phenyl-2,2'-bithiophene (**PBT**) to be 413 nm. This lay between those of **BT** (362 nm) and **TT** (426 nm) (Table 3.7). Furthermore, the shape of the fluorescence spectrum of **PBT** was similar to that of **TT**. These data correlated well with those found by us for **4**, **6^{Br}** and **8^{Br}** and indicated once again that the degree of substitution around the phenyl ring had little impact on the fluorescence properties, *i.e.*, that the essential chromophore was **PBT**-like.

The fluorescence maxima of **3**, **5^{Br}** and **7^{Br}** were compared to those of **T**, **BT**, and **TT**. Becker *et al.*¹⁶ reported **T** as having no fluorescent properties, whereas **BT** and **TT** had fluorescence maxima at 362 and 426 nm, respectively. This further supported our

previous observation in that the monothienyl substituted benzenes (**3**, **5^{Br}** and **7^{Br}**) had a higher degree of conjugation than thiophene alone.

3.3.5 Electrochemical Experiments

3.3.5.1 Electrochemical Polymerization

Polymers of **1**, **2** and **4** have been prepared previously; however, an in depth comparison between these polymers has yet to be conducted. Furthermore, to our knowledge, polymerization of compound **3** has not been reported. Thus, our goals were to prepare polymers of compounds **1** – **4** (**P1** – **P4**), to investigate the effects of extended conjugation (**1** and **3** vs. **2** and **4**), and to determine whether cross-linking between polymer chains had an effect on the stability and conductivity of these polymers (**1** and **2** vs. **3** and **4**).

Polymers of compounds **1** – **4** were prepared by potentiodynamic synthesis using Method A (Section 2.2, p.19), unless stated otherwise. The cyclic voltammograms (CVs) of **1** and **3** (Figure 3.6) were very similar in that they both possessed (1) an irreversible wave at *ca.* 1.6 V due to oxidation of the monomers; (2) a broad reversible wave at *ca.* 1.3 V due to oxidation of neutral polymer, coupled with its return wave (due to reduction of cationic polymer) at *ca.* 1.1 V; and (3) a small irreversible wave at *ca.* 1.0 V due to the oxidation of an unknown compound. Moreover, during cycling of the potential, all waves grew, which indicated that the electrode was chemically modified by deposition of polymer. In the case of wave (2) there was very little difference between **1** and **3**. In both cases, it grew to approximately the same extent with a maximum current of *ca.* 4×10^{-5} A/cm² after 10 cycles. However, these two monomers differed slightly in that the CV of **3**

showed a second reversible wave at lower potential due either (i) to the reduction of neutral polymer (0.39 V) and oxidation of the anionic polymer so produced (0.20 V); or (ii) to a redox process associated with decomposition of p-doped polymer. In addition, the film generated from **1** was green in color – similar to films of poly(**BT**) – while the film produced from **3** was also green but had a brown ring along the outer edge. Mitsuhashi *et al.*¹⁷ reported similar coloring for **P1**.

In contrast to those of monomers **1** and **3**, the CVs of **2** and **4** were completely different. The CV of **2** (Figure 3.6) showed one irreversible wave at 1.1 V due to oxidation of the monomer, and two broad reversible waves at 1.0 V and 1.3 V, each with its own return wave at 1.1 V and 0.72 V. It is thought that these two waves corresponded to two distinct oxidations of the polymer, followed by the corresponding stepwise reduction of the so generated cationic polymer. Polymer **4**, on the other hand (Figure 3.6), displayed an irreversible wave at *ca.* 1.2 V (oxidation of the monomer) and only a single broad wave at *ca.* 0.95 V (oxidation of the neutral polymer) followed by one broad return wave at *ca.* 0.56 V (reduction of the cationic polymer). Furthermore, the extent of polymer deposition over 10 cycles was different for these two monomers: **2** was deposited much more easily than **4**, a fact that was demonstrated by the approximate 2-fold increase in the maximum current (1.25×10^{-4} A/cm² vs. 0.75×10^{-4} A/cm²). This also indicated that both **2** and **4** produced higher maximum current than **1** and **3**. The films of **P2** and **P4** were both orange-brown in color.

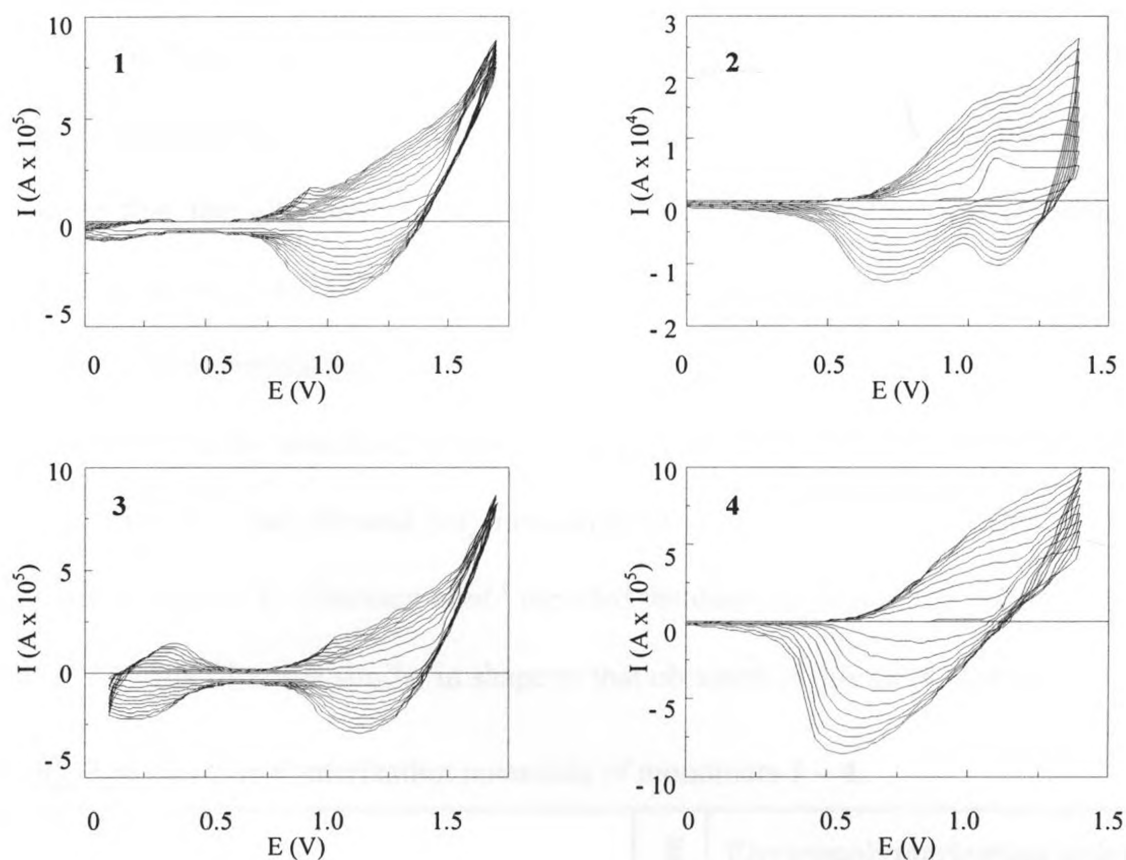


Figure 3.6: Potentiodynamic syntheses of polymers from monomers **1** and **3** (in CH₃CN solution over the potential range of 0 – 1.6 V and 0.1 – 1.6 V, respectively), and **2** and **4** (in CH₂Cl₂ solution over the potential range of 0 – 1.4 V).

The electropolymerization potential of **1** has not been reported in the literature, and that found by us for **2** was similar to that reported by Cherioux *et al.*¹ It should be noted that the potential reported in the literature was referenced to Fc/Fc⁺ (0.23 V vs. Ag/Ag⁺)¹⁸ (Table 3.8). The electropolymerization potential of tri-substituted compound **4** was comparable to but greater than that reported in the literature. This difference may have been due to the instability of the Ag/Ag⁺ reference electrode used. Published reports used SCE as the reference electrode (0.042 V vs. Ag/Ag⁺). In the case of **3**, Cherioux *et al.*¹ reported that it was impossible to deposit a polymer film and, consequently, reported

only the anodic peak potential for this compound. They attributed this failure to the high reactivity of the cation radical of **3**, which may have reacted with a molecule of solvent or suffered nucleophilic attack.¹ Although it was not reported, we think that it was also possible that the oligomers formed during electropolymerization were soluble in the synthesis solution (CH₂Cl₂), and diffused away from the electrode surface, thus preventing polymerization. We, however, found that **3** was indeed polymerizable in CH₃CN solution by potentiodynamic synthesis. Presumably this decreased the solubility of the oligomers and allowed polymerization to occur. When the potential was cycled between 0 and 1.5 V, Cherioux *et al.*¹ reported the deposition of a thin polymer film of **4**. The CV of this film was similar in shape to that obtained in this work (Section 3.3.5.2).

Table 3.8: Electropolymerization potentials of monomers **1** – **4**.

Polymer	Abbreviation	Electropolymerization potential of monomer (V) ^a (Literature value/literature value corrected to Ag/Ag ⁺ reference)
Poly(1,3-bis{2'-thienyl}benzene)	P1	1.55 (N/A) ^{19,20}
Poly(1,3-bis{5'-[2',2''-bithienyl]}benzene)	P2	1.09 (0.81 ^b /1.04) ²¹
Poly(1,3,5-tris{2'-thienyl}benzene)	P3	1.60 (1.06 ^{c,d} /1.10) ¹
Poly(1,3-tris{5'-[2',2''-bithienyl]}benzene)	P4	1.22 (1.05 ^d /1.09) ¹

^a Potentials measured vs. Ag/Ag⁺ at scan rate of 100 mV/s, in CH₃CN solution, with 0.1 M TBAPF₆ electrolyte. ^b Potentials measured vs. Fc/Fc⁺ at scan rate of 100 mV/s, in CH₂Cl₂ solution, with 0.1 M TBAPF₆ electrolyte. ^c Anodic peak potential. ^d Potentials measured vs. SCE at scan rate of 1 V/s, in CH₂Cl₂ solution, with 0.1 M Et₄NClO₄ electrolyte.

3.3.5.2 Cyclic Voltammetry (CV) of Polymers

A series of CVs was obtained for all four polymers. Measurements were carried out in CH_3CN solutions containing 0.1 M TBAPF_6 at a scan rate of 100 mV/s. In the case of **P1** and **P3**, the films produced were visibly thinner than those of **P2** and **P4**, and were stable only over a narrow potential range (*i.e.*, from -1.0 to 1.1 V). Cycling beyond these potentials led to a dramatic decrease in current after the first cycle, and a gradual decrease with subsequent cycling. The cause of this instability is unknown. The estimated available window potential of the electrolyte solution was -2.5 to 2.5 V,²² which eliminated the possibility that the p-doped polymer reacted with solvent radicals at higher potentials (*i.e.*, 1.7 V). Figure 3.7 shows the overlaid anodic (-0.5 to 1.4 V) and cathodic (0 to -2.0 V) CVs for **P1** and **P3**. The general shapes of the CVs for these two polymers were similar: they both possessed an irreversible p-doping wave at *ca.* 1.0 V, and a reversible p-doping wave at higher potential (*ca.* 1.2 V), together with its return wave. The peak oxidation and reduction potentials are given in Table 3.9, together with the scan limits.

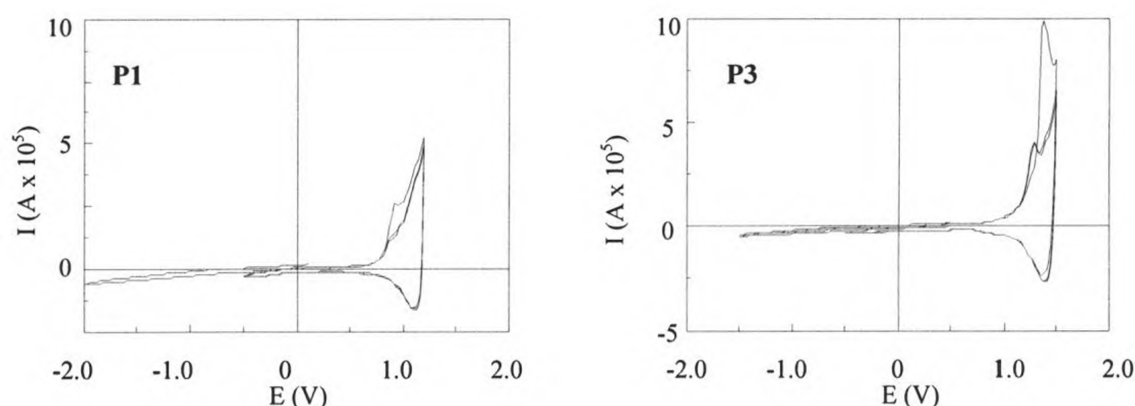
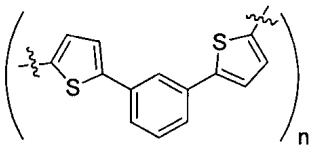
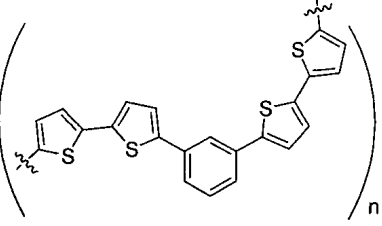
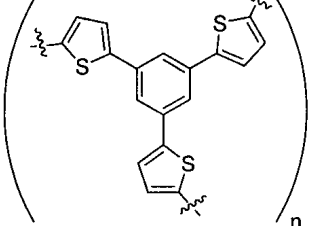
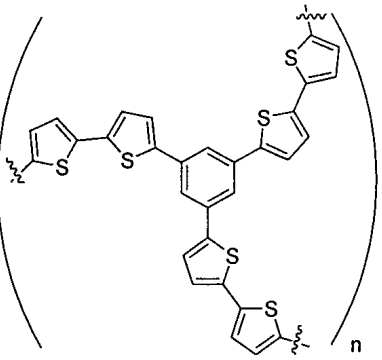


Figure 3.7: Cyclic voltammograms (3 cycles) of **P1** and **P3**. Polymers were deposited on a Pt electrode by potentiodynamic synthesis over 10 cycles (0 to 1.7 V).

Table 3.9: p-Doping and n-doping potentials and voltammetry scan limits for **P1 – P4**.

Polymer	Oxidation Potential of Polymer (p-doping) (V)	Reduction Potential of Polymer (n-doping) (V)	Negative Potential Limit (V)	Positive Potential Limit (V)
 <p>P1</p>	0.89, 1.2	N/A	-1.1	<1.2
 <p>P2</p>	1.3, 1.6	-1.9	-2.2	1.7
 <p>P3</p>	1.3, 1.5	N/A	-1.1	<1.2
 <p>P4</p>	1.3, 1.5	-1.75	-2.0	1.6

When **P1** and **P3** were cycled anodically to higher potentials (*e.g.*, 1.6 V), new irreversible reduction waves appeared at *ca.* 0 V. The growth of these peaks occurred concurrently with the decrease in current of the p-doping wave at *ca.* 1.0 V (Figure 3.8). Various potential ranges (*e.g.*, -1.0 V to 0.75 V, -1.0 to 1.3 V and -1.0 to 1.75 V) were assayed for the appearance of these new waves. Only when potentials higher than 1.3 V were applied did the waves at *ca.* 0 V appear. Therefore, these waves almost certainly corresponded to reduction of decomposition products of the p-doped polymer.

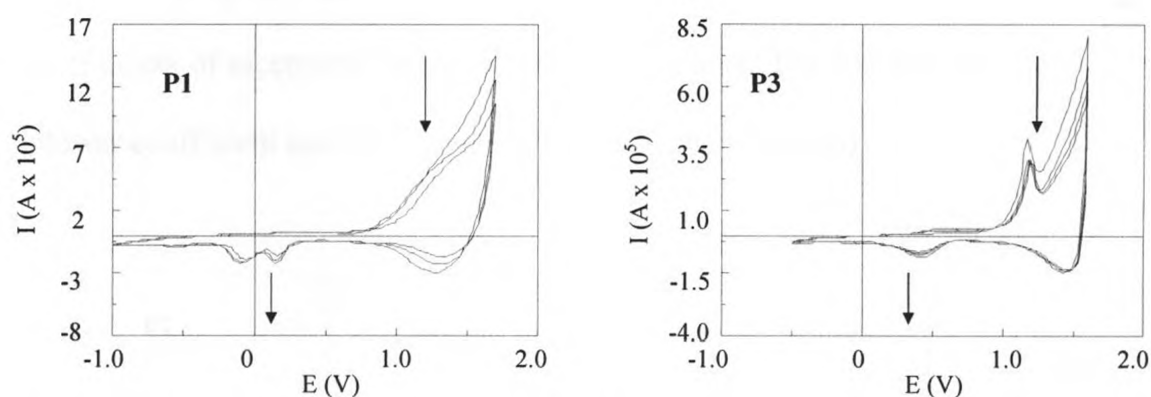


Figure 3.8: Cyclic voltammograms of **P1** and **P3**. Polymers were deposited on a Pt electrode by galvanostatic synthesis (3×10^{-5} A/cm² for 50 s, discharged at 0 V for 100 s to convert to the undoped state.)

In comparison to films of **P1** and **P3**, films of **P2** and **P4** were visibly thicker and were stable over a larger potential range (*e.g.*, -2.0 to 1.6 V). Figure 3.9 shows the overlaid anodic (0 to 1.7 V) and cathodic (0 to -2.0 V) CVs for **P2** and **P4**. The enhanced stability may have been due to a decrease in steric hindrance in those polymers that have four thienyl rings as opposed to two between each phenyl ring, which allowed polymerization to occur more smoothly. In addition, the CVs of **P1/P3** and **P2/P4** were different in shape. The latter polymers showed two quasi-reversible p-doping waves and

one quasi-reversible n-doping wave, whereas the former polymers showed two irreversible p-doping waves and no reduction wave.

When comparing **P2** and **P4**, we observed that **P2** had a higher maximum current density. In an ideal sense, **P2** was a linear polymer with significant electronic communication between the meta bithienyl units across the phenyl ring. On the other hand, **P4** was a crossed linked polymer. Roncali *et al.*²³ reported similar differences in the maximum current densities of polymers of trithienobenzene core linear and star-shaped monomers (Figure 1.2, p.9). This difference was attributed to a difference in diffusion coefficients of electrolyte between the two polymers. The star-shaped polymer exhibited a lower coefficient and thus possessed a lower current density.

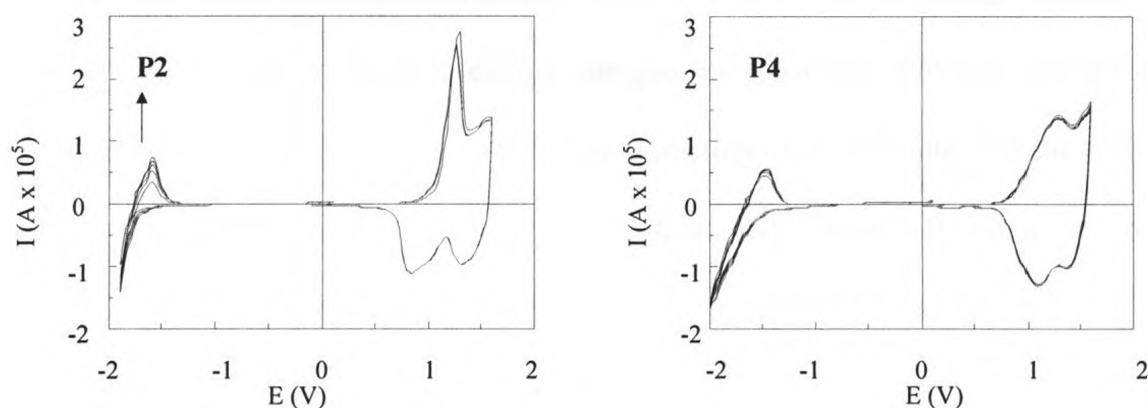


Figure 3.9: Cyclic voltammograms (5 cycles) of **P2** and **P4**. Polymers were deposited on a Pt electrode by galvanostatic synthesis (3×10^{-5} A/cm² for 50 s, discharged at 0 V for 100 s to convert it to the undoped state).

3.3.5.3 Spectroelectrochemical Studies

In these experiments, the UV-visible absorption spectra of thin films of **P2** and **P4**, which had been deposited onto ITO plates (Method B, Section 2.2, p.19), were recorded at various potentials. The chosen potentials were based on the redox events observed in the CV of each polymer.

The UV-visible absorption spectra of **P2** during p-doping (0 to 1.2 V) (A, Figure 3.10), showed a decrease in the absorption intensity of the original high-energy intergap transition (*ca.* 475 nm) and an increase in absorption intensity of two low-energy transitions (*ca.* 650 and 750 nm) at each subsequent p-doping level (0 – 1.2 V).

The UV-visible absorption spectrum during cathodic doping (from –1.0 to –2.0 V) (B, Figure 3.10) showed similar trends as during anodic doping: a decrease in the absorption intensity of the high-energy intergap transition (*ca.* 425 nm) and the increase in absorption intensity of two low-energy transitions (*ca.* 675 and 775 nm). However, during cathodic doping, the low-energy transitions were more defined and more intense than those in the corresponding spectra during anodic doping. Furthermore, the appearance of these transitions occurred rapidly between –1.5 and –2.0 V, whereas the low-energy transitions observed during anodic doping exhibited a slow growth over the range of 0.5 to 1.2 V.

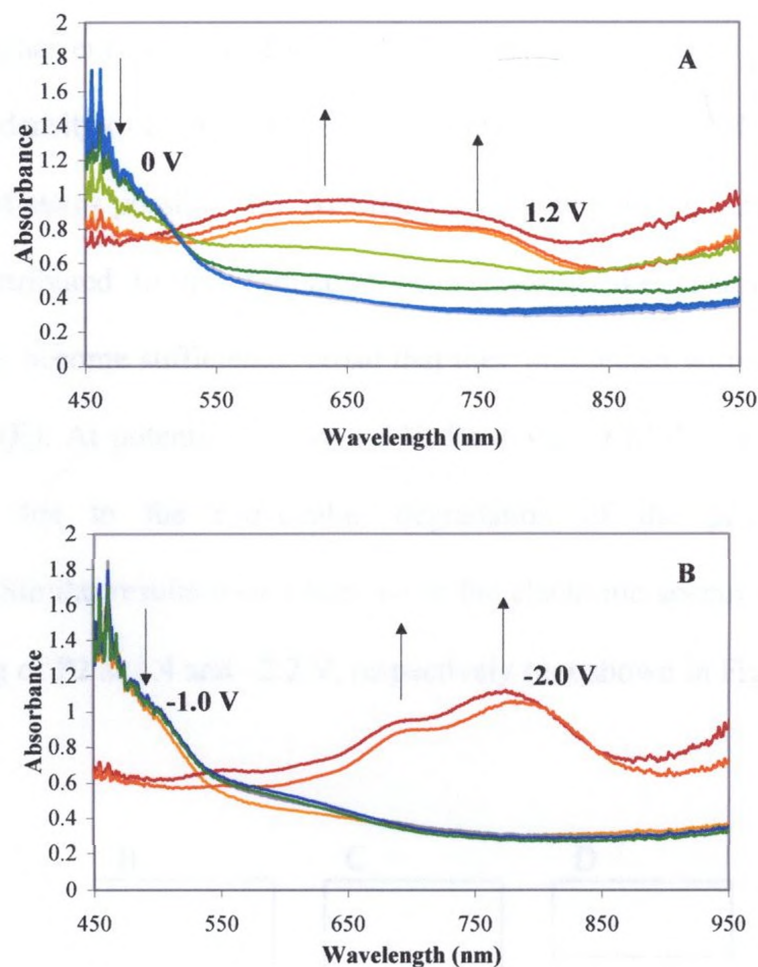


Figure 3.10: Electronic absorption spectra of **P2** as a function of oxidation potential from 0 to 1.2 V (A) and reduction potential from -1.0 to -2.0 V (B) vs. Ag/Ag^+ .

Reynolds *et al.*²⁴ reported similar results for a series of alkoxy-substituted poly(phenylene bithienylene)s and attributed the increase in absorption intensity of the low-energy transitions to an increase in the density of the charge carriers, polarons and bipolarons. The progression of the optical spectra as a function of oxidation potential was explained using the band-structure diagram shown in Figure 3.11. In the undoped form, the absorption band of the polymer was assigned to a $\pi - \pi^*$ transition with an onset energy of E_g (A). As an anodic potential was applied, the initial charge carriers, a

combination of polarons and bipolarons, were formed causing a shift in the initial $\pi - \pi^*$ transition to higher energy (B and C). A further increase in anodic potential caused an increase in the density of bipolarons, which could then be represented as bands due to the large number of states possible (D). At even higher potentials, the change in the optical spectra was attributed to the formation of a metallic-like charge carrier: intergap bipolaron bands become sufficiently broad that they intersected with the conduction and valence bands (E). At potentials above 1.5 V, Reynolds *et al.*²⁴ observed a decrease in electroactivity due to the irreversible degradation of the polymers caused by overoxidation. Similar results were observed in the electronic spectra during anodic and cathodic doping of **P2** at 1.4 and -2.2 V, respectively (not shown in Figure 3.11).

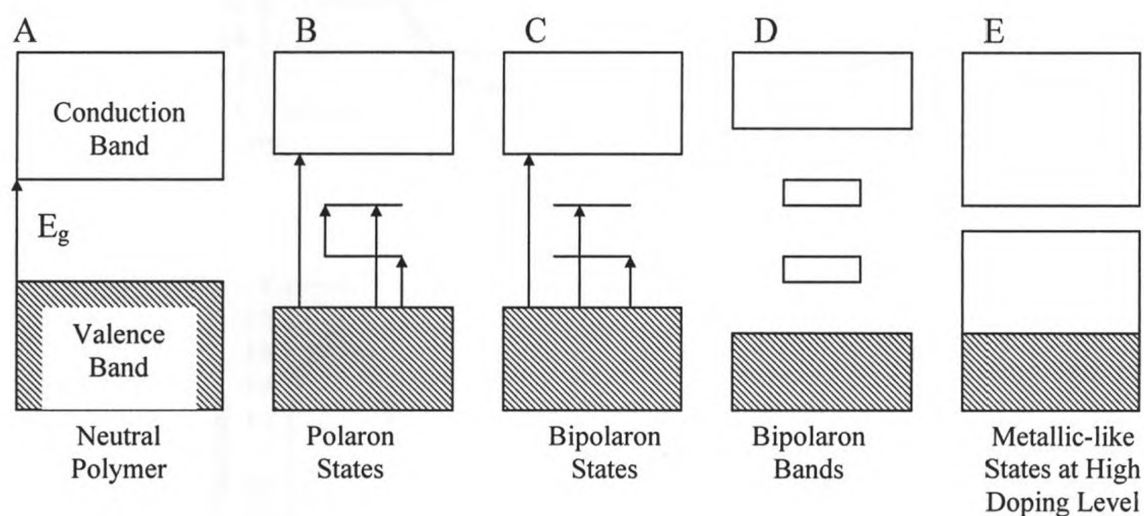


Figure 3.11: Electronic band diagram for nondegenerate ground-state conjugated polymers showing (A) neutral state, (B) polaron states, (C) bipolaron states, (D) bipolaron bands, and (E) metallic-like bands.

Upon anodic doping (from 0 to 1.2 V), the UV-visible absorption spectrum of **P4** showed similar behavior to that of **P2**. However, the appearance of the two low-energy transitions (A, Figure 3.12) was more pronounced and occurred over a shorter potential range (1.0 to 1.4 V). Furthermore, cathodic doping (from -1.0 V to -2.0 V) had no effect on the absorption spectrum of this polymer. Results from previous CV measurements of **P4** have shown that cathodic doping does occur but only at very negative potentials (*ca.* -2.0 V). Therefore, these experiments will need to be repeated.

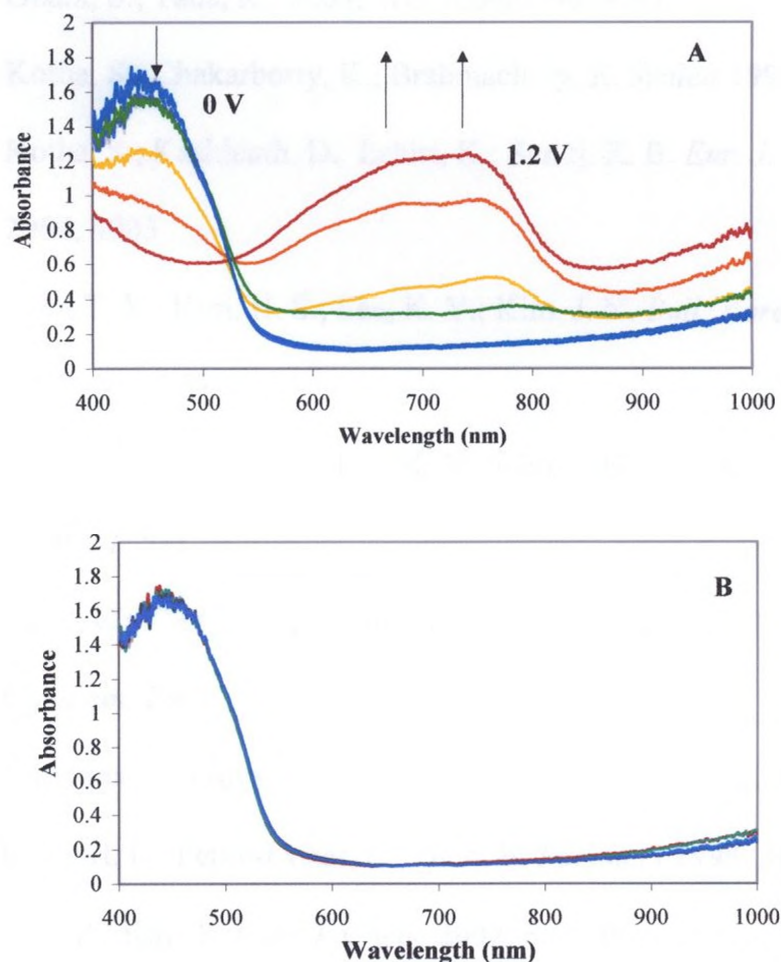


Figure 3.12: Electronic absorption spectra of **P4** as a function of oxidation potential from 0 to 1.2 V (A) and reduction potential from -1.0 to -2.0 V (B) vs. Ag/Ag^+ .

3.4 References

- (1) Cherieux, F.; Guyard, L. *Adv. Funct. Mater.* **2001**, *11*, 305.
- (2) Sato, T.; Hori, K.; Fujitsuka, M.; Watanabe, A.; Ito, O.; Tanaka, K. *J. Chem. Soc., Faraday Trans.* **1998**, *94*, 2355.
- (3) Pelter, A.; Jenkins, I.; Jones, D. E. *Tetrahedron* **1997**, *53*, 10357.
- (4) Mitchell, W. J.; Kopidakis, N.; Rumbles, G.; Ginley, D. S.; Shaheen, S. E. *J. Mater. Chem.* **2005**, *15*, 4518.
- (5) Satoru, O.; Kentaro, T. 2004; EP 1535 942 A1.
- (6) Obara, S.; Tada, K. 2004; WO 2004/009669 A1.
- (7) Kotha, S.; Chakarborty, K.; Brahmachary, E. *Synlett* **1999**, 1621.
- (8) Kotha, S.; Kashinath, D.; Lahiri, K.; Sunoj, R. B. *Eur. J. Org. Chem.* **2004**, 4003.
- (9) Kim, T. Y.; Kim, H. S.; Lee, K. Y.; Kim, J. N. *Bull. Korean Chem. Soc.* **1999**, *20*, 1255.
- (10) Kim, T. Y.; Kim, H. S.; Lee, K. Y.; Kim, J. N. *Bull. Korean Chem. Soc.* **2000**, *21*, 521.
- (11) Belot, C.; Filiatre, C.; Guyard, L.; Foissy, A.; Knorr, M. *Electrochem. Commun.* **2005**, *7*, 1439.
- (12) Cherieux, F.; Guyard, L.; Audebert, P. *Chem. Commun.* **1998**, 2225.
- (13) Rebourt, E.; Pepin-Donat, B.; Dinh, E. *Polymers* **1995**, *36*, 399.
- (14) Gan, Z.; Roy, R. *Can. J. Chem.* **2002**, *80*, 908.
- (15) Song, C.; Swager, T. M. *Macromolecules* **2005**, *38*, 4569.
- (16) Becker, R. S.; Seixas de Melo, J.; Maçanita, A. L.; Elisei, F. *J. Phys. Chem.* **1996**, *100*, 18683.

- (17) Mitsuhashi, T.; Kaeriyama, K.; Tanaka, K. *Chem. Commun.* **1987**, 764.
- (18) Wang, K.; Stiefel, E. I. *Science* **2001**, 291, 106.
- (19) Pelletier, A.; Maud, J. M.; Jenkins, I.; Sadka, C.; Coles, G. *Tetrahedron Lett.* **1989**, 30, 3461.
- (20) Sato, T.; Hori, K.; Tanaka, K. *J. Mater. Chem.* **1998**, 8, 589.
- (21) Song, C.; Swager, T. M. *Macromolecules* **2005**, 38, 4569.
- (22) Bard, A. J.; Faulkner, L. R. *Electrochemical Methods, Fundamentals and Applications*; 2nd. ed.; Wiley: New York, 2001.
- (23) Nicolas, Y.; Blanchard, P.; Levillain, E.; Allain, M.; Mercier, N.; Roncali, J. *Org. Lett.* **2004**, 6, 273.
- (24) Child, A. D.; Sankaran, B.; Larmat, F.; Reynolds, J. R. *Macromolecules* **1995**, 28, 6571.

4 C₂-Symmetric Thienyl Benzene Compounds

4.1 General Introduction

In the mid-1930s, Hammett proposed his now eponymous equation (4.1) to relate the nature of a substituent X to the reactivity of a side chain Y in compounds of type XGY, where G is a skeleton group (very often benzene) to which X and Y are attached.^{1,2}

$$\log (k/k_0) = \sigma\rho \quad (4.1)$$

Here k and k_0 are rate constants for reactions of the substituted (XGY) and the unsubstituted (HGY) compounds, respectively (but equilibrium constants K , K_0 can also be used); σ is the substituent constant, which depends on the nature and position of the R group (*i.e.*, meta, σ_m , or para, σ_p); and ρ is the reaction constant for a given reaction under a given set of conditions.^{1,2}

It is now well established that the physical properties of thiophenes (and of their respective polymers) can be tuned by the introduction of electron-donating or withdrawing groups to the ring, *e.g.*, a linear relationship has been found between the oxidation potential of 3-substituted thiophenes and the Hammett sigma parameter of the substituent group.³⁻⁷ In 1994, Ferraris *et al.*⁴ reported the electrochemical polymerization of a series of 3-(*p*-R-phenyl)thiophene monomers (R = -CMe₃, -Me, -OMe, -H, -F, -Cl, -Br, -CF₃, -SO₂Me) and demonstrated that the oxidation potentials of the monomers (Figure 4.1) and the resulting polymers (Figure 4.2) were well correlated with the Hammett sigma constants of the substituents.

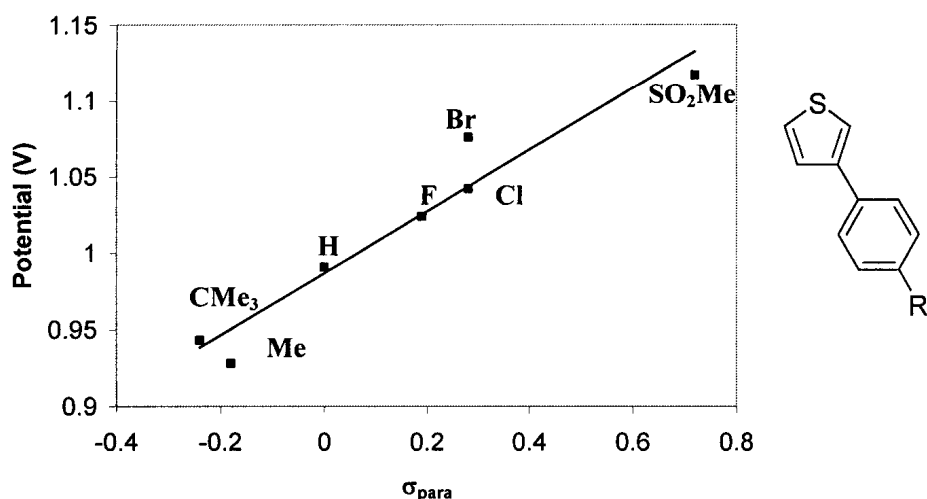


Figure 4.1: Plot of the oxidation potentials of 3-(*p*-R-phenyl)thiophene monomers against σ_p values of the R group.⁴

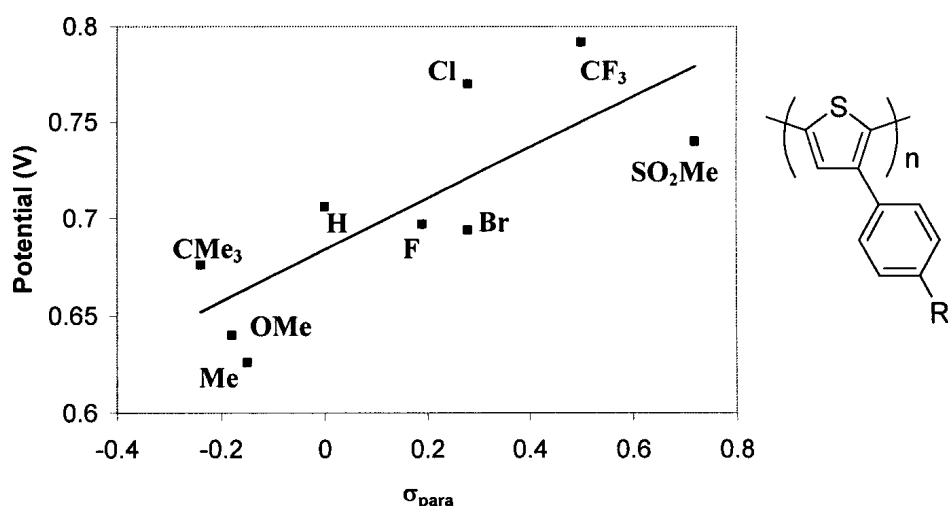


Figure 4.2: Plot of oxidation potentials for the polymers of 3-(*p*-R-phenyl)thiophene against σ_p values for the R group.⁴

As expected, the addition of an electron-donating substituent ($\sigma_p < 0$) to the *para*-position on the phenyl ring shifted the redox potentials cathodically, whereas addition of electron-withdrawing substituents ($\sigma_p > 0$) shifted them anodically. Furthermore, the resulting oxidation potentials were influenced by a combination of inductive (σ_I) and resonance (σ_R) effects of the pendant groups; the relative extent to which these effects

contributed depended on the nature of the group and its position (*i.e.*, meta vs. para).³ These results clearly demonstrated that the electrochemical properties of poly(thiophene)s were amenable to rational tuning. We hoped that the same would be the case in our systems.

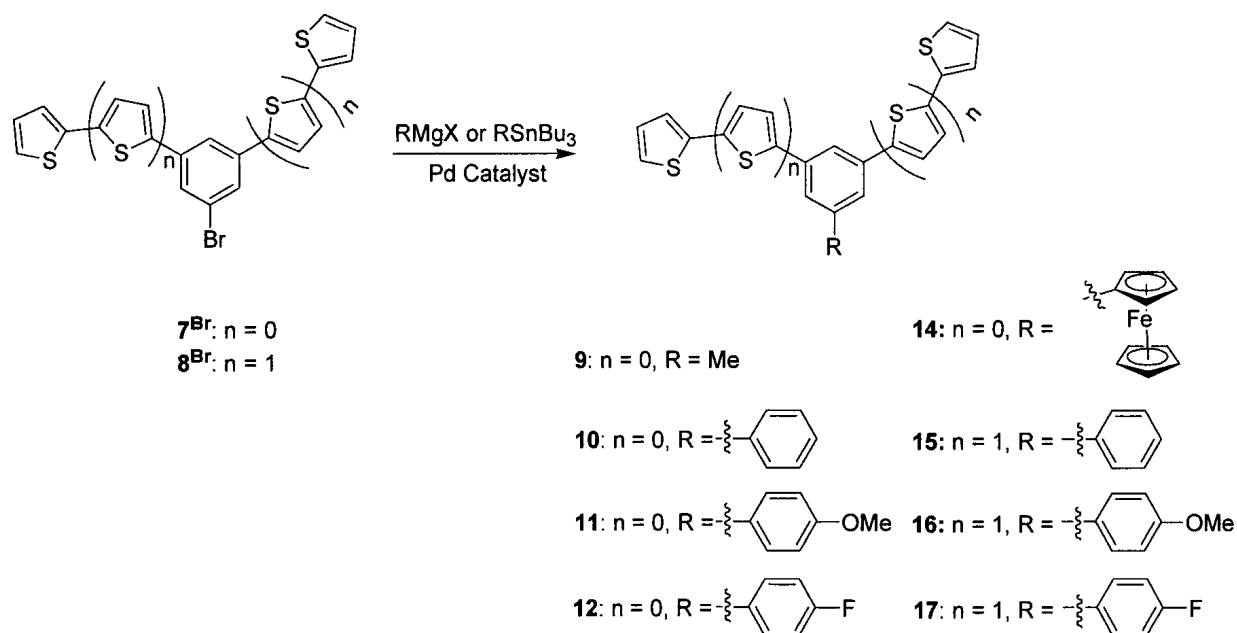
4.2 Synthesis of 1,3-bis(thienyl)-5-R-phenyl compounds

See Experimental Section 2.6, p.43.

4.3 Results and Discussion

4.3.1 Synthesis of 1,3-bis(thienyl)-5-R-phenyl compounds

In order to explore the effects of electron-donating and –withdrawing groups on the physical properties of the thiophene rings in our system, we made a series of compounds of the general formula 1,3-bis(thienyl)-5-R-benzene ($R = -\text{Me}$, $-\text{C}_6\text{H}_5$, $-\text{C}_6\text{H}_4\text{OCH}_3$ and $-\text{C}_6\text{H}_4\text{F}$) (**9** – **12** and **15** – **17**, Scheme 4.1). Our approach to synthesis was inspired by the success of the syntheses of **1** and **3** using Kumada cross-coupling reactions. Thus, the coupling of 1-bromo-3,5-bis(2'-thienyl)benzene (**7^{Br}**) or 1-bromo-3,5-bis{5'-(2',2''-dithienyl)}benzene (**8^{Br}**) with the appropriate Grignard reagent in the presence of $\text{PdCl}_2(\text{dppf})$ as catalyst (Scheme 4.1) gave compounds **9** – **12** and **15** – **17** in modest to good yields (35 – 84 %, Table 4.1). Slight excesses of the Grignard reagent (1.5:1 Grignard reagent:thienyl starting material) and low catalyst loading (3 mol %) were used. To the best of our knowledge, none of the compounds discussed in this section has yet been reported in the literature.



Scheme 4.1: Syntheses of **9** – **12** and **14** – **17** by reaction of bromothienyl compounds with RMgX or RSnBu₃.

Table 4.1: Reaction type and yields for the synthesis of compounds **9** – **17**.

Compound	Coupling Reaction	Isolated Yield (%)
9	Kumada	52
10	Kumada	68
11	Kumada	52
12	Kumada	84
13 ^a	Sonogashira	68
14 ^b	Stille	8
15	Kumada	68
16	Kumada	35
17	Kumada	71

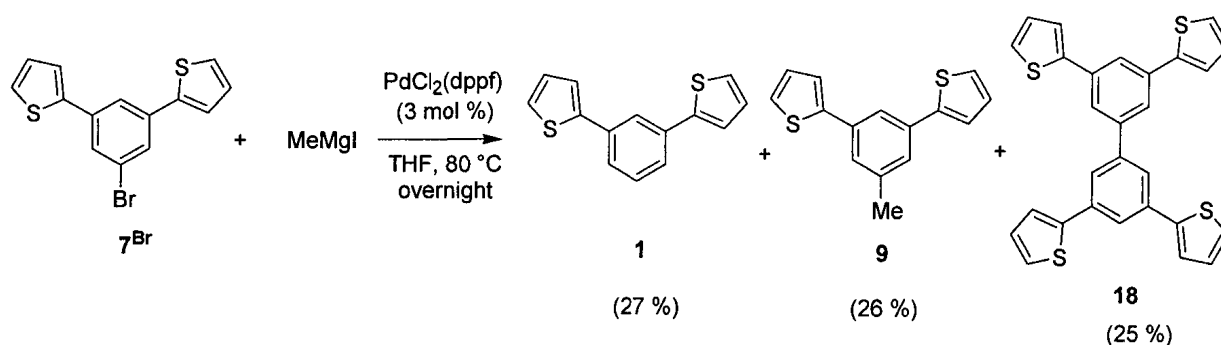
Reactions were conducted in refluxing THF over 18 h, unless otherwise stated.

^a1:1 mixture of THF:Et₃N, 24 h at 60 °C

^bToluene, 35 h at 90 °C.

Initial attempts to synthesize compound **9** involved the coupling of the Grignard reagent MeMgI and compound **7**^{Br} under Kumada conditions. In these experiments,

MeMgI was made in house by reacting MeI, Mg turnings and I₂ in refluxing THF over 24 h. Although all the Mg had not been consumed after this time, compound **7^{Br}** and PdCl₂(dppf) were added regardless. This reaction gave three products: **9**, **1** and the homocoupled compound **18** (Scheme 4.2). Compound **1**, which resulted from the hydrolysis of the Grignard reagent derived from **7^{Br}**, could not be separated from **7^{Br}** using column chromatography. The second byproduct of this synthesis, **18**, was isolated in 25 % yield. It is thought that this compound was made *via* the Kumada coupling reaction between compound **7^{Br}** and its corresponding Grignard reagent.



Scheme 4.2: Pd-catalyzed Kumada coupling of **7^{Br}** with MeMgI to give **9** and the homocoupled by-product, **18**.

In order to generate **18** in a rational manner, and in higher yields, 2 equiv. of **7^{Br}** were mixed with 1 equiv. Mg turnings and a few crystals of I₂ in refluxing THF; there was no visible reaction after 24 h. MeI (2 equiv.) was then added and the desired compound, **18**, was obtained in 25 % yield. The formation of **1** and **9** was confirmed by TLC; however, these compounds were not isolated. These results suggest that MeI was necessary in order for the production of the corresponding Grignard reagent of **7^{Br}** but the reason for this is unknown.

Compound **13** (Figure 4.3, Section 4.3.2) was obtained in moderate yield (68 %) using a Sonogashira coupling reaction between **7^{Br}** and phenyl acetylene. A slightly higher catalyst loading was required in this reaction (5 mol % Pd(PPh₃)₂Cl₂ and 10 mol % CuI) than in the Kumada reactions. Sonogashira conditions were chosen because the starting material, phenyl acetylene, could be obtained commercially and did not require further functionalization.

Compound **14** was obtained using a Stille cross-coupling reaction between tributylstannylferrocene and **7^{Br}** using PdCl₂(dppf) as the catalyst. The synthesis of the ferrocenyl starting material was straightforward: ferrocene was lithiated with ^tBuLi at 0 °C before being quenched with SnBu₃Cl at r.t.. Purification of this compound, like other stannyl reagents prepared previously (Section 3.3.2, p.64), was by vacuum distillation at high temperature (~ 450 °C), which may have contributed to low yields (50 – 60 %). Onward reaction of the stannyl reagent with **7^{Br}** gave a mixture that contained stoichiometric tributylstannyl bromide that was difficult to separate from the desired product.

4.3.2 Electronic Spectroscopic and Electrochemical Measurements

The effect of the electron-donating and -withdrawing properties of the appended R groups (Figure 4.3) on the physical and electronic properties of compounds **1**, **2** and **9** – **17** were investigated using electronic spectroscopy (*i.e.*, UV-visible absorption and fluorescence spectroscopies) as well as by electrochemical experiments. Although the measurements conducted on these compounds were preliminary, general statements about their properties could be made. The pertinent absorption and fluorescence data are given in Table 4.2 and Table 4.3 along with the anodic peak potential (E_{pa}) for each compound. Electrochemical experiments were conducted according to Method C (Section 2.2, p.19).

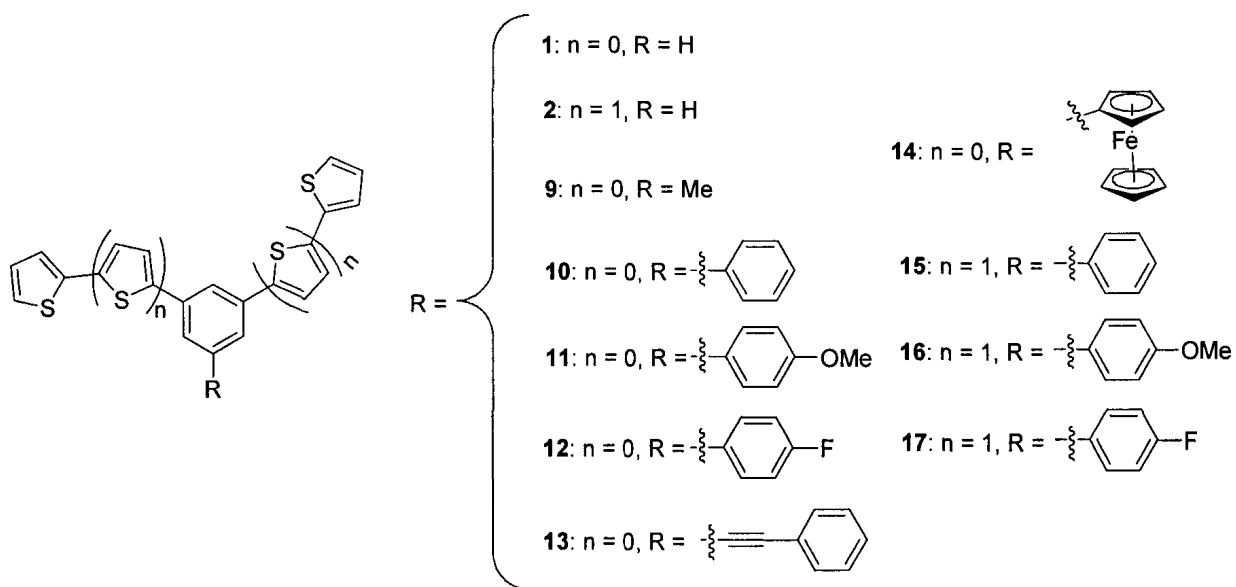
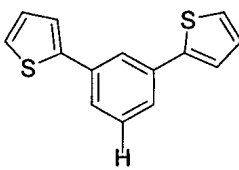
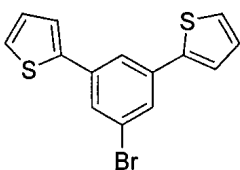
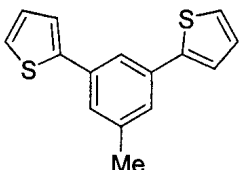
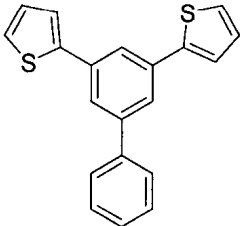
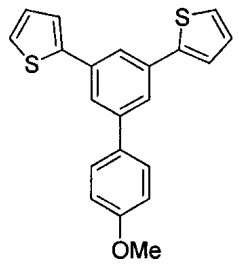
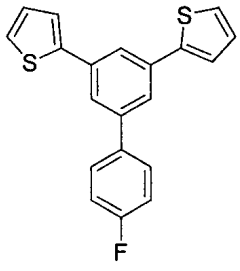
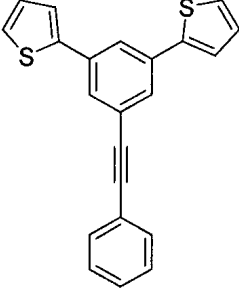
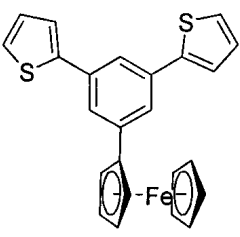


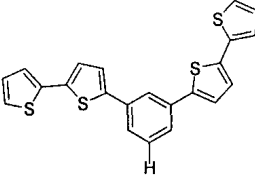
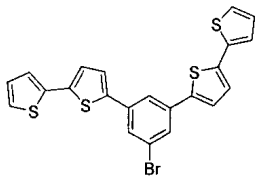
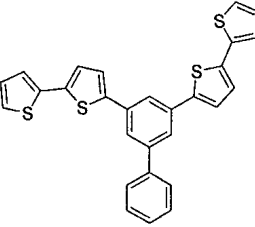
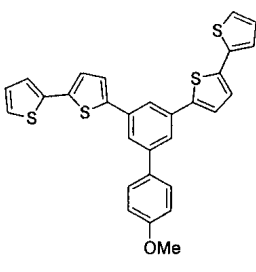
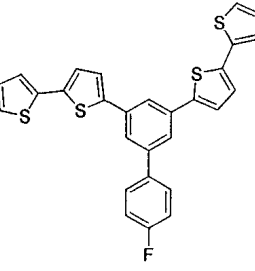
Figure 4.3: Structures of compounds **1**, **2** and **9** – **17**.

Table 4.2: Absorption, fluorescence and anodic peak potential (E_{pa}) data for compounds **1**, **7^{Br}** and **9 – 14**.

Compound	Absorption (λ_{max}/nm)	Fluorescence (λ_{max}/nm)	E_{pa} (V) ^a	Compound	Absorption (λ_{max}/nm)	Fluorescence (λ_{max}/nm)	E_{pa} (V) ^a
 1	299	361	1.35	 7^{Br}	298	360	1.31
 9	310	363	1.30	 10	246	376	1.29
 11	310	375	1.15	 12	276	374	1.24
 13	306	379	1.32	 14	298	381	0, 1.13

^a vs. Fc/Fc^+ in CH_3CN solution using 0.1 M TBAP as supporting electrolyte.

Table 4.3: Absorption, fluorescence and anodic peak potential (E_{pa}) data for compounds **2**, **8^{Br}** and **15 – 17**.

Compound	Absorption (λ_{max} /nm)	Fluorescence (λ_{max} /nm)	E_{pa} (V) ^a	Compound	Absorption (λ_{max} /nm)	Fluorescence (λ_{max} /nm)	E_{pa} (V) ^a
 2	312	423	1.12	 8^{Br}	358	408	1.23
 15	310	419	0.90	 16	310	420	1.22
 17	310	418	1.27				

^a vs. Fc/Fc^+ in CH_2Cl_2 solution using 0.1 M TBAP as supporting electrolyte.

Compounds containing monothienyl substituents (**1** and **9 – 13**) were colorless solids or, in the case of **14**, a red liquid. In contrast, compounds containing bithienyl substituents (**2** and **15 – 17**) were yellow solids. All compounds possessed intensely blue-purple fluorescence. The absorption and fluorescence maxima of the “monothienyl”

compounds (**1** and **10 – 12**) uniformly appeared at higher energy than those of the corresponding “bithienyl” compounds with the same R group (**2** and **15 – 17**). These results were expected because an increase in the length of the thiophene unit (*i.e.*, from thiophene to bithiophene) increased the degree of conjugation and shifted the optical features to longer wavelengths. Furthermore, the results were consistent with those observed previously for mono-, bi- and trisubstituted thienyl compounds (**3**, **5^{Br}** and **7^{Br}** vs. **4**, **6^{Br}** and **8^{Br}**) (Section 3.3.4, p.71). Typical absorption and fluorescence spectra are shown in Figure 4.4.

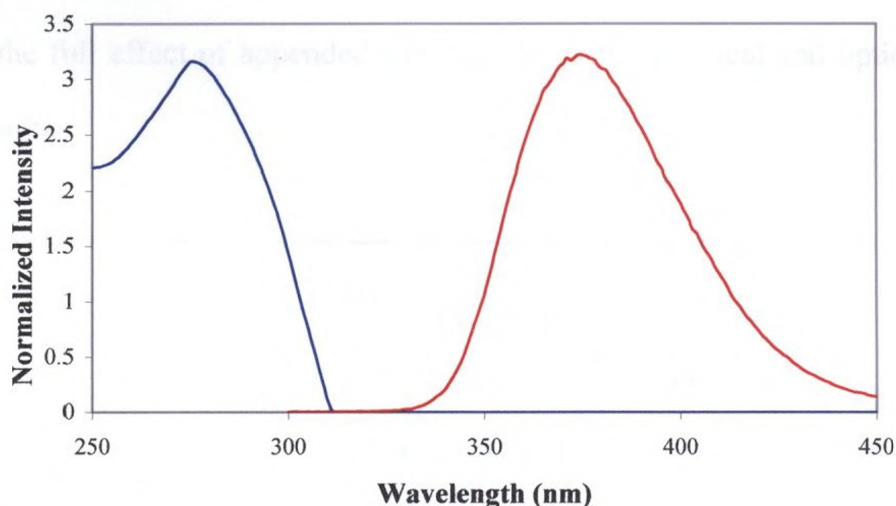


Figure 4.4: Absorption (blue) and fluorescence (red) spectra of **12**.

Electrochemical measurements were conducted on compounds **1**, **2** and **9 – 17** (Table 4.2 and Table 4.3). An increase in length of thiophene oligomers has been correlated to a decrease in oxidation potential and a bathochromic shift in absorption maximum.⁸ As a result, compounds containing bithiophene units (**2** and **15 – 17**)

possessed lower E_{pa} than compounds containing thiophene units (**1** and **10 – 12**) with the same R substituent.

The E_{pa} of the “monothienyl” compounds (**1**, **7^{Br}** and **9 – 14**) and the “bithienyl” compounds (**2**, **8^{Br}** and **15 – 17**) were plotted against their σ_m values⁹ (Figure 4.5 and Figure 4.6, respectively) in order to examine the effects of the electron-donating and -withdrawing properties of the appended R groups on the electronic properties of compounds. Unfortunately, there was not a good correlation between these two sets of values. The results from these preliminary studies suggested that these systems are not as straightforward as originally thought, as they did not exhibit the expected shifts in E_{pa} as predicted by the Hammett equation. Further research is warranted in this area in order to determine the full effect of appended substituents on the physical and optical properties of thienyl units.

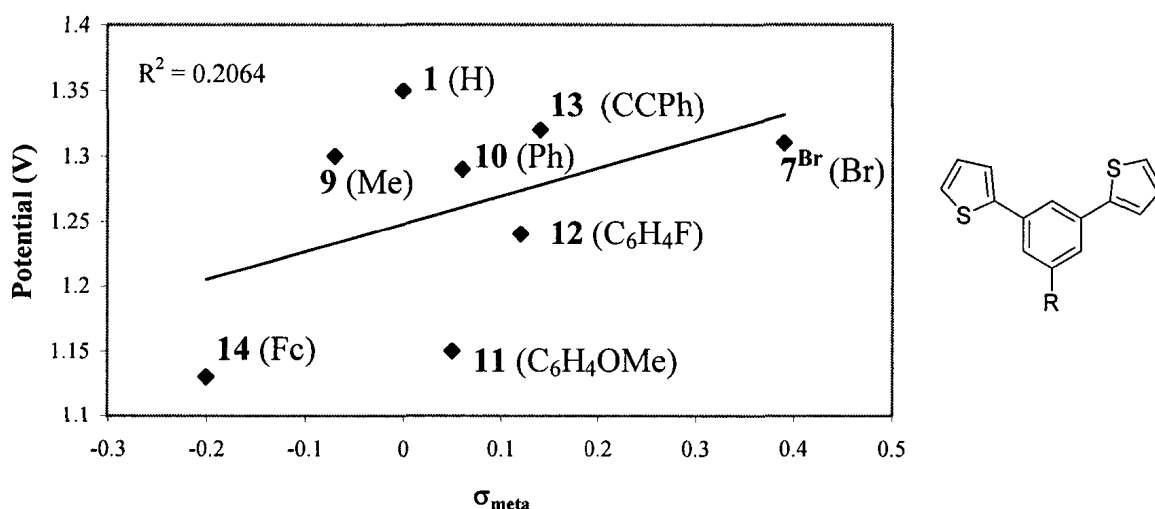


Figure 4.5: Plot of oxidation potentials of **1**, **7^{Br}** and **9 – 14** against σ_m values of the R group.

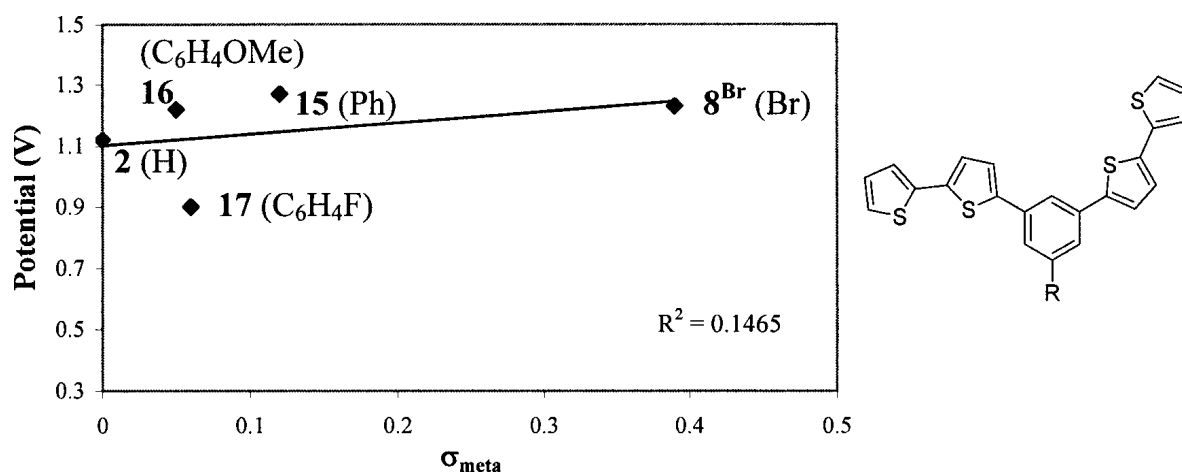


Figure 4.6: Plot of oxidation potentials of **2**, **8^{Br}** and **15 – 17** against σ_{m} values of the R group.

4.4 References

- (1) Jaffé, H. H. *Chem. Rev.* **1953**, 53, 191.
- (2) March, J. *Advanced Organic Chemistry*; 4th ed.; Wiley: New York, NY, 1992.
- (3) Alhalasah, W.; Holze, R. *Microchim. Acta.* **2007**, 156, 133.
- (4) Guerrero, D. J.; Ren, X.; Ferraris, J. P. *Chem. Mater.* **1994**, 6, 1437.
- (5) Sarker, H.; Gofer, Y.; Killian, J. G.; Poehler, T. O.; Searson, P. C. *Synthetic Met.* **1997**, 88, 179.
- (6) Sato, M.; Tanaka, S.; Kaeriyama, K. *Makromol. Chem.* **1989**, 190, 1233.
- (7) Waltman, R. J.; Bargon, J. *Can. J. Chem.* **1986**, 64, 76.
- (8) Roncali, J. *Chem. Rev.* **1992**, 92, 711.
- (9) Hansch, C.; Leo, A.; Hoekman, D. *Exploring QSAR - Hydrophobic, Electronic and Steric Constants*; American Chemical Society: Washington, DC, 1995.

5 Conclusions and Plans for Future Work

Target compounds **1** and **3** were produced in high yields (80 % and 86 %, respectively) using a reliable Kumada cross-coupling reaction between 2-thienylmagnesium bromide and the appropriate halobenzene starting material. Unlike reported syntheses, this method used low catalyst loadings (3 mol %), slight excesses of thienyl starting material and mild reaction conditions. Obara and Tada reported the synthesis of **3** in higher yield (90 %); however, this route involved the Suzuki cross-coupling reaction between 1,3,5-tribromobenzene and 2-thienyl-5-boronic acid, which is often difficult to synthesize. The advantage to our syntheses was that the starting material, 2-thienylmagnesium bromide, could be obtained straightforwardly from the reaction of 2-bromothiophene, which is commercially available, and Mg turnings. The syntheses of **1** and **3** have also been reported using Negishi coupling reactions (65 and 60 % yield, respectively); however, this synthetic route is not as efficient as our Kumada coupling reaction (80 % and 86 % yield, respectively).

Compounds **2** and **4** were obtained in high yields using Stille and Suzuki cross-coupling reactions (83 % and 90 %). Although the Suzuki coupling reaction was high yielding, synthesis of the boronic acid starting material was unreliable and often gave no product. A Stille coupling strategy gave **4** in only 18 % yield; however, the starting material, 5-tributylstannyl-2,2'-bithiophene, could be made straightforwardly and in moderate yield (76 %). To our knowledge, these are the first reported syntheses of **4** using metal-catalyzed coupling reactions. The synthesis of **4** has been reported *via* the cyclotrimerization of 5-acetyl-2,2'-bithiophene in modest yield (56 – 65%), but, this synthesis was irreproducible in our hands.

Compounds **1** – **4** were polymerized by potentiodynamic synthesis. The polymeric films produced from **1** and **3** were different from those produced from **2** and **4**: they were visibly thinner and stable over a shorter potential range (from –1.0 to 1.1 V vs. –2.0 to 1.1 V). Furthermore, when films of **P1** and **P3** were cycled above 1.3 V, two reduction peaks at *ca.* 0 V appeared due to the reduction of decomposed polymer. On the other hand, **P2** and **P4** displayed no decomposition when cycled to potentials as high as 1.8 V. In addition, the CVs of **P1/P3** and **P2/P3** were different in shape. The latter polymers showed two quasi-reversible p-doping waves and one quasi-reversible n-doping wave, whereas the former polymers showed two irreversible p-doping waves and no reduction waves. Finally, the CV of **P2** displayed a higher maximum current density than of **P3**. This was thought to be due to a difference in diffusion coefficients of the electrolyte in these two systems. Further research is warranted in order to investigate the effects of cross-linking in these systems.

Spectroelectrochemical studies of **P2** and **P4** were also conducted. With increased anodic doping, we observed a decrease in the absorption intensity of the high-energy intergap transition and an increase in the absorption intensity of two low-energy transitions due to the formation of charge carriers. This effect was more pronounced and occurred over a shorter potential range in **P4**. Similar energy transitions occurred in the spectrum of **P2** during cathodic doping; however, these experiments need to be repeated in order to investigate the effects of cathodic doping in **P4**.

The absorption and fluorescence spectra of the mono-, di- and tri- substituted compounds (**5^{Br}** and **6^{Br}**, **7^{Br}** and **8^{Br}**, and **3** and **4**) revealed that there was limited

extended conjugation through the benzene and that the chromophore in these molecules was most likely the phenyl (bi)thiophene unit.

The eminently valuable meta-substituted benzene compounds (**7^I** and **8^I**) were isolated from the Pd-catalyzed syntheses of **3** and **4**. Targeted approaches to the bromo analogues of these compounds using Kumada (**7^{Br}**) and Stille (**8^{Br}**) coupling conditions gave the desired products in 46 % and 27 % yield, respectively. Further elaboration of these compounds using Kumada, Stille and Sonogashira coupling reactions gave a series of compounds with the general structure 1,3-bis(thienyl)-5-R-benzene, where R = –Me, –C₆H₅, –C₆H₄OCH₃, –C₆H₄F, –CCPh or –Fc, in low to good yields (8 – 84 %).

Preliminary investigations into the physical and optical properties of these compounds revealed that they were more complex than originally predicted. There was no correlation between the E_{pa} and the Hammett σ_{m} parameters of these compounds: electron-donating and -withdrawing groups did not shift the E_{pa} of these compounds as expected (*i.e.*, electron-donating groups were expected to shift the E_{pa} cathodically, and electron-withdrawing groups anodically). Therefore, further experiments and calculations are required in order to determine the effect of these groups on the physical properties of the meta-thienyl substituted benzenes.

Appendix 1: Crystal Structure Data for 2

Table A1. Crystallographic Experimental Details for 2

Identification code	06161	
Empirical formula	C ₂₂ H ₁₄ S ₄	
Formula weight	406.57	
Temperature	150(2) K	
Wavelength	0.71073 Å	
Crystal system	Monoclinic	
Space group	P 21	
Unit cell dimensions	a = 7.2032(3) Å	α = 90°
	b = 8.0310(5) Å	β = 98.419(3)°
	c = 16.0829(8) Å	γ = 90°
Volume	920.35(8) Å ³	
Z	2	
Density (calculated)	1.467 Mg/m ³	
Absorption coefficient	0.519 mm ⁻¹	
F(000)	420	
Crystal size	0.35 x 0.30 x 0.16 mm ³	
Theta range for data collection	2.56 to 27.48°	
Index ranges	-9 ≤ h ≤ 9, -10 ≤ k ≤ 8, -20 ≤ l ≤ 20	
Reflections collected	8413	
Independent reflections	3568 [R(int) = 0.0410]	
Completeness to theta = 27.48°	99.7 %	
Absorption correction	Semi-empirical from equivalents	
Max. and min. transmission	0.9201 and 0.8391	
Refinement method	Full-matrix least-squares on F ²	

Table A1. Crystallographic Experimental Details for **2** (continued)

Data / restraints / parameters	3568 / 363 / 279
Goodness-of-fit on F^2	1.068
Final R indices	[$I > 2\sigma(I)$] $R_1 = 0.0350$, $wR_2 = 0.0761$
R indices (all data)	$R_1 = 0.0453$, $wR_2 = 0.0800$
Absolute structure parameter	0.08(7)
Largest difference peak and hole	0.195 and -0.274 e.Å ⁻³

Appendix 2: Crystal Structure Data for 4

Table A2. Crystallographic Experimental Details for 4

A. Crystal Data

Formula	C ₃₀ H ₁₈ S ₆
Formula weight	570.80
Crystal dimensions (mm)	0.45 × 0.09 × 0.02
Crystal system	orthorhombic
Space group	<i>P</i> 2 ₁ 2 ₁ 2 ₁ (No. 19)
Unit cell parameters ^a	
<i>a</i> (Å)	7.3457 (5)
<i>b</i> (Å)	23.4327 (16)
<i>c</i> (Å)	29.416 (2)
<i>V</i> (Å ³)	5063.4 (6)
<i>Z</i>	8
ρ _{calcd} (g cm ⁻³)	1.498
μ (mm ⁻¹)	0.561

B. Data Collection and Refinement Conditions

Diffractometer	Bruker PLATFORM/SMART 1000 CCD ^b
Radiation (λ [Å])	graphite-monochromated Mo Kα (0.71073)
Temperature (°C)	−80
Scan type	ω scans (0.3°) (20 s exposures)
Data collection 2θ limit (deg)	50.00
Total data collected	35079 (−8 ≤ <i>h</i> ≤ 8, −27 ≤ <i>k</i> ≤ 27, −34 ≤ <i>l</i> ≤ 34)
Independent reflections	8902 (<i>R</i> _{int} = 0.1312)
Number of observed reflections (<i>NO</i>)	5414 [<i>F</i> _o ² ≥ 2σ(<i>F</i> _o ²)]
Structure solution method	direct methods (<i>SHELXS</i> –86 ^c)
Refinement method	full-matrix least-squares on <i>F</i> ² (<i>SHELXL</i> –93 ^d)
Absorption correction method	multi-scan (<i>SADABS</i>)
Range of transmission factors	0.9889–0.7865
Data/restraints/parameters	8902 [<i>F</i> _o ² ≥ −3σ(<i>F</i> _o ²)] / 5 ^e / 664
Flack absolute structure parameter ^f	0.46 (11)
Goodness-of-fit (<i>S</i>) ^g	1.045 [<i>F</i> _o ² ≥ −3σ(<i>F</i> _o ²)]
Final <i>R</i> indices ^h	
<i>R</i> ₁ [<i>F</i> _o ² ≥ 2σ(<i>F</i> _o ²)]	0.0609
<i>wR</i> ₂ [<i>F</i> _o ² ≥ −3σ(<i>F</i> _o ²)]	0.1463
Largest difference peak and hole	0.407 and −0.356 e Å ⁻³

^aObtained from least-squares refinement of 2262 reflections with 4.44° < 2θ < 36.62°.

Table A2. Crystallographic Experimental Details for **4** (continued)

^bPrograms for diffractometer operation, data collection, data reduction and absorption correction were those supplied by Bruker.

^cSheldrick, G. M. *Acta Crystallogr.* **1990**, *A46*, 467–473.

^dSheldrick, G. M. *SHELXL-93*. Program for crystal structure determination. University of Göttingen, Germany, 1993.

^eThe following pairs of interatomic distances within the disordered thienyl group were constrained to be equal (within 0.001 Å) during refinement: d(S82A–C85) = d(S82B–C85); d(S82A–C88A) = d(S82B–C88B); d(C85–C86A) = d(C85–C86B); d(C86A–C87A) = d(C86B–C87B); d(C87A–C88A) = d(C87B–C88B).

^fFlack, H. D. *Acta Crystallogr.* **1983**, *A39*, 876–881; Flack, H. D.; Bernardinelli, G. *Acta Crystallogr.* **1999**, *A55*, 908–915; Flack, H. D.; Bernardinelli, G. *J. Appl. Cryst.* **2000**, *33*, 1143–1148. The Flack parameter will refine to a value near zero if the structure is in the correct configuration and will refine to a value near one for the inverted configuration. The value observed herein is indicative of racemic twinning, and was accommodated during the refinement (using the *SHELXL-93* TWIN instruction [see reference *d*]).

^g $S = [\sum w(F_o^2 - F_c^2)^2 / (n - p)]^{1/2}$ (n = number of data; p = number of parameters varied; $w = [\sigma^2(F_o^2) + (0.0619P)^2 + 0.3930P]^{-1}$ where $P = [\text{Max}(F_o^2, 0) + 2F_c^2]/3$).

^h $R_1 = \sum ||F_o| - |F_c|| / \sum |F_o|$; $wR_2 = [\sum w(F_o^2 - F_c^2)^2 / \sum w(F_o^4)]^{1/2}$.